

October 2022

A Holistic Investigation of Acidosis in Breast Cancer

Bryce Ordway
University of South Florida

Follow this and additional works at: <https://digitalcommons.usf.edu/etd>



Part of the [Biology Commons](#), [Medicine and Health Sciences Commons](#), and the [Physiology Commons](#)

Scholar Commons Citation

Ordway, Bryce, "A Holistic Investigation of Acidosis in Breast Cancer" (2022). *USF Tampa Graduate Theses and Dissertations*.
<https://digitalcommons.usf.edu/etd/9801>

This Dissertation is brought to you for free and open access by the USF Graduate Theses and Dissertations at Digital Commons @ University of South Florida. It has been accepted for inclusion in USF Tampa Graduate Theses and Dissertations by an authorized administrator of Digital Commons @ University of South Florida. For more information, please contact digitalcommons@usf.edu.

A Holistic Investigation of Acidosis in Breast Cancer

by

Bryce Ordway

A dissertation submitted in partial fulfillment
of the requirements for the degree of
Doctor of Philosophy
Department of Cell Biology, Microbiology, and Molecular Biology
College of Arts and Sciences
University of South Florida

Co-Major Professor: Robert J. Gillies, Ph.D.
Co-Major Professor: Shari Pilon-Thomas, Ph.D.
Gina DeNicola, Ph.D.
Andriy Marusyk, Ph.D.
Patricia McDonald, Ph.D.
Paul Stewart, Ph.D.
Pawel Swietach, Ph.D.

Date of Approval:
October 10, 2022

Keywords: Warburg phenotype, Aerobic fermentation, Low pH, Tumor evolution

Copyright © 2022, Bryce T. Ordway

Dedication

I dedicate this work to two people, whose unconditional support made it possible, and who will not be here to see its completion. My grandmother, Susan Lynn Phillips, was my biggest supporter. I could do no wrong in her eyes, and she believed in whatever I set my sights on. Although I am far from perfect, she truly believed I was. My family suffered her loss on August 30th, 2019, roughly one year after the start of my PhD. After her passing, life was hard for me and continuation of this work was not guaranteed. I was inspired to press-on by the other person with whom this work is dedicated, my late mentor Robert J. Gillies. Bob took me on as his last graduate student knowing his time was limited. He treated me as an equal and supported things most mentors would not. He believed in me and my ideas, more than I believed in myself. Most importantly, he gave me his time and energy, two things that were scarce at the end of his life. He dedicated himself to building me up, regardless of whether I deserved it or not, and wanted to ensure my success above all else. Working with Bob was the most humbling experience I have had. On June 7th, 2022, the world lost an amazing scientist and visionary, but the people who had the privilege of working with him lost so much more.

No matter the evidence for the contrary, these two people believed in me, and without them I would not be where I am today.

Acknowledgments

There are many people who deserve recognition for supporting me and my work throughout my PhD. First off, I would like to thank my family and friends. My mother, Tisha Phillips, and grandfather, Stanley Phillips, for encouraging me to dream big and for teaching me to work hard and be honest. They both worked very hard to provide me with the necessary resources that allowed me to be successful. I would like to thank my lovely girlfriend, Ilda Miguel, for always supporting me and for loving me even though this lifestyle isn't always conducive of a successful relationship. We have both made sacrifices for this, and her resilience is overdue for applause. I would also like to thank the Charity family for treating me as one of their own. Brian and Holly Charity have provided me with so much in the past and present, with no expectation for anything in return. Their encouragement motivated me to push the limits of the norm and aim for something higher. My best friend, Grayson Charity, and his soon to be wife, Megan Clary, would do anything for me, and our long late night discussions helped me get through the tough times. I wouldn't be me without each and every one of these people.

Next, I would like to thank those who have supported my work at Moffitt Cancer Center. Mehdi Damaghi took me on as a mentee and showed me what it really means to be a scientist. Long days and lots of problems are the norm, but hard work and persistence reward you in the end. He dedicated a lot of effort to mentoring me when it was not something he was obligated to do, and I am grateful for this. I would like to thank Samantha Byrne for her technical assistance, throughout my work. I would also like to thank Veronica Estrella, Arig Ibrahim Hashim, Rachel Snayd, Fiorella Lanatta, Bruna Victorasso Jardim-Perassi, Smitha Pillai, Dominique Abrahams, Pietro Irrera, Mustafa Urfi, Michal Tomaszewski, Emmanuel Stimphil, Stanislav Avdieiev,

Shonagh Russell and the rest of the Gillies/Gatenby family, past or present, for their friendship and support.

Outside of our lab, Pawel Swietach, a friend and mentor, provided me a lot of technical training and guidance throughout my Ph.D. work and during his visits to Tampa. I also would like to acknowledge my collaborators Joel Brown and Audrey Freischel for their friendship and sparking the interesting work we have done together.

A special acknowledgement is due for Shari Pilon-Thomas. Upon Bob Gillies passing, Shari was instrumental in making sure the work in the Gillies lab continued and the people in the lab were taken care of. She was also kind enough to accept the responsibility of being my mentor for the remainder of my time at Moffitt Cancer Center.

Table of Contents

List of Figures	viii
Publications	x
Abstract	xi
Chapter 1: Introduction	1
BREAST CANCER EPIDEMIOLOGY	1
<i>Breast cancer's global impact</i>	<i>1</i>
<i>Age and ethnicity related statistics</i>	<i>1</i>
CHARACTERIZATION OF BREAST CANCER	2
<i>Staging of breast tumors</i>	<i>3</i>
<i>Molecular characterization of breast tumors</i>	<i>4</i>
INTRODUCTION TO ACIDOSIS IN BREAST CANCER	5
Chapter 2: Metabolic Dynamics in the Breast Tumor Microenvironment	8
PHYSIOLOGY OF THE BREAST TUMOR	8
HOW DOES THE PHYSIOLOGY OF A BREAST TUMOR LEAD TO PERTURBED METABOLISM?	9
HOW DOES PERTURBED METABOLISM ALTER BREAST TUMOR PHENOTYPE?	10
<i>Molecular mechanisms of microenvironmental sensing</i>	<i>10</i>
<i>Heritable epigenetic modifications acquired through microenvironmental sensing</i>	<i>14</i>
<i>Effects of heritable epigenetic modification on tumor metabolism</i>	<i>18</i>
<i>Consequences of epigenetically altered metabolism on tumor progression</i>	<i>21</i>
HETEROGENEITY OF METABOLIC PHENOTYPES IN BREAST CANCER	22
FIGURES	24
Chapter 3: Breast Cancer Adaptation to Acidic Microenvironment Induces a Partial Epithelial to Mesenchymal Transition State	27
INTRODUCTION	27
RESULTS	31
<i>RNA sequencing of acid-adapted and non-adapted MCF7 cells unravels the EMT mechanism of breast cancer cells</i>	<i>31</i>
<i>Integrative analysis of transcriptomics and proteomics of acid-adapted and non-adapted MCF7 cells reveals the role of S100 proteins in acid- induced epithelial to mesenchymal transition</i>	<i>32</i>
<i>Acid-adapted MCF7 cells express higher S100A6 and S100B proteins</i>	<i>34</i>
<i>S100A6 expression correlates with survival in breast cancer patients</i>	<i>35</i>
DISCUSSION	36

METHODS	38
<i>Cell Culture and Acid Adaptation in vitro</i>	38
<i>RNA Sequencing</i>	38
<i>RNA Sequencing Data Processing and Analysis</i>	40
<i>Proteomics</i>	40
<i>SILAC LABELING</i>	40
<i>LYSIS AND DIGESTION</i>	40
<i>ISOELECTRIC FOCUSING FRACTIONATION</i>	41
<i>LC-MS/MS</i>	41
<i>NETWORK CONSTRUCTION</i>	42
<i>MOTIF EXPLORING AND MOTIF RANKING</i>	42
<i>Proteomics and Transcriptomics Integrative Data Analysis</i>	44
<i>Examining Survival and Gene Alteration Changes</i>	45
<i>Immunofluorescence</i>	45
<i>Immunohistochemistry</i>	45
<i>Statistical Analysis</i>	46
FIGURES	47
Chapter 4: Inhibition of Glycolysis Allows for Breast Cancer Control	56
INTRODUCTION.....	56
RESULTS.....	59
<i>Diclofenac and koningic acid reduce the glycolytic activity of cancer cells</i>	59
<i>Diclofenac inhibits MCT activity</i>	59
<i>Diclofenac and koningic acid decrease the viability of cancer cells</i>	60
<i>Diclofenac and koningic acid reduce the Warburg phenotype of cancer cells</i>	62
<i>Reducing Warburg phenotype can change population dynamics</i>	63
<i>Evolutionary designed therapy controls tumor growth and metastasis in vivo</i>	64
DISCUSSION	65
METHODS	66
<i>Cell culture</i>	66
<i>Hypoxia cell culture</i>	67
<i>Transfection (GFP/RFP Plasmids)</i>	67
<i>Mettler Toledo Five EasyTM/FiveGoTM pH Meter</i>	67
<i>Viability assays</i>	67
<i>Glycolytic rate measurements (Seahorse)</i>	68
<i>Metabolic profiling</i>	69
<i>MCT activity</i>	69
<i>pHi measurement</i>	70
<i>Spheroid mono- and co-culture</i>	70
<i>Animal experiment</i>	71
FIGURES	73
Chapter 5: Implications of Findings and Future Directions	82
IMPLICATIONS OF FINDINGS, LIMITATIONS, AND FUTURE DIRECTIONS.....	82

<i>Chapter 3: Breast Cancer Adaptation to Acidic Microenvironment Induces a Partial Epithelial to Mesenchymal Transition State</i>	82
<i>Chapter 4: Inhibition of Glycolysis Allows for Breast Cancer Control</i>	87
CONCLUDING REMARKS	93
References	94
Appendices	113
APPENDIX 1: IACUC APPROVAL LETTER	113
APPENDIX 2: COPYRIGHT STATEMENTS	114
<i>Copyright statement for “Causes and Consequences of Variable Tumor Cell Metabolism on Heritable Modifications and Tumor Evolution”</i>	114
<i>Copyright statement for “Integrative Analysis of Breast Cancer Cells Reveals an Epithelial-Mesenchymal Transition Role in Adaptation to Acidic Microenvironment”</i>	114
<i>Copyright statement for “Targeting of Evolutionarily Acquired Cancer Cell Phenotype by Exploiting pHi-Metabolic Vulnerabilities”</i>	114
APPENDIX 3: PUBLICATIONS	115

List of Figures

Figure 2.1.	Phases of Breast Cancer Progression.	24
Figure 2.2.	Mechanisms of environmental sensing and their effects on epigenetic modifiers.	24
Figure 2.3.	Epigenetic alterations mediated by environmentally induced epigenetic modifiers.	25
Figure 2.4.	The effect of environmentally induced epigenetic modifications on tumor cell expression and metabolism.	26
Figure 3.1.	Acid adapted cells show partial EMT phenotype.	47
Figure 3.2.	Interaction map of our motif packs, obtained from STRING database illustrating the first shell of interactions for each motif pack.	48
Figure 3.3.	RNA sequencing motif analysis unravels EMT related genes involved in acid adaptation.	49
Figure 3.4.	Integrative analysis of proteomics and transcriptomics data to discover the acidic microenvironment induced EMT genes.	50
Figure 3.5.	SILAC proteomics analysis of DCIS breast cancer cells.	51
Figure 3.6.	Validation of higher expression of acid-induced EMT markers by Immunocytochemistry.	52
Figure 3.7.	Clinical validation of S100A6 expression correlation to acid phenotype in breast cancer.	53
Figure 3.8.	Survival analysis of patients with high and low expression of S100A6 in different stages from IDC, and IDC with local metastasis respectively.	54
Figure 3.9.	RNA sequencing data analysis workflow and the methodology of network analysis	55
Figure 4.1.	Diclofenac and koningic acid reduce the glycolytic activity of cancer cells.	73
Figure 4.2.	Glucose consumption was reduced in both MCF7 and MDA-mb-231 cells after 72 hours treatment with diclofenac, KA, or both.	74

Figure 4.3. ICC Analysis of MCT Expression in Breast Cancer Cell Lines.	75
Figure 4.4. Diclofenac and koningic acid decrease the viability of cancer cells.	76
Figure 4.5. Media pH of cells treated with diclofenac, KA, or combination of both.....	77
Figure 4.6. Survival assay of breast cancer cell lines in different microenvironmental conditions.	77
Figure 4.7. Diclofenac and koningic acid reduce the Warburg phenotype of cancer cells.	78
Figure 4.8. Spheroid 3D co-culture shows the role of evolutionary designed treatment in tumor cells population dynamics.	79
Figure 4.9. Mono- and co-culture of fluorescently tagged breast cancer cell lines.....	80
Figure 4.10. Animal experiments confirm the efficiency of evolutionary designed therapy	81

Abstract

In the early 20th century, Nobel laureate Otto Warburg made the observation that cells of a carcinoma had considerably higher glycolytic metabolism and considerably lower oxidative metabolism compared to cells of a normal tissue. He postulated that within this observation was the key to deciphering the differences between malignant and normal tissue. It is now well established that tumors of the breast are unequivocally acidic, caused by an abnormal amount of aerobic glycolysis, colloquially known as the Warburg effect. Over the last decades, our group, led by Dr. Robert J. Gillies, has set out to characterize the causes and consequences of this acidity in cancer. Major strides have been made in understanding how the acidic environment is developed, and the effects it has on the progression of the tumor. Important questions still exist in understanding how this acidity affects the phenotype of cellular populations within the tumor, how we can effectively target this acidic phenotype in the treatment of cancer, and how the glycolytic phenotype of cancer cells is regulated by acidity. The aim of this work was to contribute to the understanding of the two questions posited in the preceding text.

Chapter 3: Early ducts of breast tumors are unequivocally acidic. High rates of glycolysis combined with poor perfusion lead to congestion of acidic metabolites in the tumor microenvironment, and pre-malignant cells must adapt to this acidosis to thrive. Adaptation to acidosis selects cancer cells that can thrive in harsh conditions and are capable of outgrowing the normal or non-adapted neighbors. This selection is usually accompanied by phenotypic changes. Epithelial mesenchymal transition (EMT) is one of the most important switches correlated to malignant tumor cell phenotype and has been shown to be induced by tumor

acidosis. New evidence shows that the EMT switch is not a binary system and occurs on a spectrum of transition states. During confirmation of the EMT phenotype, my results demonstrated a partial EMT phenotype in the acid-adapted cell population. Using RNA sequencing and network analysis we found 10 dysregulated network motifs in acid-adapted breast cancer cells playing a role in EMT. The further integrative analysis of RNA sequencing and SILAC proteomics resulted in recognition of S100B and S100A6 proteins at both the RNA and protein level. Higher expression of S100B and S100A6 was validated in vitro by Immunocytochemistry (IHC). I further validated our finding both in vitro and in patients' samples by IHC analysis of Tissue Microarray (TMA). Correlation analysis of S100A6 and LAMP2b as a marker of acidosis in each patient from Moffitt TMA approved the acid related role of S100A6 in breast cancer patients. Also, ductal carcinoma *in situ* (DCIS) patients with higher expression of S100A6 showed lower survival compared to lower expression. We propose essential roles of acid adaptation in cancer cells EMT process through S100 proteins such as S100A6 that can be used as therapeutic strategy targeting both acid-adapted and malignant phenotypes.

Chapter 4: Evolutionary dynamics can be used to control cancers when a cure is not clinically considered to be achievable. Understanding Darwinian intratumoral interactions of microenvironmental selection forces can be used to steer tumor progression towards a less invasive trajectory. Here, we approach intratumoral heterogeneity and evolution as a dynamic interaction among subpopulations through the application of small, but selective biological forces such as intracellular pH (pHi) and/or extracellular pH (pHe) vulnerabilities. Increased glycolysis is a prominent phenotype of cancer cells under hypoxia or normoxia (Warburg effect). Glycolysis leads to an important aspect of cancer metabolism: reduced pHe and higher pHi. We recently showed that decreasing pHi and targeting pHi sensitive enzymes can reverse the Warburg effect (WE) phenotype and inhibit tumor progression. Herein, I used diclofenac (DIC) repurposed to control MCT activity, and konigic acid (KA) that is a GAPDH partial inhibitor, and

observed that one could control the subpopulation of cancer cells with WE phenotype within a tumor in favor of a less aggressive phenotype without a WE to control progression and metastasis. In 3D spheroid co-cultures, I showed that our strategy can control the growth of more aggressive MDA-MB-231 cells, while sparing the less aggressive MCF7 cells. In an animal model, we show that our approach can reduce tumor growth and metastasis. We thus propose that evolutionary dynamics can be used to control tumor cells' clonal or sub-clonal populations in favor of slower growth and less damage to patients. We propose that this can result in cancer control for tumors where cure is not an option.

In total, this work has provided knowledge to the field by better describing how cellular populations of breast cancer cells adapt to an acidic environment, and how fermentative glycolysis can be exploited to control breast cancer populations.

Chapter 1: Introduction

The focus of this work was on the causes and consequences of acidosis in breast cancer. In order to best set the stage for the work done, this chapter will describe the clinical underpinnings of breast cancer, how breast cancer affects the global population, and the prior significance of acidosis in breast cancer.

EPIDEMIOLOGY OF BREAST CANCER

Breast cancer's global impact

According to the Global cancer Observatory (GCO) by the World Health Organization (WHO), breast cancer is the most commonly diagnosed malignancy, with 47.8 out of every 100,000 people being diagnosed in 2020 [1], with cases almost exclusively seen in women. Breast cancer also represents the 2nd highest cause of cancer death with 13.6 people per 100,000 people dying from breast cancer per annum, globally; being beaten only by lung cancer at 18.0 per 100,000 [1]. When looking only at cancer mortality in women, breast cancer beats out lung cancer as the number one cause of cancer death. As research pushes forward, one major problem is that the cure rate for breast cancer is hardly making strides. In low-income countries, breast cancer mortality rates are increasing, and in high-income countries mortality rates are stagnating [2]. While these outcomes are far from desirable, there has been a net improvement in treatment outcomes, but due to increased incidence rates mortality rates are not decreasing [3]. There exists a need to decrease breast cancer mortality rates, as it still remains the number one cause of cancer mortality among all women [4].

Age and ethnicity related statistics

The current mean age of breast cancer diagnosis, in the United States, is 58.6 years old with a standard deviation of 9.4 years [5]. There exists a range of diagnosis ages based on ethnicity, with non-Hispanic white women having the highest mean age of diagnosis at 60.4 with a standard deviation of 9.2 years, compared to Hispanic women who have the lowest mean age of diagnosis at 57.0 with a standard deviation of 9.5 years [5]. This disparity gets larger when looking at the percentage of breast cancer deaths that happen before the age of 50. Within this younger than 50 years old group, deaths from breast cancer occur in only 7.6% of non-Hispanic white women, compared to 20.1% of Hispanic women [5].

When discussing incidence rate, the trends from ethnicity do not follow the mortality rates. Of women under 50 years of age in the United States, despite having the lowest mortality rate, non-Hispanic white women have the highest incidence rate for invasive breast cancer at 49.2 per 100,000. Native American women represent the lowest incidence for this group at 28.6 per 100,000. As for incidence of advanced stage breast cancer before the age of 50 years old in the United States, non-Hispanic black women have the highest rate at 23.1 per 100,000. Native American women again represent the lowest incidence for this group, at 13.4 per 100,000 [5].

Differences in overall incidence, age of incidence, mortality, and stage among different ethnic groups likely stem from differences in genetic background, environmental exposures and socioeconomic status.

CHARACTERIZATION OF BREAST CANCER

The term breast cancer represents a wide variety of diseases that have been characterized and categorized in order to best describe a given patient's disease, with the end goal of finding their best treatment strategy. These categorizations can be broken down into tumor staging, and molecular characterization.

Staging of breast tumors

Current guidelines for the staging of cancer are provided by the American Joint Committee on cancer (AJCC) and the Union for International cancer Control (UICC). The staging system maintained by these two groups is known as the TNM staging system, in which the (T) represents the overall status of the tumor, (N) represents the degree of lymph node involvement, and (M) represents metastatic presence. Following information regarding staging was obtained from the cancer Research UK website [6].

The T stage of breast cancer can be broken down into 7 groups Tx, Tis (DCIS), Tis (Paget), T1, T2, T3, and T4. Tx represents a tumor size that cannot be determined, regardless of reason. Tis (DCIS) represents a ductal carcinoma *in situ* breast tumor, in which the tumor is confined to the ducts of the breast and has not invaded into surrounding breast tissue. Tis (Paget) represents a rare skin condition of the nipple that is associated with an early rash, irrespective of invasive status of the tumor. T1 represents a tumor that is 2 cm or less in diameter. T2 represents a tumor that is >2 and <5 cm in diameter. T3 represents a tumor that is >5 cm in diameter. Stage 4 represents an invasive tumor that has spread to the chest wall, breast skin, or both; sometimes also encompassing an inflammatory carcinoma.

The N staging of breast tumors is divided into two groups, the pathological (pN) and the clinical (cN). pNX and cNX represent a nodal status that cannot be assessed. Both the pathological and clinical nodal staging methods go from a scale of pN1-pN3 or cN1-cN3, respectively; with the N number increasing with severity of the nodal involvement. The main differentiator between the two nodal staging methods is that the pathological system takes into account the number of lymph nodes involved, which the clinical staging method is focused mainly on the location of the nodes in which cells have disseminated to.

The M staging of tumors is given only 4 different possible designations. M0 represents a patient status in which no metastases are present. cMo(i+) is used to designate a patient in which medical imaging and physical examination do not show the presence of metastasis, but cancer cells can be found in laboratory tests, not localized to the primary tumor. cM1 represents a patient who does present visually of physically detectable metastases in a part of the body other than the breast. pM1 is the pathological designation used when metastasis larger than 0.2mm across are observed upon tissue examination.

Molecular characterization of breast tumors

With advances in nucleic acid technologies, it has now become commonplace that patients in the clinic presenting with breast cancer are profiled for the presence of germ-line mutations, somatic mutations, or changes in gene expression. The purpose of this testing is to better characterize the patient and their tumor, with the goal of using the best treatment available for their specific case.

The protein expression markers most synonymous with the subtyping of breast cancer are the estrogen receptor (ER), progesterone receptor (PR), and the human epidermal growth factor receptor 2 (HER2). The significance of ER expression in breast cancer was demonstrated early in the molecular characterization of breast cancer with many papers in the late 1970's implicating low expression of ER with increased tumor recurrence, faster cell proliferation rates, and decreased response to chemotherapy [7-9]. Around this same time, the PR status of breast tumors was taking shape with studies showing presence of a progesterone receptor in 1/3 of breast cancer patients tested [10], and the hope was this would be another marker of hormone status, as ER status was not sufficient to predict patient response to endocrine treatment. The significance of HER2 expression as a marker was demonstrated by that fact that it is overexpressed in 25%-30% of breast cancer patients, it was associated with poor clinical outcome, and it was almost exclusively caused by an amplification of the HER2 gene, which

would be clinically observable [11]. Expression of the ER and PR genes are positively correlated with one another, while the expression of HER2 is inversely correlated with their expression [12]. Molecular characterization of breast cancer was defined in a landmark study of gene expression in breast cancer patients. In this study, it was observed that ER+ patients expressed many proteins associated with luminal cells, placing them in the luminal category [13]. The luminal category of breast tumors has been further broken down into luminal A and luminal B, based on the expression of Ki67, with luminal A expressing low levels of Ki67 and luminal B expressing high levels of Ki67 [14]. It was also demonstrated that the ER- cancers should be placed in two distinct expression categories based on their expression of HER2, with tumors negative for ER and HER2 being deemed triple-negative basal-like tumors, and tumors negative for ER expression but positive for HER2 expression, being deemed HER2+ [13]. While the differentiation between these breast tumor types is not on the basis of metabolism, the metabolic profiles of these different tumor types vary greatly [15].

INTRODUCTION TO ACIDOSIS IN BREAST CANCER

Berlin, Germany 1925. Otto Warburg published an observation that, despite the presence of oxygen, cells of a carcinoma have considerably lower oxidative metabolism and considerably higher fermentative metabolism when compared to their normal counterparts. This phenotype has been deemed, “the Warburg effect”. Warburg himself postulated that within his observation was the key to deciphering what the true difference between a cancerous cell and a normal cell is. These insights have led to nearly a century of scientific investigation to answer one simple question, “Why do cancers have high aerobic glycolysis?”. This question has plagued some researchers for their entire careers, spawned endless debates about the “true” metabolic phenotype of cancer cells, and led to the investigation of countless subfields all centering around the increased propensity of cancer cells to carry out aerobic glycolysis. No

matter one's opinion on the subject, it is hard to deny the vast impact this observation has had on cancer research for the past century.

In breast cancer the highly fermentative phenotype has been well established, with studies demonstrating increased glucose uptake via Fluorodeoxyglucose-Positron Emission Tomography (FDG-PET) [16], decreased extracellular pH via chemical exchange saturation transfer (CEST) magnetic resonance imaging (MRI) [17], and increased ratios of lactate:glucose in the serum of breast tumors compared to the bodily serum [18]. This increase in fermentative glycolysis does not come without consequence. The excess lactate and protons produced as a result of high fermentative glycolysis elicit tremendous changes in the tumor, stromal, and immune cell populations [19-23].

Associations between breast cancer and acidosis first began with anecdotal clinical cases of patients who presented with lactic acidosis of the blood [24, 25], with some noting that the lactic acidosis was resolved with the use of antineoplastic treatment [26]. It would later come to be accepted that the pH within tumors is much lower than that of normal tissue, associated with this increase in lactic acid fermentation and poor perfusion [27-30]. Major studies into the effects this high concentration of protons may have on tumor phenotype and progression began with the demonstration that low pH in the tumor microenvironment contributed to the local invasion of the tumor [19]. Since then, there has been interest surrounding how this low pH environment may affect the phenotype of tumor cells themselves, or drive evolution of the tumor cell population.

With the investigation into how low pH may affect tumor cell populations, there also exists considerable interest in the targeting of an acidic tumor microenvironment. It is known that the acidic environment promotes invasion [19], and that cell populations adapted to survive in the acidic environments are pushed toward an aggressive phenotype [31], and a partial epithelial to mesenchymal transition (EMT) state [21]. It has also been demonstrated that the

acidic environment in cancer is a significant force in the inhibition of immune function caused by the tumor microenvironment [32]. With all of this taken into account, there exists considerable interest in the targeting of the acidic microenvironment, either by preventing acid production or buffering the existing environment [33-35].

In this body of work, I set out to make contributions towards answering two questions relating to gaps in our understanding of the causes and consequences of acidosis in breast cancer. These questions are:

1. How does the adaptation to an acidic microenvironment alter breast cancer cell phenotype?
2. Can one target fermentative glycolysis in the treatment of breast tumors with the goal of controlling their progression?

By investigating these questions, I hoped to gain a better understanding of how acidosis influences breast cancer progression, and how fermentative glycolysis could be targeted for the treatment of patients. Current treatment strategies using chemotherapeutic and targeted agents provide relief to many patients, while in others they fall short of providing a durable response. Alternative view points in the treatment of breast cancer, such as the ones proposed here, may be able to provide less morbid treatment options for those who would have been successful with current therapies, and also provide an efficacious treatment for those who would have failed.

Chapter 2: Metabolic Dynamics in the Breast Tumor Microenvironment

The metabolism of tumors is highly dependent on their environmental influences. Cell of origin, growth dynamics, heterogeneity, nutrient access, and current metabolic state, all play together to influence the metabolism of a tumor. This chapter will lay out the hypothetical factors leading to a fermentative phenotype in Breast Cancer and demonstrate how tumor metabolism can feedback to further alter metabolism, both transiently and stably.

PHYSIOLOGY OF THE BREAST TUMOR

In order to set the stage for the metabolic perturbations observed in breast carcinomas, one must first understand the physiology of a breast tumor. Of all observed breast tumors, 95% are classified as adenocarcinomas. As defined by the NIH on the *cancer.gov* website, adenocarcinomas are cancers that form from the lining of glandular tissues, which function to secrete a variety of fluids necessary for normal bodily function.

The anatomy of a breast is composed of adipose and glandular tissue, held together by connective ligaments. Lobes of the breast are comprised of lobules containing alveoli with mammary secretory epithelial cells. Small and large ducts connect the alveoli for each lobe, in order to drain the secretions to the areola [36, 37]. These ducts are where the beginnings of breast malignancies take place. Epithelial cells line the ducts of the breast. Upon malignant transformation, ductal epithelial cells begin to grow into the duct forming a nodule within the duct. This nodule will grow into the duct, and likely reach a point at which it grows to the capacity of the duct. When confined to the inter-lumen of the duct, these tumors are labelled as Ductal Carcinoma *in situ* (DCIS) (Figure 2.1). Invasion into the area surrounding the duct is common, and represents a jump in staging to an invasive ductal carcinoma (IDC) (Figure 2.1).

Once at this stage, tumors can be classified as either IDC with metastases, or IDC without metastases.

HOW DOES THE PHYSIOLOGY OF A BREAST TUMOR LEAD TO PERTURBED METABOLISM?

As mentioned previously, growth of a breast tumor happens within the breast duct. Vasculature of the duct is localized to the outer region, where the epithelial lining resides. As with most solid tumors, breast malignancies grow away from these vascularized regions as they expand into the lumen of the duct. Vasculature is responsible for the exchange of new and expended nutrients, an essential process for proper cellular function and tissue maintenance. As tumors grow and cells are increasingly separated from vascular networks, cells become deprived of essential nutrients and are enveloped in their own toxic waste products, relying only on a nutrients diffusion distance through the tissue for supply. Cells have mechanisms for sensing this lack of vascularity in their local region, and activate pathways to induce the growth of vascular network. This attempt to grow the vasculature usually is not sufficient to adequately perfuse cells and still results in cells deep in the tumor to be subject to harsh conditions. In order for cells to survive this, they must acclimate their metabolic strategies to fit the environment they are presented with. Two of the most important nutrients required for cellular metabolism are oxygen and glucose. In most normal functioning cells of the body, Glucose is converted into Pyruvate via a chain of enzymatic reactions known as Glycolysis. Pyruvate is then converted into acetyl-CoA and shuttled in the tricarboxylic acid cycle (TCA), which fuels the electron transport chain of the mitochondria. This is where oxygen is reduced, and large sums of adenosine triphosphate (ATP) are produced. Alternatively, a process known as fermentative glycolysis can take place in which pyruvate is converted into lactate, and lactate is shuttled out of the cell. This process is not energetically favorable, but can be done in the absence of oxygen. In the absence of glucose, the TCA cycle can be fueled by other methods such as the

uptake of glutamine or lactate. In 2004, a landmark paper was published by Robert Gatenby and my advisor, Robert Gillies [38], laying out a framework for how cells may adapt to have a highly fermentative phenotype. The key principle that causes this adaptation in cancer comes down to the diffusion limit of the nutrients. In tissues, oxygen diffuses a much shorter distance than does glucose. What this means for a tumor, is that there exists a population of cells within the tumor that is a distance away from vasculature that does not allow for adequate enough oxygenation to carry out oxidative phosphorylation, but does have concentrations of glucose sufficient to carry out glycolysis. Cells in this “zone” if you will, are pushed toward a glycolytic phenotype via hypoxia signaling mechanisms. Further discussion on how signaling mechanisms may regulate this process will take place in later sections. It is hypothesized that populations subjected to these environments will evolve to be better suited to the highly glycolytic dependent environment, or may acclimated via epigenetic mechanisms.

HOW DOES PERTURBED METABOLISM ALTER BREAST TUMOR PHENOTYPE?

This section comes from work previously published by myself, Pawel Swietach, Robert J. Gillies, and Mehdi Damaghi [39]. I was the major contributor to the writing of this article and aided in concept development.

Molecular mechanisms of microenvironmental sensing

Cancer evolution operates through selection, which requires a degree of phenotypic diversity to present a range of possible responses to microenvironmental selection forces, some of which confer selective advantage [40, 41]. Tumors can be described as complete ecosystems, containing cancer cells, stromal cells, vasculature, extracellular matrix, and the chemical milieu consisting of variables such as pH and oxygen tension [42-44]. During tumorigenesis - and similarly in response to therapy - the tumor ecosystem shows considerable plasticity because cancer cells shape their microenvironment, to which subsequent generations of them must

adapt to thrive, and these adaptations, in turn, fine-tune the microenvironment [45]. During the various stages of tumor progression, cells can be exposed to highly variable chemical stimulations, largely attributed to variable blood perfusion; for example, oxygen deprivation (hypoxia), nutrient deprivation, metabolic end-product build-up, and increased acidity. Overall, these stimuli would be considered, by normal standards, to be survivable to most cells but exerts some cost on cells fitness, and it is therefore axiomatic that cancer cells must adapt to these conditions if they are to thrive. Although the stimuli are survivable, they still impose stress on the cells which changes their fitness, requiring acquisition of a novel homeostatic balance that costs more energy for cells and can be lethal for cells in competition with other cells.

Hypoxia is one of the main environmental factors a cancer cell must face in order to survive, thrive, and progress. Hypoxia imposes a metabolic stress on the cell, hindering its ability to carry out aerobic respiration. Therefore, the cell must be able to adapt to a hypoxic environment in order to survive. The cellular response to hypoxia is robust, and exerts most of its force via the transcription factors HIF-1 α and HIF-2 α . Another HIF family protein, HIF-3 α , functions to repress the responses directed by HIF-1 α and HIF-2 α . All three of these proteins carry out their function via dimerization with constitutively expressed HIF β proteins in the nucleus which allows them to directly modulate transcription of proteins involved in the hypoxia response [46, 47], or in the case of HIF-3 α repress the transcriptional response. HIF-1 α is a constitutively expressed protein, whose activity is regulated by the hydroxylation of conserved proline residues. In microenvironments of high oxygen tension (>5%), the proline residues are hydroxylated, tagging the protein for degradation by E3 ubiquitin ligases [48]. When oxygen concentrations are below the tolerable threshold for a given cell type, HIF-1 α is not degraded, and increases in concentration to allow HIF-1 α to induce transcription of its client genes [49].

Nutrient deprivation is another major stressor within the tumor microenvironment. When the cell experiences a critical reduction in a particular nutrient, it must swiftly adjust in order to

maintain productivity in the terms of metabolism, proliferation, migration, or other processes essential to evolutionary success and survival. Two main nutrient sensing proteins implicated in cancer are AMP-activated protein kinase (AMPK) and the mammalian target of rapamycin (mTOR) [50, 51]. These proteins are capable of sensing the current energy status of the cell and nutrient availability, respectively.

The metabolic pathway directed by AMPK is highly context-specific; depending on the nutrient status of the cell. AMPK is responsible for the cellular response to glucose deprivation and acts as a metabolic switch from a highly glycolytic state to an oxidative state depending on the availability of glucose. This is particularly important in the context of cancer and the highly plastic nature of cancer metabolism. AMPK is activated by 5'-AMP, which indicates that the cell is not regenerating ATP at a fast-enough rate to meet demand. This induces the uptake of glucose and the induction of glycolysis to replenish the cellular ATP [50]. The induction of glycolysis via-a-vis respiration is likely due to the promptness with which glycolytic activation can occur [52].

mTOR is present in the form of two different complexes, mTORC1 and mTORC2. These two complexes participate in associated, but distinct signaling pathways in nutrient sensing. mTORC1 becomes activated in response to various growth factors and amino acids that promote cell growth and proliferation. When inactive, mTORC1 represses growth and induces an autophagic response. mTORC2 is a sensor of glucose but also plays a role in amino acid signaling. mTORC2 is activated by acetyl-coenzyme A (Ac-CoA), which is produced in the cytoplasm via citrate lyase, when glycolytic flux is abundant. The result of mTORC2 activation is increased cell proliferation, in response to the increased glucose metabolism. mTORC2 has also been implicated in amino acid sensing by having the ability to suppress the function of the glutamine-cysteine transporter, system Xc transporter-related protein [51].

Aberrant perfusion in the tumor microenvironment allows a significant build-up of metabolites in the tumor interstitial fluid. The main metabolite that is commonly accumulated in the tumor interstitial fluid is lactic acid, which is associated with a decrease in pH. A decrease in extracellular and intracellular pH can dramatically modulate the activities of enzymes, some of which are more sensitive than others, depending on how significant the change in pH is and the isoelectric point of the enzymes optimal activity [53]. These alterations in enzyme activity are pleiotropic and leads to metabolic reprogramming. Lactate in the tumor microenvironment is a by-product of increased glucose fermentation, which occurs even in the presence of oxygen, known as aerobic glycolysis or the Warburg Effect. Once produced, lactate is shuttled out of the cell, stoichiometrically with a proton, by monocarboxylate transporters (MCTs) 1-4. Sensing of extracellular pH is accomplished through a variety of plasma membrane associated proteins including two major classes of acid-sensing receptors: i) G-protein coupled receptors (GPCR) such as Ovarian cancer G protein-coupled receptor 1 (OGR1), G-protein coupled receptor 4 (GPR4), T-cell death-associated gene 8 (TDAG8), and ii) Acid-sensitive ion channels (ASICs) which include 7 proteins from 4 genes: 1a/b, 2a/b, 3, 4, 5, and Ca^{2+} channel that includes transient receptor protein channel vanilloid subfamily 1 and 2 (TRPV1 and TRPV2) [54]. Lactate can also be sensed and regulate cellular functions by activating the G protein-coupled receptors HCA₁/GPR81, HCA₂/GPR109A, and HCA₃/GPR109B. These hydroxy-carboxylic acids (HCA) receptors control physiological homeostasis under changing metabolic and dietary conditions [55].

Cancer cells commonly overexpress many of the aforementioned acid sensors, and this can be correlated to tumor progression and poor outcome [56, 57]. Therefore, investigating these sensors as a factor in malignancy may identify relevant prognostic biomarkers or may reveal new therapeutic vulnerabilities. The sensors can be connected to pathways to activate transcription factors or overexpress other genes and proteins (Figure 2.2). However,

considering the ever-changing state of the microenvironment, we propose that epigenetic regulation may be a more effective factor in stabilization of emerging phenotypes in cancer cells. Adaptation to an acid-microenvironment has been shown to alter cell state by pushing cells into a partial EMT phenotype [58]; this may be a manifestation of these acid sensors inducing a stable epigenetic change.

Heritable epigenetic modifications acquired through microenvironmental sensing

One mechanism enabling cancer cells to adapt is through changes to gene expression via epigenetic regulation. Some modalities of epigenetic regulation are transient (e.g. histone acetylation) and are imposed to help cancer cells survive acute disruptions in their microenvironmental homeostasis. In contrast, other epigenetic mechanisms are more persistent (e.g. DNA methylation) and have the ability to be passed down through generations to endow further generations with memory on how to survive in the tumoral microenvironment.

The term epigenetics was first created by CH Waddington who described it as “the causal interactions between genes and their products, which bring the phenotype into being”. While a commonly agreed upon definition is hard to find today, the term epigenetics in the modern era is commonly described as a permanent change in the way genes are expressed. Types of epigenetic regulation include histone modifications, DNA Methylation, and non-coding RNA [59], which can all impact one another to create a complex regulatory dynamic. A major question is: “How do the external factors of the tumoral microenvironment play into altering this complex dynamic”?

It is commonly known that the epigenetic signatures of cancer cells are different compared to their untransformed counterparts [60-64]. Many of these epigenetic alterations exert their function by altering the metabolism of cancer cells [65], and are acquired by signaling cascades initiated by sensing of the extracellular environment. Some of the signaling cascades

that can lead to changes of epigenetic signatures were implied in the previous section and the specific alterations they are involved in will be discussed herein.

In many solid tumors, intra-ductal hyperplasia leads to significant alterations in the physical microenvironment, especially in peri-luminal cells that are far (>160 microns) from their blood supplies. Importantly, the diffusion distance of oxygen in tissues is 100-200 microns [66], meaning that the periluminal cells of DCIS can be profoundly hypoxic. The depth and duration of hypoxia is dependent on the blood flow of the surrounding stroma. Hypoxia eventually selects for metabolic reprogramming, leading to acidosis, as well as exacerbating nutrient deprivation. Over many years in this environment, these forces (hypoxia, acidity, nutrient deprivation) select for cells with more highly adaptable, aggressive, de-differentiated phenotypes [38, 45]. The resulting acidosis leads to genome instability, which could increase the rate of cancer evolution [67]. The source of cytoplasmic (and nuclear) acidosis is lactate accumulation as a byproduct of glycolysis. Lactate has been shown to have a variety of effects on the epigenetic mechanisms of the cell, some of which are confounding. Direct inhibition of histone deacetylases (HDACs) by lactate has been shown in separate studies [68, 69]; while others have reported multiple times on the increase in activity of the Sirtuin family of histone deacetylases upon exposure of cells to a chronically acidic extracellular environment [70, 71]. These examples represent combined sensing and epigenetic effector mechanisms that act directly on altering the epigenetic status of the cell.

The oxygen sensing protein HIF-1 α can regulate epigenetics in a variety of ways. Upon activation, HIF-1 α leads to downstream signaling cascades important for the survival of cells in low oxygen environments. The ultimate effect of some of these signaling cascades is the epigenetic alteration of gene regulation (Figure 2.2). Two epigenetic mechanisms influenced by HIF-1 α are histone methylation and DNA methylation (Figure 2.2). Unlike other epigenetic mechanisms, histone methylation can act in both activating and repressing fashions depending on the specific location of the covalent modification. The histone demethylase JMJD2B is

activated by HIF-1 α (Figure 2.2), and is specifically targeted to H3K9me2/3 to demethylate the mark to a monomethylated state [72, 73]. The expression of ten-eleven translocation proteins 1/3 (TET1/3) is also upregulated upon stabilization of HIF-1 α . TET1/3 are 5-methylcytosine (5mC) oxidases, which convert 5mC into either 5-hydroxymethylcytosine (5hmC), 5-formylcytosine (5fC), or 5-carboxylcytosine (5caC) via sequential reactions [74]. The result of these reactions is the deactivation of the methylation mark and the subsequent reactivation of the sequence being repressed by the methylation. This has been validated in neuroblastoma where it was shown that HIF-1 α can induce HIF-1 α /hypoxia specific DNA methylation signatures [75]. The fact that HIF-1 α activates DNA methylation supports the hypothesis of inheritable epigenetic changes to next generation that can be tracked in cancer cells. Contrary to the upregulation of TET by hypoxia-induced transcriptional programs, TET proteins have been shown to have their activity reduced directly by low oxygen availability in a tumor setting. TET activity is lost *in vitro* when exposed to hypoxic conditions, possibly via hypermethylation of tumor suppressor promoters in hypoxic regions of tumor samples [76]. The opposing forces of the transcriptional and functional regulation of TET proteins may demonstrate a physiological feedback system for regulating the epigenetic response to oxygen deprivation in order to attenuate the response (Figure 2.2).

The sensing of nutrients by a cell is vitally important to its survival and can have long term effects on the downstream lineage of that cell via epigenetic modifications. Having this feed forward system of epigenetic regulation directed by nutrient signaling allows for increased fitness for subsequent generations. As mentioned previously, cellular nutrient sensing is mainly achieved through 3 essential proteins and protein complexes: AMPK, mTORC1, and mTORC2 (Figure 2.2). AMPK is activated in response to cellular metabolic stress, and modulates gene transcription epigenetically in order to respond to this stress. Unlike the mTORC1/2 complexes, AMPK is able to modulate transcription directly by phosphorylation of Ser³⁶ on histone H2B [77].

This phosphorylation mark directly promotes the transcription of response genes needed to handle metabolic stress. Other papers report the direct phosphorylation of Ser³⁶ on H2B by S6K1 [78], which is also a player in the LKB1-AMPK-mTORC1 signaling axis, with S6K1 being phosphorylated by mTORC1. mTORC1 is another player in the epigenetic response to nutrient sensing. As mentioned previously, mTORC1 is capable of sensing various growth factors and amino acids. A downstream target of mTORC1 nutrient sensing is SIRT4, which is repressed in response to mTORC1 activation [79]. SIRT4 is a lysine deacetylase (Figure 2.3) [80], that has the ability to inhibit glutamine metabolism by inhibiting glutamate dehydrogenase (GDH). This inhibition of SIRT4 is achieved at the transcriptional level by mTORC1 stabilizing the CREB2- β TrCp complex, preventing CREB2 from activating transcription of SIRT4 [79]. mTORC2 exerts its epigenetic function by activation of the AKT and SGK1 proteins. The effect of these proteins on epigenetic regulation is the inhibition of KMT2D, which is a histone methyltransferase specifically targeting H3K4 (Figure 2.3) [81]. Inhibition of KMT2D has been shown to have anti-tumor effects in some cancers by not allowing the FOXA1-PBX-ER complex to access the DNA for transcription [82].

While the aforementioned mechanisms involve the sensing of nutrients to transduce downstream epigenetic changes, alterations in acetate level can directly influence the epigenetic status of the cell. Free Acetyl-CoA in the cell nucleus is produced by Acetyl-CoA synthetase (ACSS2), which catalyzes the conversion from Acetate, and by ATP-citrate lyase (ACLY) which catalyzes the conversion from citrate. The levels of free Acetyl-CoA directly influence the global acetylation status of histones [83], and henceforth have the ability to regulate epigenetics without the direct manipulation of an enzyme intermediate. While there is no direct sensing mechanism, this level of regulation could be seen as a sensor of the glycolytic state of the cell considering it has been shown that decreasing the amount of glucose available to a cell reduces the Acetyl-CoA abundance and lowers global histone acetylation [84].

A recently described mechanism of both environmental sensing and epigenetic modification is that of histone lactylation. In 2019, Zhang et al. described for the first time the modification of histones by lactate [85]. As is commonly known, lactate is built-up as a byproduct of glycolysis. This epigenetic modification may provide a direct mechanism for the regulation of gene expression in response to fermentative glycolytic activity of the cell.

Effect of heritable epigenetic modifications on tumor metabolism

Many epigenetic alterations that are acquired throughout tumor progression alter the metabolism of the tumor's cellular population. While the previous section covered specific epigenetic alterations that occur in response to the metabolic microenvironment, this section will describe the role of epigenetic modifications in altering cancer cell metabolism.

Lactate itself has the ability to alter the activity of epigenetic modifier proteins. The inhibition of HDAC's by lactate demonstrated in previous studies [68, 69] has yet to be phenotypically implicated in the alteration of metabolic processes; yet it is likely this lactate-mediated mechanism will play a role in altering metabolism. The activation of SIRT1 by extracellular acidosis, which is a consequence of acid-inhibition of glycolysis and the subsequent build-up of NAD⁺, has been shown to alter cellular metabolism through histone deacetylation leading to increased transcription of HIF-2 α . This SIRT1/HIF-2 α axis promotes the oxidative metabolism of glutamine, and suppresses the effects of HIF-1 α , inhibiting hypoxia mediated induction of glycolysis [70]. Corbet et al. in a later study showed that SIRT1 as well as SIRT6 are essential for histone deacetylation and the induction of fatty acid metabolism when cells are chronically exposed to an acidic extracellular environment [71]. From a cell survival standpoint, this switch to other methods of energy metabolism when lactate has accumulated is intuitive, and has relevancy in the context of cancer progression that is discussed later.

In response to hypoxia, HIF-1 α activation leads to the induction of JMJD2B activity. JMJD2B has been shown to be upregulated in ER-positive breast cancer [86] and bladder cancer [87], and its upregulation has been directly linked to induction by HIF-1 α in colorectal cancer [88] and gastric cancer [89]. This activation of JMJD2B directly drives the demethylation of H3K9me2/3 to its monomethylated state (Figure 2.3). JMJD2B has been shown to play a role in altering the expression of many cancer associated genes including cyclin-dependent kinase 6 (CDK6) [87], and carbonic anhydrase 9 (CA9) [88], which can directly affect the transmembrane pH gradient. Also induced by hypoxia and HIF-1 α activation are the expression of TET proteins 1 and 3 [74]. As mentioned previously, TET proteins are 5mC oxidases that allow for the expression of genes repressed by DNA methylation. Induction of TET in neuroblastoma has been shown to increase transcription of hypoxia response gene [90], and TET1 has been shown to be overexpressed in triple negative breast cancer (TNBC) where it is associated with hypomethylation (Figure 2.3) [91]. Hypomethylation increases the expression of associated genes such as Hexokinase II (HK2) in liver cancer [92] and glioblastoma multiforme [93]. Hexokinase II catalyzes the conversion of glucose to glucose-6-phosphate, an essential step in glycolysis. While CA9 and HK2 are both direct transcriptional targets of the HIF-1 α mediated hypoxic response, this epigenetic regulation is important because it imposes the upregulation of these proteins over longer time scales and allows for the maintenance of the metabolic phenotype independently of oxygen status.

Epigenetic marks induced by nutrient sensing proteins and complexes have the ability to greatly alter cellular metabolism, making a useful feed-forward mechanism for acclimation and adaptation to the current metabolic microenvironment. The phosphorylation of Ser³⁶ on Histone 2B is a significant epigenetic mark made by two proteins involved in nutrient sensing: AMPK and S6K1 [77, 78]. It has been shown that phosphorylation of Ser³⁶ on Histone 2B is significantly increased upon treatment of cells with 2-Deoxy Glucose [77], which mimics a

glucose deprived environment. The resulting effect on the cellular transcription from phosphorylation of Ser³⁶ on Histone 2B by AMPK is the recruitment of EZH2 [78]. EZH2 is a histone methyltransferase that trimethylates Lysine 27 on histone 3 when recruited. It has been shown in *Drosophila* that trimethylation of Lysine 27 on histone 3 reduces the glycolytic tendencies of the cell [94]. Considering the presence of this mark in glucose-deprived cellular states, it would intuitively make sense that the presence of this mark would decrease the glycolytic capacity of the cell.

The suppression of SIRT4 by mTORC1 has profound effects on the metabolism of cancer cells, specifically inhibiting glutamine metabolism through inhibition of GDH. In colorectal cancer, decreased SIRT4 expression has been correlated with progression and increased invasive potential of cancer cells [95], and in both colorectal and gastric cancers lower SIRT4 expression is associated with poor prognosis [95, 96]. All in all, this leads to the conclusion that when in the presence of sufficient amino acids and growth factors, the activation of mTORC1 will lead to the inhibition of SIRT4 and the subsequent reactivation of glutamine metabolism which can promote tumor growth (Figure 2.3).

mTORC2 has the ability to modulate activity of KMT2D. KMT2D is inhibited downstream during mTORC2 activation, which in response, inhibits the access of the FOXA1-PBX1-ER complex from binding the DNA. Prevention of this complex from binding the DNA has been shown to reduce the expression of key proteins including: GREB1, SERPINA1, cFOS, and MYC [97]. Of these proteins, MYC has been shown to have the most substantial effects on reprogramming cancer metabolism in a type-specific manner. A comprehensive list of metabolic alterations in specific cancer types driven by MYC has recently been reviewed [98]. The effect MYC has on glycolysis is highly variable depending on the cancer type, with a MYC-associated increase in non-small cell lung cancer and hepatocellular carcinoma, and a MYC associated decrease in renal cell carcinoma and prostatic intraepithelial neoplasia. MYC's effect on

glutaminolysis was cohesive in the various cancer types, with an associated increase demonstrated in hepatocellular carcinoma, pancreatic ductal adenocarcinoma, and renal cell carcinoma.

In addition to the previously mentioned alterations in gene expression caused by stimulus-induced epigenetic modifications, epigenetic upregulation of MCT4 via hypomethylation of the SLC16A3 promoter has been shown in renal cancers [99]. Although no specific mechanism can be tied to this alteration, this increase in MCT4 expression will have profound consequences on the long-term progression and evolution of the tumor.

Consequences of epigenetically altered metabolism on tumor progression

As described previously, a resulting consequence of oxygen deprivation and stabilization of HIF-1 α is the induction of TET1/3 and hypomethylation of the genome. Hypomethylation has been shown to upregulate the expression of Hexokinase 2 [92, 93], which is associated with an increase in glycolysis (Figure 2.4). Increased glycolysis will increase acidosis in the tumor microenvironment that can induce extracellular matrix remodeling [54]. Thus increased glycolysis and its sequelae are barriers that cancer cells must overcome in order to meet the energy demands of rapid proliferation and to survive and thrive in a more hostile environment. Altered glycolysis can also lead to Warburg phenotype leading to even more acidic microenvironment and more altered genome and epigenome alteration [38, 100].

Despite the differing sensing mechanisms of the mTORC1/mTORC2 complexes and SIRT1, all mechanisms converge on a single metabolic alteration caused by epigenetic modification: the increase of glutamine metabolism. This may pose the opportunity to target glutamine metabolism as a cancer therapeutic, an idea that has drawn enough attention to warrant various reviews on that subject alone [101, 102]. Although this may seem like a rational therapeutic target, cautionary narratives have been proposed as to the possible outcome of

creating a resistant cellular population with a heightened metabolic capacity [103]. While glutamine metabolism is non-essential in a normally proliferating cell, under periods of rapid proliferation, like tumor growth, glutaminolysis is an essential process [104]. This phenotype is selected for due to the high demand for metabolic building blocks produced from the TCA cycle. In the TCA cycle alpha-ketoglutarate can be carboxylated to citrate, which, if in abundance, is translocated to the cytoplasm where it is used for fatty acid synthesis. The end product of glutaminolysis is alpha-ketoglutarate, which is shunted into the TCA cycle to accelerate the process [105]. Supporting the TCA cycle with the necessary building blocks will give more chance to glucose to be turned into lactate in glycolysis and augment a Warburg phenotype. Glutamine-fed TCA cycle can also give more freedom to cancer cells to use glycolysis for their fluctuating ATP demand as a quick local source of energy for cancer cells [52].

HETEROGENEITY OF METABOLIC PHENOTYPES IN BREAST CANCER

This section comes from a soon to be published review paper written by, myself, Bruna Victorasso Jardim-Perassi, Enakshi Sunassee, and Nimmi Ramanujam. I was involved in developing the idea for the paper, I directed all writing for the manuscript, and I contributed to writing the manuscript.

While fermentative glycolysis is the main highway for the carbon metabolism in a breast tumor, the spatial heterogeneity within a breast tumor could lead to a variety of metabolic phenotypes, and it is well characterized that TNBC tumors are phenotypically diverse with respect to their markers of metabolism [106]. In a previous review we outlined how this process may be carried out through feedback between the environment and epigenetic regulation [39]. Access to vasculature is one of the main determinants for how a cell will decide to carry out its metabolic processes. Vasculature allows for an exchange of metabolic resources and products between the cancer cell population and the body at large [38]. Deprived of this exchange, cells deep in the tumoral lumen must adapt strategies to survive. There are two possible strategies

for how a cell might go about surviving in this environment. Strategy one requires that a cell become highly efficient in scavenging glucose from the microenvironment and become resistant to the toxic inhibitory effects of the by-products of glycolytic metabolism. This strategy is exemplified by the triple-negative breast cancer (TNBC) cell line, MDA-MB-231, with its lowly oxidative and highly glycolytic phenotype. It is also important to note, that in order for this strategy to be successful there must be a non-zero amount of glucose present. Strategy two is one in which the cells take a back-seat, and rely on fuel stores within the cell, entering into a quiescent state [107]. In an environment of high cell turnover, the former, more metabolic strategy may prevail in producing more of a cell's lineage. In the case of ample vasculature access, it may be the case that a more oxidative metabolic phenotype is favored over a glycolytic phenotype due to the increased access to oxygen. In reality, the dynamic nature of the tumor microenvironment places cells in both perfused, oxygenated environments as well as, desolate nutrient-deprived environments. The ideal solution for this scenario is a plastic metabolic phenotype that allows cells to utilize both glycolytic and oxidative avenues of energy production. Work done in yeast suggests this "best of both worlds" phenotype may not exist, due to what is known in evolution as a pareto front. A pareto front is the dividing line of a restricted trait space the likes of which an organism cannot access. It was demonstrated in yeast, that the maximal of both fermentative and respiratory phenotypes was inaccessible [108].

FIGURES

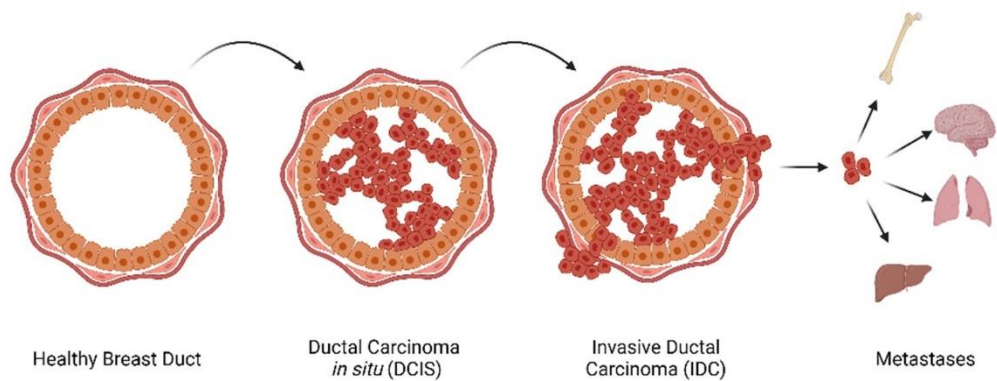


Figure 2.1. Phases of Breast Cancer Progression.

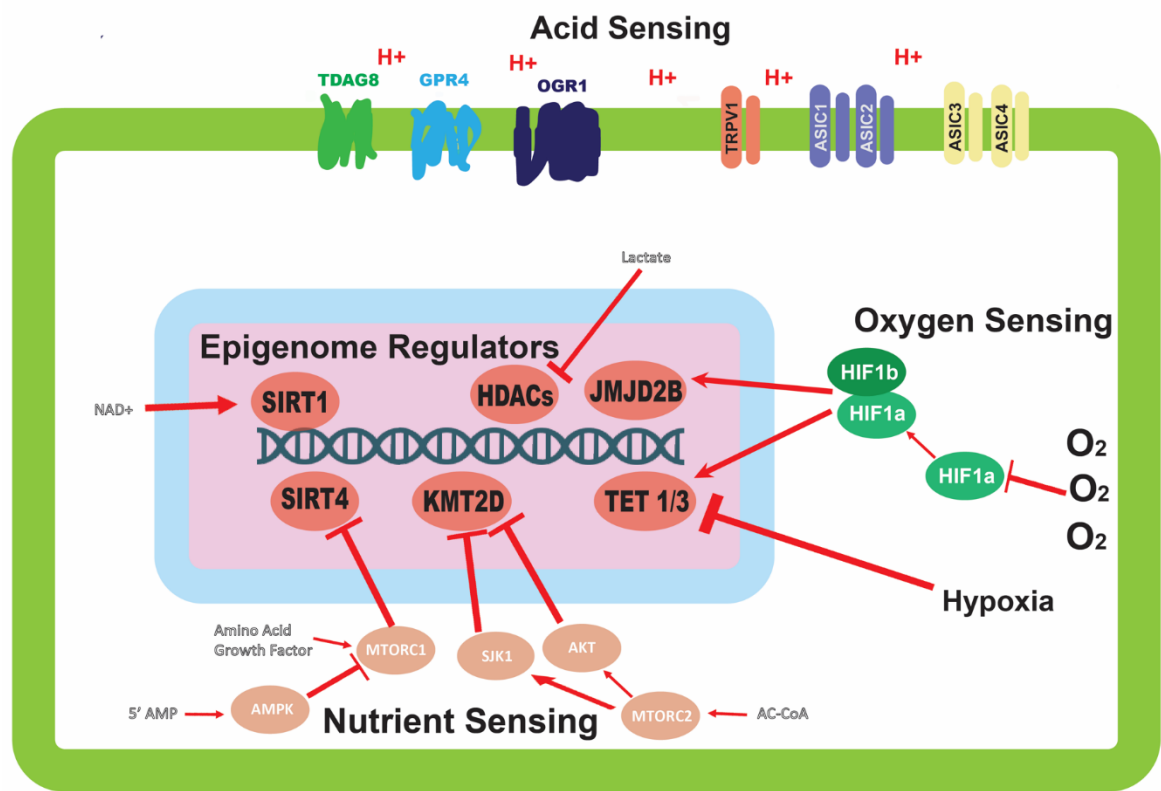


Figure 2.2. Mechanisms of environmental sensing and their effects on epigenetic modifiers. This figure depicts the various avenues by which cells are able to detect perturbations in the environment, and the downstream effects of this sensing on epigenetic modifiers. Oxygen sensing mechanisms trigger dimerization of HIF-1α and HIF-1β proteins to affect epigenetic modifiers; oxygen also direct modulates activity of epigenetic modifiers. Nutrient sensing can initiate a signaling cascade, largely mediated by the mTORC complexes and AMPK protein, with the ability to alter the activity of epigenetic modifying proteins. Acid sensing proteins located

on the outer membrane of the cell are able to sense the extracellular pH, but have no clear mechanism for altering the activity of epigenetic modifiers.

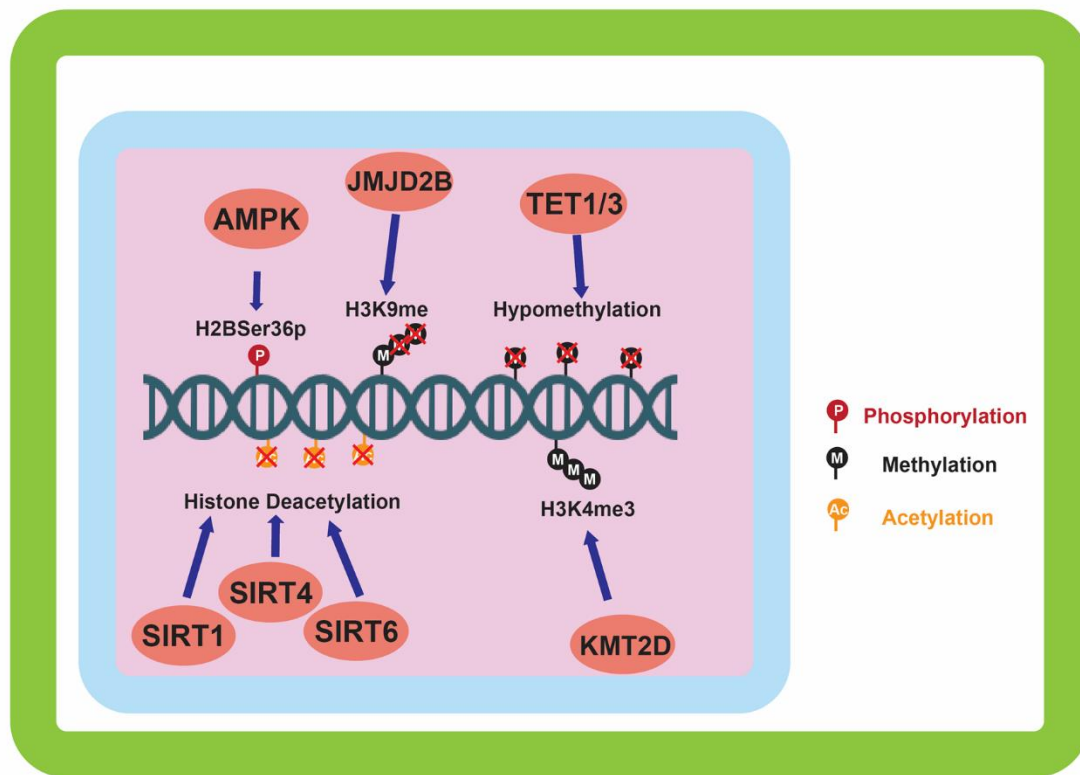


Figure 2.3. Epigenetic alterations mediated by environmentally induced epigenetic modifiers. The epigenetic modifiers altered by the sensing of the cellular environment go on to carry out a variety of modifications to the epigenome. DNA methylation, and histone methylation and acetylation are the main downstream targets of the environmental sensing. Phosphorylation of histones by AMPK is also carried out in response to environmental sensing.

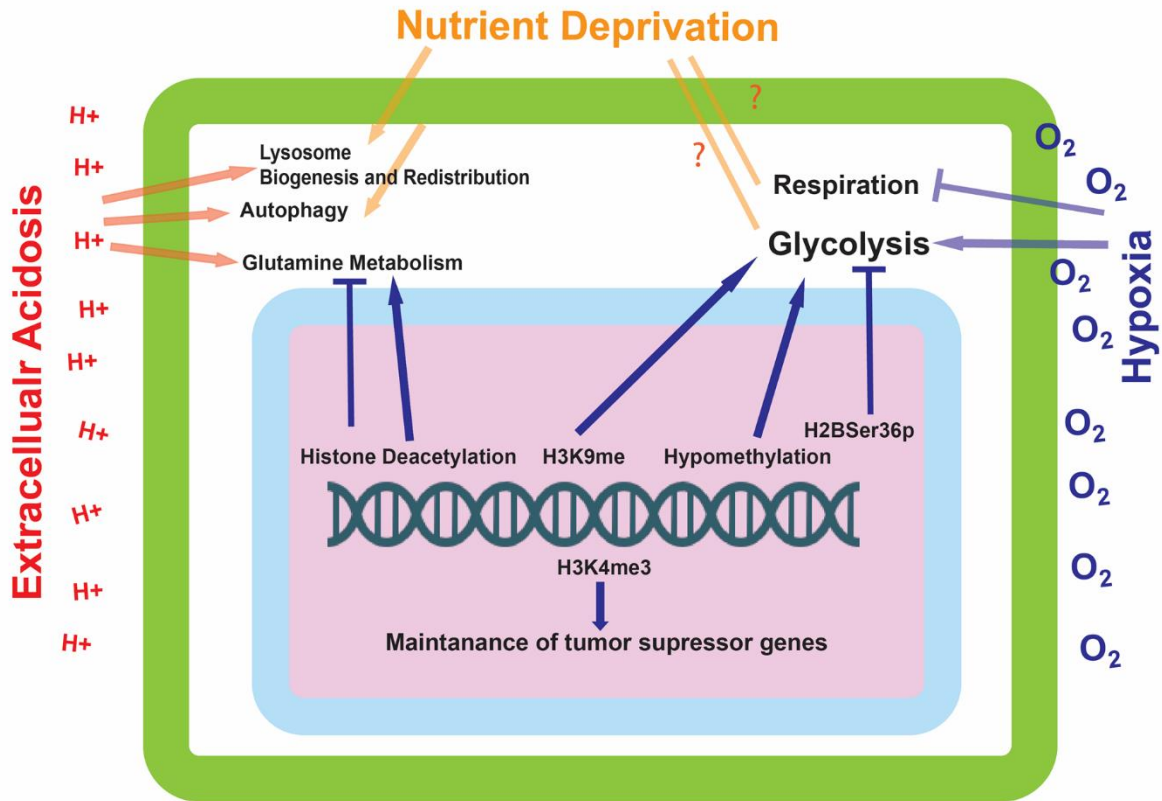


Figure 2.4. The effect of environmentally induced epigenetic modifications on tumor cell expression and metabolism. The epigenetic modifications made by the proteins influenced by the environmental sensing mechanisms go on to alter the metabolic state of the cell. These modifications can alter the cells ability to metabolize glutamine and carry out glycolysis, as well as influence the transcriptional status of tumor suppressor genes.

Chapter 3: Breast cancer adaptation to acidic microenvironment induces a partial epithelial to mesenchymal transition state

This work is adapted from the previous publication listed below. Mehdi Sadeghi, from Semnan University in Iran, completed and supervised the bioinformatics analysis in this work. All aspects of the biological study were completed or supervised by our team. We published our findings in *Frontiers in Oncology* [58].

INTRODUCTION

The principal driver of evolutionary processes is the concept of survival of the fittest. Those given populations that are the most well adapted to survive in an environment are the ones that will persist. In higher order organisms, the surviving populations are those that have a set of static traits that make them successful in a given environment. At a cellular selection level, organisms have the ability to acclimate to a given environment and alter their phenotype to be more successful in surviving. This ability to alter phenotype in order to acclimate to a given environment is particularly important in the context of cancer cell survival. In order for a cancerous cell population to persist, it must be able to adapt and evolve to maintain its' fitness within a given tumoral environment [109-111]. Those cellular populations with the ability to more rapidly and efficiently adapt to the environment will have an advantage over the other cell populations when facing the challenges of a new or changing environment [112]. Epithelial to mesenchymal transition (EMT) is one of the phenotypic switches that promote cancer progression, invasion and metastasis. EMT tests a cancer cells ability to efficiently change cellular states in response to changing conditions, also denoted as cellular plasticity, which also often referred to in the cancer stem cell model [113, 114]. Although denoted as a transition, It

has been recently observed that the EMT process is non-binary and occurs on a spectrum of transition states that can have the characteristics of both epithelial and mesenchymal phenotypes [115, 116]. The transition to one of the intermediate states between epithelial and mesenchymal phenotype has been denoted partial EMT (pEMT), with cells expressing both markers of epithelial and mesenchymal cell status. pEMT states compared to complete EMT carry different migratory patterns during cancer metastasis [117, 118], and demonstrate the elevated plasticity of their epithelial progenitors [116]. Another cause of EMT can be functional heterogeneity of cancer cells that is the result of genetic and epigenetic makeup as well as their interactions with the microenvironment. It has been recently shown that phenotypic heterogeneity is a dynamic reversible state of highly plastic cancer cells and their response to microenvironmental changes in GBM [119]. Lately, there have been proposals for a strong connection between tumor plasticity and recreating intra-tumoral phenotypic heterogeneity [120] and also emphasizing the role of microenvironment in shaping spatial and temporal heterogeneity [121]. It looks like the relationship between tumor cell plasticity, and intra-tumoral heterogeneity with emerging new phenotypes such as EMT or pEMT in everchanging cancer microenvironments is getting more attention and will be new area of research. It has been shown that growth factors, such as epidermal growth factor (EGF), transforming growth factor- β (TGF- β), and basic fibroblast growth factor (bFGF/FGF2) are also able to induce EMT [122, 123]. It has also recently reported that tumor microenvironment conditions such as hypoxia and acidosis can induce EMT [124, 125].

Adenocarcinomas initiate and evolve within the hostile microenvironment of avascular ducts, which are characterized by acidosis, hypoxia, reactive oxygen species (ROS), and nutrient deprivation [42, 126]. In particular, the acidic microenvironment of tumors strongly influences cancer progression and evolution. We have proposed that chronic acidosis induces genomic instability and selects for emergence of aggressive clones, leading to genomic diversity

and increased tumor heterogeneity [127-131], a proximal cause of malignancy and resistance [132]. Specifically, the acidified habitat imparts a Darwinian selection pressure that favors cells that adapt mechanisms to resist acid-mediated cell death. Further, the acidic microenvironment is also manifested in locally invasive cancers where it confers cancer cells a selective advantage over the stromal cells, leading them to invade to surrounding stroma. Indeed, an acidic microenvironment stimulates invasion and metastasis and also promotes remodeling of the extracellular matrix (ECM) [19, 20, 45, 54, 133]. Further, acidosis promotes angiogenesis via the release of VEGF [134](31) and impairs immune surveillance [135, 136]. Acid adaptation also pushes cancer cells toward a more aggressive phenotype through lysosomal redistribution [137] and plays a major role in subpopulation formation and evolution of solid tumors.

Integrative analysis has received a lot of attention lately in biology and cancer biology specifically, due to its nature of inter-validating data in different levels of biology such as genome, transcriptome, proteome, and metabolome [138]. Different data integration approaches can help to combine various high throughput omics data to construct an integrative regulatory network. These networks can help to understand the molecular basis of carcinogenesis and provide a powerful framework for exploring new cancer biomarkers [139, 140]. With the advancements in network inference and construction methods, network analysis, and interpretation approaches it is feasible now to explore authentic and accurate molecular signatures. Another advantage of such analysis is discovery of groups of co-regulated molecules as a sub-network biomarker for treatment, diagnosis or prognosis applications.

Expression profiling is a major key to unraveling gene expression patterns and the transcriptome. RNA sequencing is a next-generation sequencing (NGS) technology that sequences cDNA in order to provide accurate measurement of transcripts levels to define biological networks [141]. Networks are the language of complex systems like biological systems. Biological networks are used widely to model biological interactions at the molecular

level to understand biological processes particularly in the case of cancer [142]. To assess biological networks different techniques have been developed; centrality analysis is one of them [143, 144]. Centrality analysis ranks the nodes (genes in gene regulatory networks) based on their significance. In centrality analysis, adding topological parameters to biological data leads to sufficiently informative results that have been shown to be effective in exploring key signature molecules in biological processes [145]. Such biological network analysis has been used in cancer biomarker discovery [146].

Here in, we studied the effect of acid adaptation on early stage breast cancer evolution using the MCF7 cancer cell line. We studied EMT phenotypic switches as regulators of acid adaptation using RNA sequencing data and gene regulatory network analysis and by integrating the results to SILAC proteomics data. For that reason, we compared acid-adapted MCF7 breast cancer cell line RNA profile to parental MCF7 cells. The differentially expressed genes in the acid-adapted cells were used to construct a gene regulatory network. This network was implemented to explore sub-network biomarkers related to EMT by a set of robust criteria. We then compared our findings with the SILAC proteomics results and found S100 family proteins such as S100A6 and S100B are abundant in both sets of omics data. I validated both S100B from RNA sequencing and S100A6 from proteomics data, by Immunocytochemistry (ICC). I furthered our validation using IHC of breast cancer patient TMAs with 160 biopsy cores. S100A6 expression was compared to LAMP2b as a biomarker of acidosis in solid tumors, and each core's LAMP2b expression was co-registered with S100A6 expression using Definiens tissue studio software analysis. The TMA co-registration analysis showed correlation of S100A6 with LAMP2b expression the most in early breast cancer stage, ductal carcinoma in situ, DCIS. Survival analysis of patients with different expression of S100A6 revealed correlation of high S100A6 expression with worse outcome in survival of breast cancer patients. When taken in total, I conclude that amongst many paths of EMT, S100 proteins may play critical roles in acid-

induced EMT that can be responsible for cancer progression and survival of cancer cells in their continuously changing microenvironments.

RESULTS

RNA sequencing of acid-adapted and non-adapted MCF7 cells unravels the EMT mechanism of breast cancer cells

In order to study the effects of acidosis on EMT of breast cancer cells at early stages such as ductal carcinoma in situ (DCIS) I first probed the effect of chronic acid adaptation on EMT status of MCF7 breast cancer cell line using quantitative reverse transcription-polymerase chain reaction (qRT-PCR) (Figure 3.1A) and Immunofluorescent (IF) (Figure 3.1B) techniques. Acid adaptation showed some of the epithelial to mesenchymal phenotypes such as high expression of Vimentin or loss of membrane β -catenin and ZO-1 and didn't show some other's such as loss of E-Cadherins (Figures 3.1A,B). So, I concluded acid adaptation is a path to complete EMT and the status observed can be explained as partial EMT induced by acid adaptation that can be completed by further adaptation to acid or other microenvironmental conditions (Figures 3.1A,B). The partial EMT is reported in other publications and referred as a measure of plasticity [116, 118]. Then we carried out sequencing of RNA on a paired sample of MCF7 cells and its acid-adapted counterpart. MCF7 cells are ER, PR, and HER2 positive with many phenotypes of early neoplastic cells such as slow metabolism, and low rate of glycolysis and Warburg phenotype that makes them a proper model of studying acidosis at early stages of breast cancer [20, 53]. They are also tumorigenic but not metastatic i.e., injection of MCF7 into immunodeficient mice will result in tumor growth but not metastasis. For RNA extraction we used acid-adapted and non-adapted MCF7 (parental) at the same passage number with similar growth rate at the time of experiment. Our collaborators identified 1,928 differentially expressed genes in acid-adapted MCF7 cells compared to non-adapted MCF7 (Supplementary Table 1). Using STRING database, a regulatory interaction network based on experimentally validated

interactions was plotted. The constructed network was replotted in Cytoscape software for better visualization (Figure 3.2). Then we searched for EMT related markers in the RNA sequencing data and found that acid adapted cells show some of epithelial markers and some of the mesenchymal markers validating the partial EMT statues of acid adapted cells (Figure 3.1C).

To obtain an interaction network, an effort to unravel the regulatory core related to EMT under the influence of acidosis was made through identifying and ranking 3-node and 3-edge motifs (Figure 3.3A). To this end, $n = 3,320$ three member motifs were identified in the network using Cytoscape NetMatchStar plugin. In order to take the significance of motifs in cellular EMT into account, GOBO terms related to EMT were explored. Then for motif ranking scheme a factor was considered for each motif based on the membership of its genes in these terms. In order to place more emphasis on EMT Cytoscape GPEC plugin was used for gene prioritization based on explored GOBP terms. It works based on a random walk with restart algorithm. GPEC helps to rank genes based on their association with specific diseases or biological pathways (EMT in our case) The obtained scores were considered as another weight in scoring function [147]. The log fold change, node degree and betweenness centrality were used in the scoring function as well. Using these factors in the scoring function the explored motifs were prioritized and ranked. The top 10 ranking motifs (Figure 3.3B) were selected for enrichment analysis toward EMT and acid adaptation. These motifs consist of 19 unique genes. Merging of these top ranked motifs leads to construct the underlying core subnetwork of the genes that were affected by acidosis and are related to EMT, differentiation and invasion of the tumor cells (Figure 3.3C).

Integrative analysis of transcriptomics and proteomics of acid-adapted and non-adapted MCF7 cells reveals the role of S100 proteins in acid-induced epithelial to mesenchymal transition

For further validation of our findings in RNA sequencing and EMT related motif analysis at the protein level, we compared all the genes in the EMT motifs with their relative protein

change in our SILAC discovery proteomics of the MCF7 cell line published previously [20] as well as the MCF-DCIS (DCIS) cell line which we conducted SILAC proteomics on for this study. Since the focus of this study is on early adaption of breast cancer cells we selected DCIS cell lines and adapted them to acid for 3–6 months in the same process as the MCF7 cells. The SILAC proteomics approach was applied to compare the whole proteome of acid-adapted cancer cells to non-adapted counterparts. SILAC or stable isotope-labeled amino acids in cell culture is a quantitative mass spectrometry (MS) based technique that is used to compare the proteome of pairs of biological samples [148] which in our case is acid-adapted and acid-naive breast cancer cell lines. To minimize the rate of false-positive biomarker association, parallel SILAC experiments were conducted for each cell lines in which the acid-adapted or non-adapted cells were labeled by growing them in SILAC “heavy” media ($^{13}\text{C}_6$ lysine and $^{13}\text{C}_{14}\text{N}_4$ arginine), while the comparator cells (acid-naive or acid-adapted cells, respectively) were cultured in media containing the corresponding amino acids of naturally occurring isotopic distribution. The labeling strategy was reversed (flipped) to eliminate potential bias due to the media and incorporation of the stable isotope-labeled amino acids (Figure 3.4A) [149]. MCF7 data was previously published for biomarker discovery of acid adaptation [20]. In DCIS SILAC proteomics, 2,841 proteins were detected with 466 unique proteins for acid-adapted DCIS cells and 323 unique proteins for non-adapted ones (Figures 3.4B,C and 3.5). We used fold change to plot our data and used 1.5-fold change cut off (Figure 3.4C). The same analysis and cut off was applied for both DCIS and MCF7 cells. To do integrative analysis, we looked for any proteins related to the five explored motif packs isolated from RNA sequencing data (Figure 3.3C) in both MCF7 and DCIS proteomics with more than 1.5 ratio change in acid-adapted vs. non-adapted condition (Figure 3.4C). In order to perform integrative proteomics and transcriptomics data analysis we focused on 10 explored motifs based on motif ranking analysis (Figure 3.3C). This analysis has been conducted to ensure consistency of proteomics and transcriptomics data. Translational pattern of 19 differentially expressed genes were assessed

in MCF7 and DCIS proteomics data. We plotted the interactome map for these altered proteins that were identified through integration of transcriptome and proteome data (Figure 3.4D). In this figure nodes in rectangular shape have both gene expression and protein translation alteration and oval nodes only present alterations in transcriptomics level. Ten proteins out of 19 discovered genes had more than 1.5-fold change in MCF7 and DCIS proteomics data (Figure 3.4E). Among these genes the ones presented in Figure 3F are differentially expressed at the proteomics level in the DCIS and MCF7 cell lines (Figure 3.4F). Due to abundance of the S100 family proteins in both transcriptomics and proteomics data, this motif pack was chosen for further experimental validation.

Acid-adapted MCF7 cells express higher S100A6 and S100B proteins

To further validate the S100 motif discovered in both RNA sequencing and proteomics data in acid-adapted EMT analysis, I performed Immunocytochemistry (ICC) experiments on the acid-adapted and non-adapted MCF7 cells. We chose S100A6 and S100B from the family because of over expression of S100A6 at the protein level in both MCF7 and DCIS cells and S100B as one marker discovered in RNA sequencing of MCF7 cells and the proteomics of DCIS. To do the experiment, both AA MCF7 and NA MCF7 were seeded on the one slide with eight chambers on it and were treated with exactly equal amounts of antibodies. Slides were imaged using a Leica TCS SP5 confocal microscope with exact settings for both cells, and samples were imaged the same day. I found higher expression of both S100B and S100A6 in acid-adapted MCF7 cells (Figures 3.6A,B). To confirm the acid adaptation status of the cells, I also stained the acid-adapted MCF7 cells and the non-adapted MCF7 cells with the known marker of acid adaptation, LAMP2b. I observed membrane localization of LAMP2b in the acid-adapted MCF7 cells (Figure 3.6C), which is characteristic of acid-adapted cell populations.

S100A6 expression correlates with survival in breast cancer patients

We then sought to clinically validate the identified S100 proteins expression in breast cancer patient Tissue Micro Arrays (TMA) that we have available at the Moffitt Cancer Center tissue core bank. On the basis of our previous findings, we hypothesized that an acidity biomarker should have two characteristics. First, due to the increase in glycolytic rate with breast cancer progression, there should be an association of progression with marker of acidity and second, the expression of the proteins should correlate somehow with the expression pattern of LAMP2b as it is a known marker of acidosis [20, 137]. In short, S100A6 and S100B proteins should increase with stage similar to LAMP2b. To test this, I analyzed protein expression of S100A6 and S100B via IHC of TMAs containing patient sample biopsies from different stages of breast cancer totaling 160 cores. While the protein expression of S100A6 showed statistically ($P < 0.0001$) higher in tumor samples compared with adjacent normal breast there was no difference for S100B. The negative results of S100B could be the cause of problems with antigen specificity or epitopes that were used. I then continued my analysis with S100A6 by measuring the positivity of each core in different stages of breast cancer. Increased S100A6 expression correlates with increased tumor progression from DCIS to invasive ductal carcinoma (Figure 3.7A). There were notably significant differences between normal breast and DCIS, Invasive Ductal Carcinomas (IDCs), and IDCs with local metastases indicating the role of this protein in cancer progression and invasiveness. I then compared the survival of patients with high and low expression of S100A6 for each biopsy cores in three categories of DCIS, IDC and IDC with local metastasis. For defining high vs. low expression, we use the median of all the cores in each category as middle point and anything below the media was taken as low and vice versa. The data was analyzed using two testing methods: Mantel-Cox and Gehan-Greslow-Willcoxon. The DCIS category showed significant difference between low and high expression (Figure 3.7B), which confirms our previous studies of DCIS as the most acidic tumors in breast

cancer. The difference wasn't significant for survival of patients with breast cancer at IDC, and IDC with local invasion stages, implying the importance of acidosis and acid related phenotype at early stages of cancer again (Figure 3.8).

To further prove the correlation of S100A6 and acidosis we compared the positivity of LAMP2b as a marker of acidosis and S100A6 as our candidate, for each biopsy core in our TMA. Comparative analysis of S100A6 positivity from each biopsy core to LAMP2b expression of the same core showed a correlation between these two proteins (Figures 3.7C,D) validating the role of S100A6 in acid adaptation.

DISCUSSION

Deregulated energetics is a hallmark of cancer progression, and the deregulation of cellular energetics has a profound effect on the growth and progression of a tumor. The creation of an acidic tumor microenvironment (TME) is one of these major consequences of deregulated cancer cell energetics. When faced with the acidic TME the cancer cell population must either adapt or perish, with the former being the usual outcome due to the extraordinary ability of cancerous cell populations to adapt to a changing environment. This adaptation to an acidic TME is not a passive action and leads to permanent changes in the phenotype of the surviving population. Little is known about the phenotypic changes that occur throughout the arduous task of adapting to the acidic TME, and deeper insight into these changes will move us a step in the direction of targeting these aggressive populations therapeutically.

Although the concept of lower pH in the tumor microenvironment is not a new discovery, the specific studying of acid-adapted cancer cell phenotypic switch is a relatively new realm of science. Previous investigations have found numerous phenotypic changes that occur during cancer cell populations adapting to an acidic environment such as, chronic autophagy [150], increased presence of lysosomal proteins in the plasma membrane [20], and heightened

aggressiveness [137]. Acidity in the intratumoral environment, not associated with acid adaptation, has also been shown to foster the stemness of cancer cell populations in osteosarcoma [151].

The aim of this study was to understand the role of acidic microenvironment in the EMT phenotypic switch, a demonstration of cancer plasticity and heterogeneity of cancer cell populations, and study their role in patient survival. We used a unique approach to identify vital regulatory sub-networks that are involved in the acid adaptation of cancer cell populations using integrative analysis of transcriptomic and proteomic data of selected cancer cells under an acid microenvironment that mimics one of the harsh selection pressures amongst many in solid breast tumors. The advantage of our approach is that our network analysis workflow encompasses different layers of information such as log fold change in cells, involvement of genes in partial and complete EMT processes and network centrality parameters which reflects gene regulatory role in the whole network. These considerations led to isolation of the motifs that may play a critical role in cancer cells' acid adaptation and pEMT. The discovered motifs also have significant regulatory function throughout the network from a structural perspective. Network centrality parameters were considered as a unique factor to weighting nodes. Log fold changes of motif genes were another parameter to rank motifs. Therefore, we have four parameters to rank the motifs: direct association of motif in EMT, motif prioritization score which is based on Cytoscape GPEC plugin and reflect indirect association of motif in EMT, centrality of the gene within the network, and expression behavior of motif in acidosis. When taken in total, these four parameters return the important motifs within the system.

Here in, we demonstrated the correlation of cancer cells acid adaptation, EMT and patient's survival, based on EMT associated markers. My findings demonstrated a partial EMT phenotype in the acid-adapted cellular populations by correlation to EMT markers accepted in the field. This partial transition may represent a heightened degree of plasticity or metastatic

ability, with cells carrying phenotypic characteristics of both epithelial and mesenchymal cells. I observed downregulation of Snai1 in the acid-adapted group, which negatively correlates with E-cadherin expression, and is not typical of a traditional EMT switch. While this was not typical of the EMT response, we did observe EMT characteristics with heightened vimentin and N-cadherin expression. Due to the observed changes in EMT markers caused by acute acidosis and acid adaptation, we believe the acid adaptation may target specific pathways in the EMT process, while neglecting others. I also proposed the importance of S100 family proteins in the acid-adapted EMT phenotype, no matter if causal or consequential of the phenotype. These findings may be used for therapeutic advances targeting the link between acidosis and EMT, while also providing a better understanding of the protein players that are associated with the ability of a cell to adapt to chronic acidic conditions.

METHODS

Cell Culture and Acid Adaptation in vitro

MCF7 cells were acquired from American Type Culture Collection (ATCC, Manassas, VA, 2007–2010) and were grown in DMEM-F12 (Life Technologies) with 10% fetal bovine serum (HyClone Laboratories) and 1% penicillin/streptomycin added. Growth medium was buffered with 25 mmol l⁻¹ each of PIPES and HEPES and the pH adjusted to 7.4 or 6.5. Cells were tested for mycoplasma contamination and authenticated using short tandem repeat DNA typing according to ATCC's. To achieve acid adaptation, cells were chronically cultured and passaged directly in pH 6.5 medium for ~2 months. Chronic low-pH-adapted cells underwent at least 20 passages.

RNA Sequencing

RNA sequencing was performed on MCF7 and acid-adapted MCF7 cells using the NuGen Ovation Encore Complete RNAseq kit, which generates strand-specific total RNAseq

libraries (Nugen, Inc., San Carlos, CA). Following quality control screening on the NanoDrop to assess 260/230 and 260/280 ratios, the samples were screened on the Agilent BioAnalyzer RNA Nano chip to generate an RNA Integrity Number (RIN) (Agilent Technologies, Santa Clara, CA). Hundred nanogram of DNase-treated total RNA was then used to generate double-stranded cDNA, which was initiated with selective random priming allowing for the sequencing of total RNA, while avoiding rRNA and mitochondrial transcripts. After primer annealing at 65°C for 5 min, a first strand cDNA synthesis reaction was performed at 40°C for 30 min using kit-supplied reverse transcription reagents. Second strand cDNA synthesis was performed in a 70 µl reaction volume at 16°C for 1 h and the reaction was stopped by adding 45 µl of stop solution. The double-stranded cDNA was then fragmented to ~200 bp with the Covaris M220 sonicator (Covaris, Inc., Woburn, MA), followed by purification with Agencourt RNAClean XP (Beckman Coulter Life Sciences, Indianapolis, IN). The fragmented DNA was suspended in 10 µl of water and end repair was performed in a 13 µl for 30 min at 25°C, followed by a heat inactivation of 70°C for 10 min. Sample-specific indexed adapter was ligated to the end-repaired DNA for 30 min at 25°C, followed by a two-step strand selection process with an intervening 1.8X volume RNAClean XP bead purification. 13 cycles of library amplification and a 1.2x volume RNAClean XP purification of the strand-selected library was performed, followed by resuspension of the library DNA in 30 µl of RNase-free water. Final libraries were screened for library fragment size distribution using an Agilent BioAnalyzer High sensitive DNA Chip. Libraries were then quantitated using the Kapa Library Quantification Kit (Roche Sequencing, Pleasanton, CA), normalized to 4 nM, and were sequenced on an Illumina NextSeq 500 150-cycle high-output flow cell in order to generate ~40 million paired-end reads of 75-base per sample (Illumina, Inc., San Diego, CA) [152].

RNA Sequencing Data Processing and Analysis

The RNA-seq data analysis workflow has been provided schematically in Figure 3.9. Raw reads were quality-filtered to obtain clear data via removal of adaptor sequences, ambiguous or low-quality reads and reads with more than 5% N, using FastQC version 0.11.8 (<http://www.bioinformatics.babraham.ac.uk/projects/fastqc/>) and Trimmomatic version 0.39 [153]. Then clean reads were aligned to the reference genome (GRCh37) using HISAT2 version 2.1.0 [154]. Finally, the read count values for aligned sequences of genes were computed to represent the expression levels of genes using HTSeq version 1.1 [155]. Differentially expressed genes (DEGs) between two groups were explored using R [156] package DESeq2 version 1.24.0 [157].

Genes with p-value <0.05 were selected as differentially expressed Genes. Benjamini-Hochberg (BH) multiple testing correction was applied on results.

Proteomics

SILAC LABELING

Acid-adapted and naive cells were labeled by SILAC. Cells were cultured in heavy SILAC media ($\Delta 6$ -lysine and $\Delta 10$ -arginine) for eight doubling time of MCF7. Extent of labeling was determined by LC–MS/MS analysis of tryptic peptides from labeled samples to ensure >90% labeling.

LYSIS AND DIGESTION

Cells were lysed by sonication in a buffer of 50% trifluoroethanol and 50 mM ammonium bicarbonate, pH 8.0, and protein was measured by the Bradford method. Protein from heavy- and light-labeled cells was combined in equal amounts, and lysis buffer was added to bring the final volume to 200 μ l. The combined protein was reduced with 100 μ l of 40 mM TCEP/100 mM

dithiothreitol for 1 h at 37°C. Proteins were alkylated with 100 µl of 200 mM iodoacetamide for 30 min in the dark at ambient temperature. The volume of the reduced and alkylated sample was brought to 1 ml with 50 mM ammonium bicarbonate, pH 8.0. Trypsin was added at a ratio of 1:50 and samples were digested at 37°C overnight. Digests were frozen at -80°C and lyophilized. Dried peptides were resuspended in HPLC water with 0.1% TFA and desalted on 100-mg Thermo hypersep C18 columns. Eluted peptides were dried in a Speed-Vac and resuspended in HPLC water for isoelectric focusing fractionation.

ISOELECTRIC FOCUSING FRACTIONATION

Tryptic peptides were fractionated using a narrow-pH-range fractionation strategy. At the end of the isoelectric focusing programme, strips were manually cut into 20 fractions. Peptides were extracted and samples were combined in the following manner to achieve 15 fractions for LC-MS/MS analysis: (anode end) samples 1–2, 3–4, 5–6, 7–8, and 9–10 were combined to make five fractions, samples 11–20 were left as individual fractions.

LC-MS/MS

Samples were analyzed as duplicate injections for each fraction. A nano-flow ultra-high performance liquid chromatograph (RSLC, Dionex, Sunnyvale, CA) coupled to an electrospray ion trap mass spectrometer (LTQ-Orbitrap, Thermo Scientific, San Jose, CA) was used for tandem MS peptide-sequencing experiments. The sample was first loaded onto a pre-column (2 cm × 75 µm ID packed with C18 reversed-phase resin, 5 µm particle size, 100 Å pore size) and washed for 8 min with aqueous 2% acetonitrile and 0.04% trifluoroacetic acid. The trapped peptides were eluted onto the analytical column (C18 Pepmap 100, 75 µm × 50 cm ID, Dionex). The 120-min gradient was programmed as: 95% solvent A (2% acetonitrile + 0.1% formic acid) for 8 min, solvent B (90% acetonitrile + 0.1% formic acid) from 5 to 15% in 5 min, 15 to 40% in 85 min, then solvent B from 50 to 90% B in 7 min and held at 90% for 5 min, followed by solvent

B from 90 to 5% in 1 min and re-equilibration for 10 min. The flow rate on the analytical column was 300 nl min⁻¹. Ten tandem mass spectra were collected in a data-dependent manner following each survey scan. The MS scans were performed in the Orbitrap to obtain accurate peptide mass measurements, and the MS/MS scans were performed in the linear ion trap using a 60-s exclusion for previously sampled peptide peaks. Mascot (www.matrixscience.com) searches were performed against the UniProt human database downloaded on 11 July 11 2012. Two missed tryptic cleavages were allowed, the precursor mass tolerance was 1.2 Da to accommodate selection of different isotopes of the peptide precursor. MS/MS mass tolerance was 0.6 Da. Dynamic modifications included carbamidomethylation (Cys), oxidation (Met), heavy lysine ($\Delta 6$) and heavy arginine ($\Delta 10$).

Quantification of differences in protein expression between SILAC-labeled samples was performed as described using MaxQuant. Results were filtered to require a posterior error probability (PEP) score < 0.05 and summed intensity > 0. Candidates were selected among proteins that consistently showed at least a 1.5-fold increase under low-pH conditions across label-flipping experiments.

NETWORK CONSTRUCTION

The STRING database is a valuable resource for the exploration and analysis of functional gene/protein interactions [158]. STRING database was used to find conserved experimentally validated gene-gene interaction networks for the explored DEGs. Since STRING builds protein-protein interaction (PPI) networks thereby our network was constructed upon coding RNAs.

MOTIF EXPLORING AND MOTIF RANKING

Networks consist of smaller and repetitive structural units which are called motifs. Network motifs can be described as recurring circuits of interactions from which the networks

are made [159]. Motifs have important roles in biological networks and suggested that they accomplish overriding functions in biological networks. In this study, Cytoscape [160] NetMatchStar plugin [161] was used to find 3-node 3-edge network motifs in the gene regulatory network which retrieved from STRING database.

In order to further our network analysis, multiple topological and biological parameters were determined and used. Log2 fold change of differentially expressed genes associated in the gene regulatory network (Supplementary Table 1), association of network's genes with biological processes involved in EMT (based on explored GOBP terms related to EMT) (Supplementary Table 2) and gene prioritization score (Supplementary Table 3) which were obtained from Cytoscape GPEC plugin [162], were considered as biological parameters. Betweenness centrality and node degree are two network topological parameters (Supplementary Table 4) which obtained using Cytoscape [160] NetworkAnalyzer [163] plugin and were considered besides biological parameters for network's robust motif ranking. Node degree indicates the number of connected edges to each node and betweenness centrality shows the control level of a node over interactions of other nodes in a network. This centrality parameter prefers the nodes that allow to connect non-directly connected clusters of a network.

The next step was to find the most important motifs in the network. For this purpose, a ranking scheme [164] was performed based on a multi objective weighting function. This scheme is based on parameters which we gathered before: (i) Topological parameters, node degree and betweenness centrality, (ii) the presence of motif genes in EMT related biological pathways (see “Discussion” for more detail), (iii) the gene prioritization score obtained from Cytoscape GPEC plugin [162], (iv) acid-adapted MCF7 cell lines gene expression log2 fold-changes (based on differential expression analysis of acid-adapted MCF7 cell lines vs. non-adapted cell lines). Using this weighted multi-objective function in Equation 1, the motif ranking was performed.

$$GS_{ij} = w_{1j} \cdot \langle nD \rangle_{i \max(nD)} + w_{2j} \cdot \langle nB \rangle_{i \max(nB)} + w_{3j} \cdot \langle PP \rangle_{i \max(PP)} + w_{4j} \cdot \langle |LFC| \rangle_{i \max(|LFC|)}$$

GS_{ij} is the ranking score for each motif ($i = 1 \dots n$) in different weighting scheme ($j = 1 \dots 13$) as said in Table 1. Different weighting values including w_{1j} to w_{4j} are used to strike importance of used factors, $\langle nD \rangle_i$: average node degree for motif's node, $\langle nB \rangle_i$: average betweenness centrality of each node in a motif, $\langle PP \rangle_i$: number of genes in a motif involved in EMT related pathways, $\langle GPS \rangle_i$: average gene prioritization score obtained from GPEC, $\langle |LFC| \rangle_i$: average absolute log2 fold change for each motif.

Five different sets of weighting scenarios including 13 different weighting schemes were applied (Table 1) to remove biasness between used parameters in motif prioritization. Each set pays more attention to specific parameters in Equation (1). In the first set, only one parameter is more important for ranking. In the sets 2–4, two, three and four parameters are important, respectively, and constantly have higher weights to the absolute LFC of the motif to explore phenotype-specific top ranked motifs. In the fifth set, equal weights allocated to all the parameters. This weighting scheme leads to 13 ranking score for each motif. After removing duplicated motifs, we selected the top 10 motifs from each weighting scenario for further analysis (Supplementary Table 5).

Proteomics and Transcriptomics Integrative Data Analysis

Integrative proteomics and transcriptomics data analysis was performed in order to ensure about consistency of proteomic and transcriptomic data regarding explored motifs. In this regard 19 differentially expressed genes of the top 10 explored motifs cross referenced with SILAC proteomics data (DCIS and MCF7 cell lines) to see which of the following transcriptomes are alternatively translated in the proteomics level.

Examining Survival and Gene Alteration Changes

cBioportal.org was used to examine the survival and gene alteration changes in breast cancer patient samples. For non-invasive breast cancer sample data, the set from Razavi et al. [165] was used, and for invasive breast cancer sample data the set from Curtis et al. [166] was used.

Immunofluorescence

Cells cultured at pH 6.5 chronically and pH 7.4 of with the same passage were rinsed with PBS, fixed in cold Methanol:Acetone (1:1) for 10 min and then blocked with 4% bovine serum albumin in PBS for 1 h. Samples were incubated with primary antibody of S100B and S100A6 (1:100) and secondary Alexa-Fluor 488 antirabbit (1:500) antibody for 1 h in room temperature. Coverslips were mounted using ProLong Gold Antifade Reagent (Life Technologies) and images were captured with a Leica TCS SP5 (Leica) confocal microscope.

Immunohistochemistry

For human tissues, a TMA containing formalin-fixed and paraffin-embedded human breast tissue specimens was constructed in Moffitt Cancer Center histology core. The TMA contains 27 normal breast tissue, 30 DCIS, 48 invasive ductal carcinomas without metastasis, 49 invasive ductal carcinomas with metastasis and 48 lymph node macro-metastases of breast cancer. Cores were selected from viable tumor regions and did not contain necrosis. A 1:400 dilution of anti-LAMP2 (#ab18529, Abcam), anti-S100A6 antibody (Prestige Antibodies Powered by Atlas Antibodies, Sigma-Aldrich) and anti S100 protein were used as primary antibodies. Positive and negative controls were used. Normal placenta was used as a positive control for LAMP2, normal breast was used as a positive control for S100 and normal kidney was used as a positive control for S100A6. For the negative control, an adjacent section of the same tissue

was stained without application of primary antibody, and any stain pattern observed was considered as non-specific binding of the secondary.

Immunohistochemical analysis was conducted using digitally scanning slides and scoring by three independent reviewers. The scoring method used by the pathologist reviewer to determine (1) the degree of positivity scored the positivity of each sample ranged from 0 to 3 and were derived from the product of staining intensity (0–3+). A zero score was considered negative, score 1 was weak positive, score 2 was moderate positive, and score 3 was strong positive (2). The percentage of positive tumors stained (on a scale of 0–3).

Statistical Analysis

Statistical analysis and estimation of correlations in this study were performed using GraphPad Prism v.6. Correlation significance calculated by Pearson correlation. The p-values reported for survival analysis measured by cox regression hazard ratio and log rank tests. All paired tests were performed by Student's t-test.

FIGURES

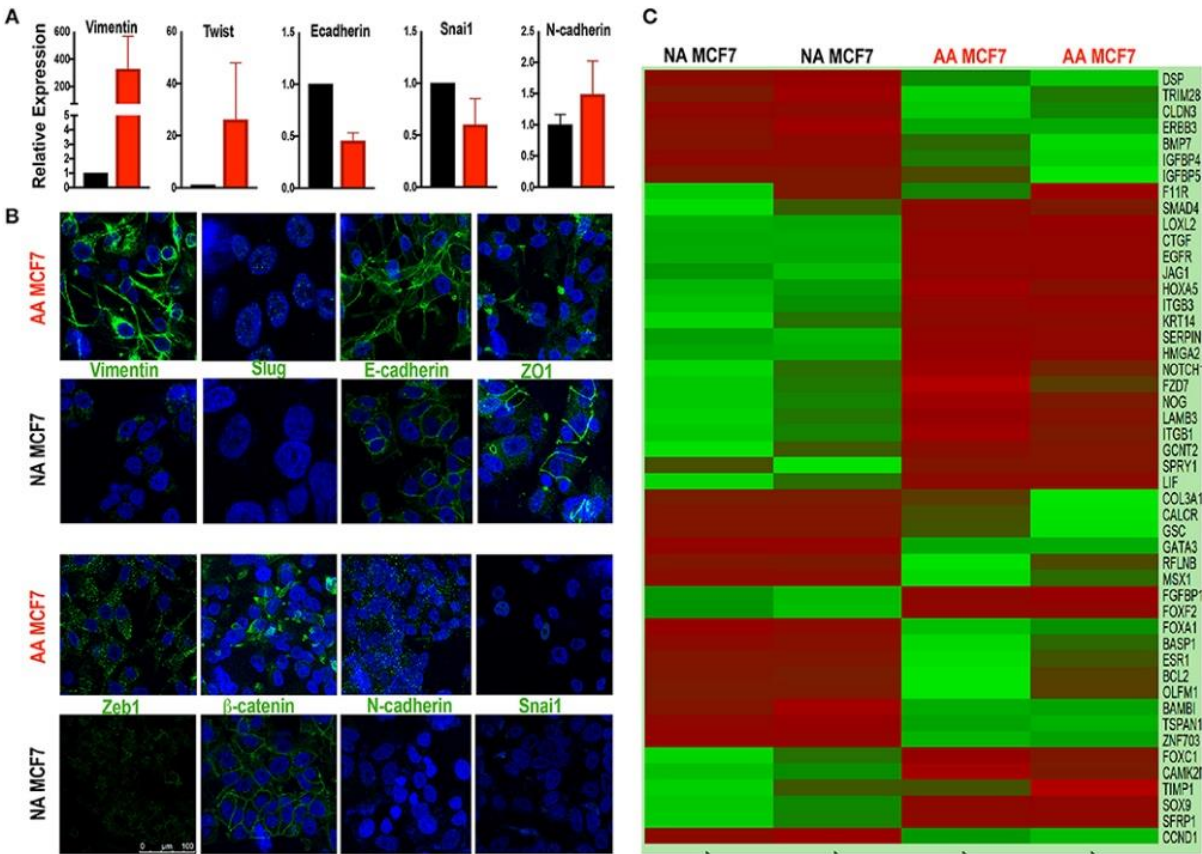


Figure 3.1. Acid adapted cells show partial EMT phenotype. (A) q-RT-PCR-analysis and (B) IF of EMT marker at RNA and protein level respectively show both markers of epithelial and mesenchymal phenotype are present in acid adapted cells confirming their transient EMT phenotype. (C) Analysis of RNA sequencing shows a mixed epithelial and mesenchymal markers. Heatmap plot for EMT related differentially expressed genes in AA-MCF7 compared to MCF7. Each row represents a gene and each columns stands for a sample. Cells color is correlated to gene count in the corresponding sample. Color code for gene count: red, high expression; green, low expression.

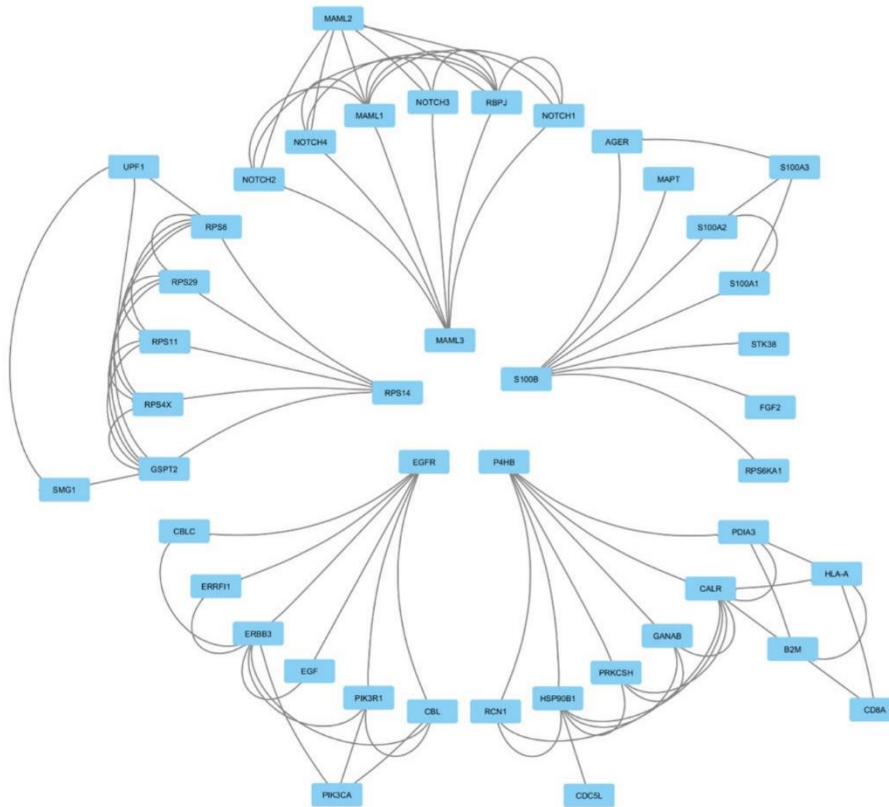


Figure 3.2. Interaction map of our motif packs, obtained from STRING database illustrating the first shell of interactions for each motif pack.

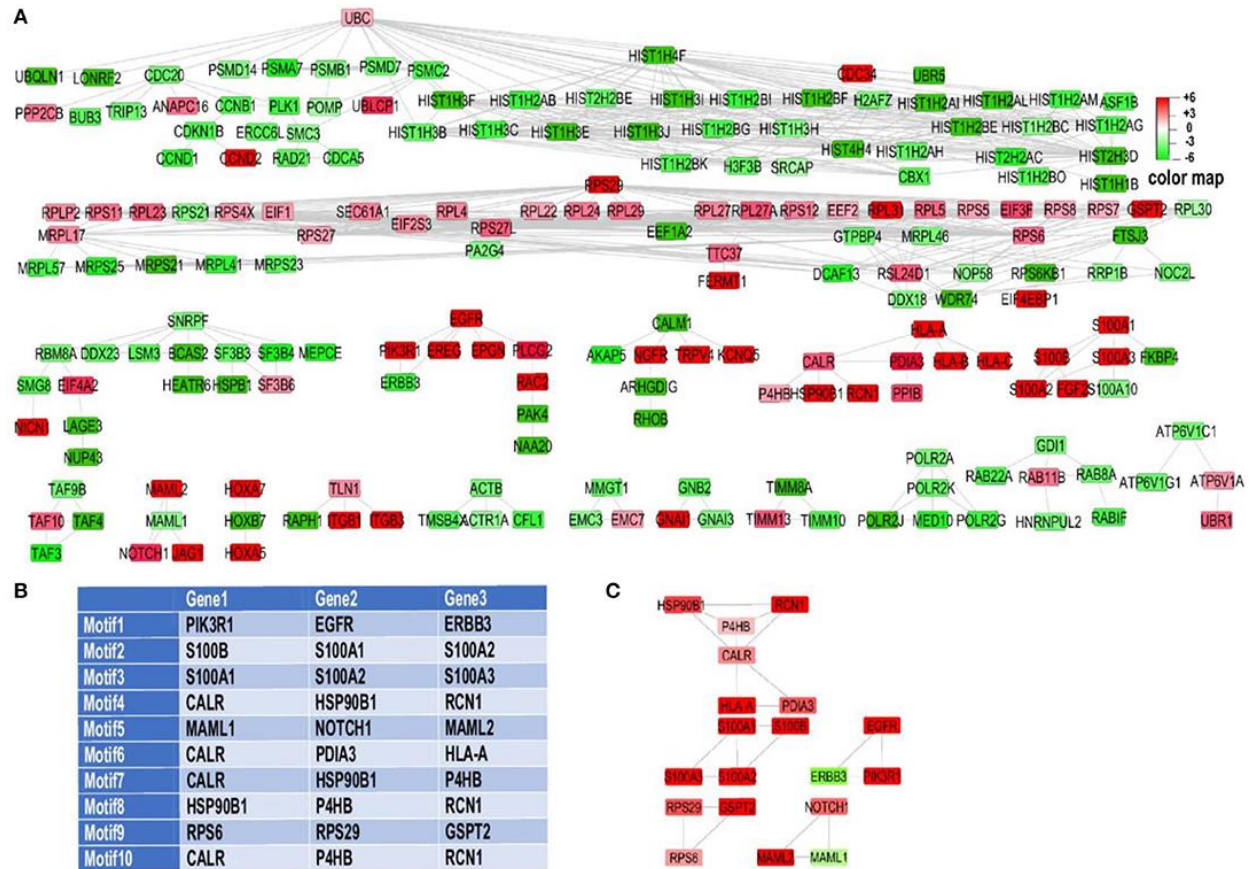


Figure 3.3. RNA sequencing motif analysis unravels EMT related genes involved in acid adaptation. (A) Experimentally validated gene regulatory networks of differentially expressed genes. For better visualization Y files layout algorithm of cytoscape was used to organize the network. Two node interactions and disconnected nodes were omitted. (B) Top ten ranked motifs of our network, directed toward EMT. (C) Top 10 explored motifs based on ranking analysis were merged together. The association of some of genes like P4HB and CALR in multiple motifs which present in top 10 motifs leads to construct a small sub-network by merging of these motifs which leads to construct core regulatory subnetwork.

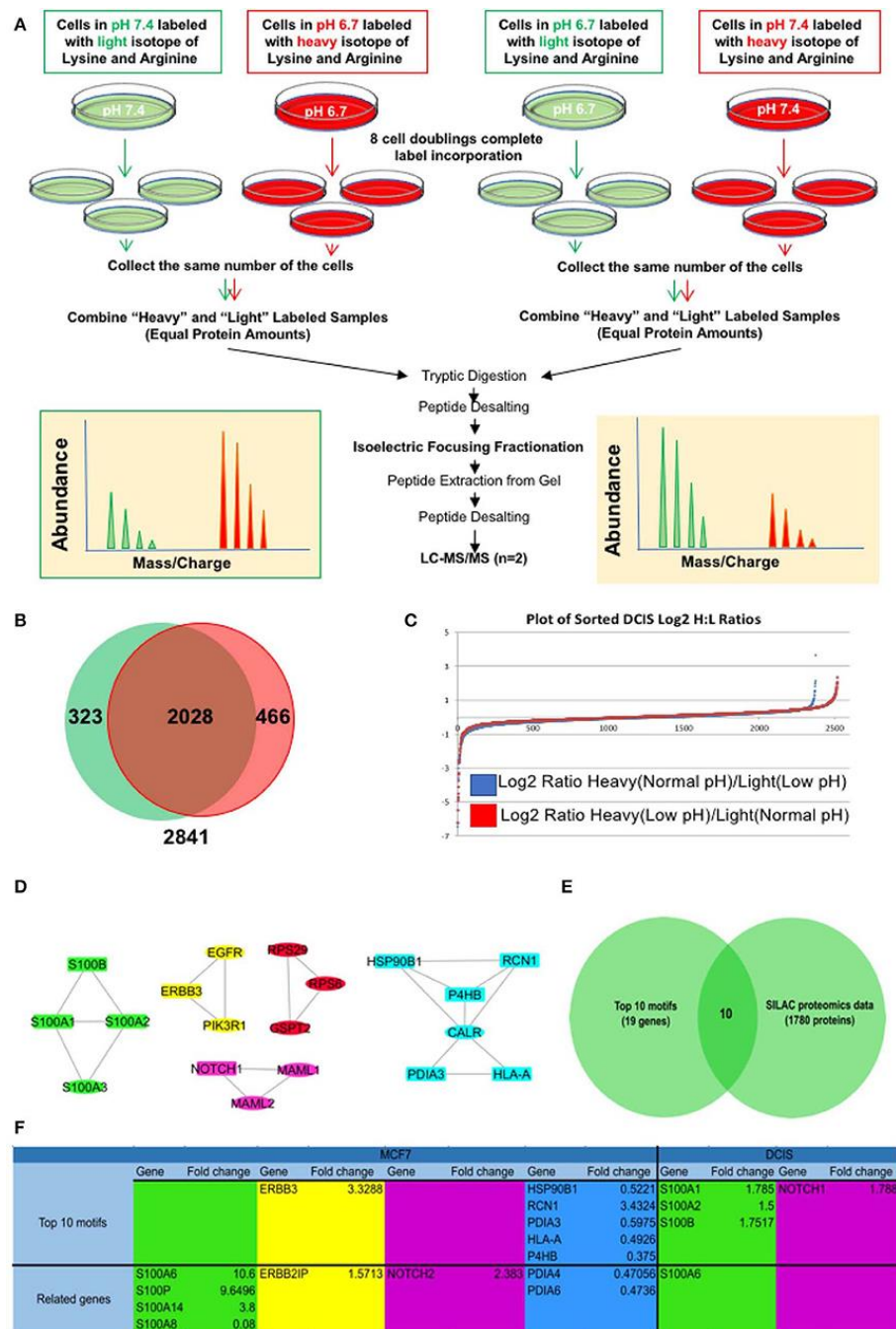
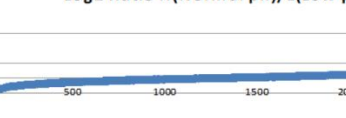


Figure 3.4. Integrative analysis of proteomics and transcriptomics data to discover the acidic microenvironment induced EMT genes. (A) A schematic of our SILAC proteomics design. We flipped the labeling to make sure the changes in protein expression is not affected by the type of labels. (B) Venn diagram and (C) Log 2 fold change of SILAC proteomics data discovered in each flipping experiment. (D) Integrated interaction map of the regulatory subnetwork and their related altered proteins in both DCIS and MCF7 cell lines. (E) Venn diagram indicating that among $n = 45$ transcripts (The subnetwork and its near interactions) $n = 12$ proteins were differentially translated with the abundance of S100 family. (F) The name of proteins that are discovered in DCIS and MCF7 proteomics and are correlated to the motif's from RNA sequencing data.

2518	2375	323	2028	466
2518	2375	2841		
Normal pH (light)	normal pH (heavy)	Combined Replicates		
Low pH (heavy)	Low pH (light)	MaxQuant ID Criteria: PEP score ≤ 0.05 Maximum Intensity > 0		

C)

Log2 Ratio H(Normal pH)/L(Low pH)




Average of log2 values = -0.081
(0.95-fold)

Stdev of log2 values = 0.4653

Median of log2 values = -0.0347
(0.98-fold)

Log2 Ratio H(Low pH)/L(Normal pH)



Average of log2 values = 0.024
(1.02-fold)

Stdev of log2 values = 0.4719

Median of log2 values = 0.0283
(1.02-fold)

51

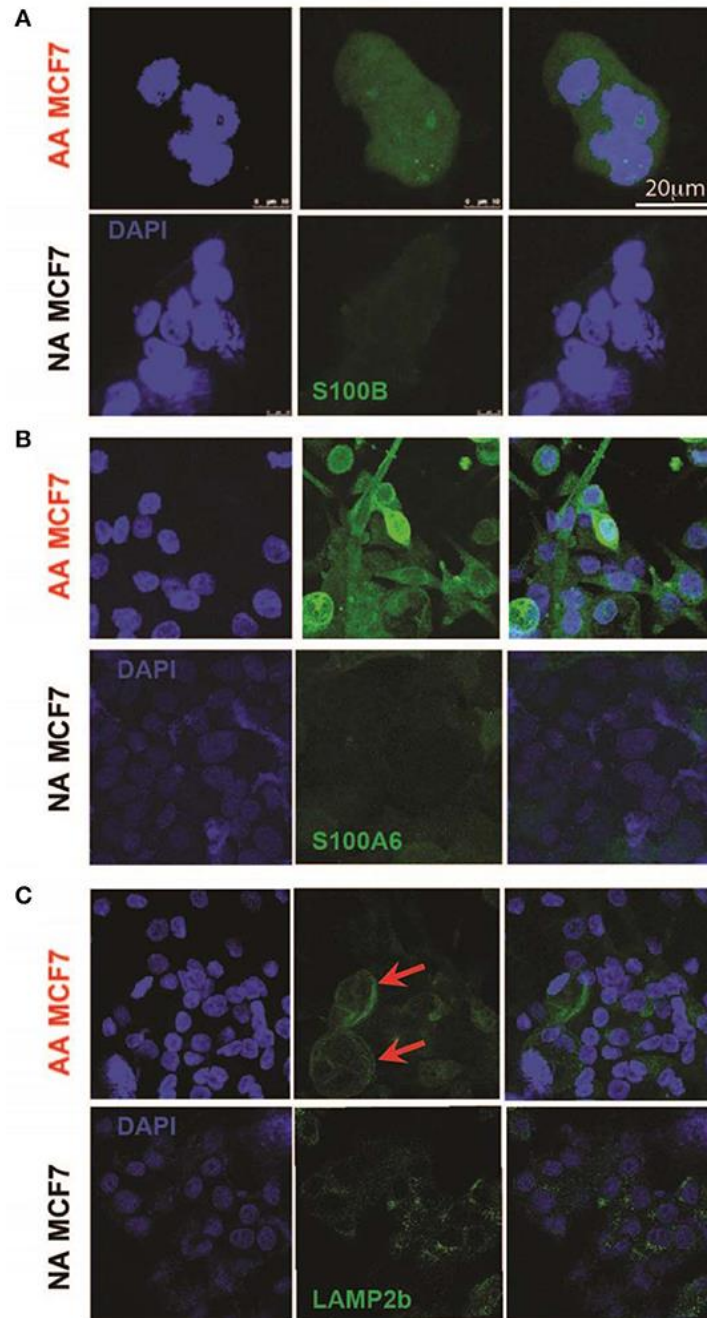


Figure 3.6. Validation of higher expression of acid-induced EMT markers by Immunocytochemistry. (A) S100B protein expression in acid-adapted and non-adapted MCF7 cells with the analysis on right. S100B expression is significantly higher in acid adapted cells. (B) S100A6 ICC of acid-adapted and non-adapted MCF7 cancer cells shows higher expression of S100A6 in AA MCF7 cells. (C) LAMP2b ICC of acid-adapted and WT MCF7 cancer cells. Acid-adapted MCF7 cells display membrane localization of LAMP2b, compared to cytoplasmic localization in non-adapted MCF7 cells.

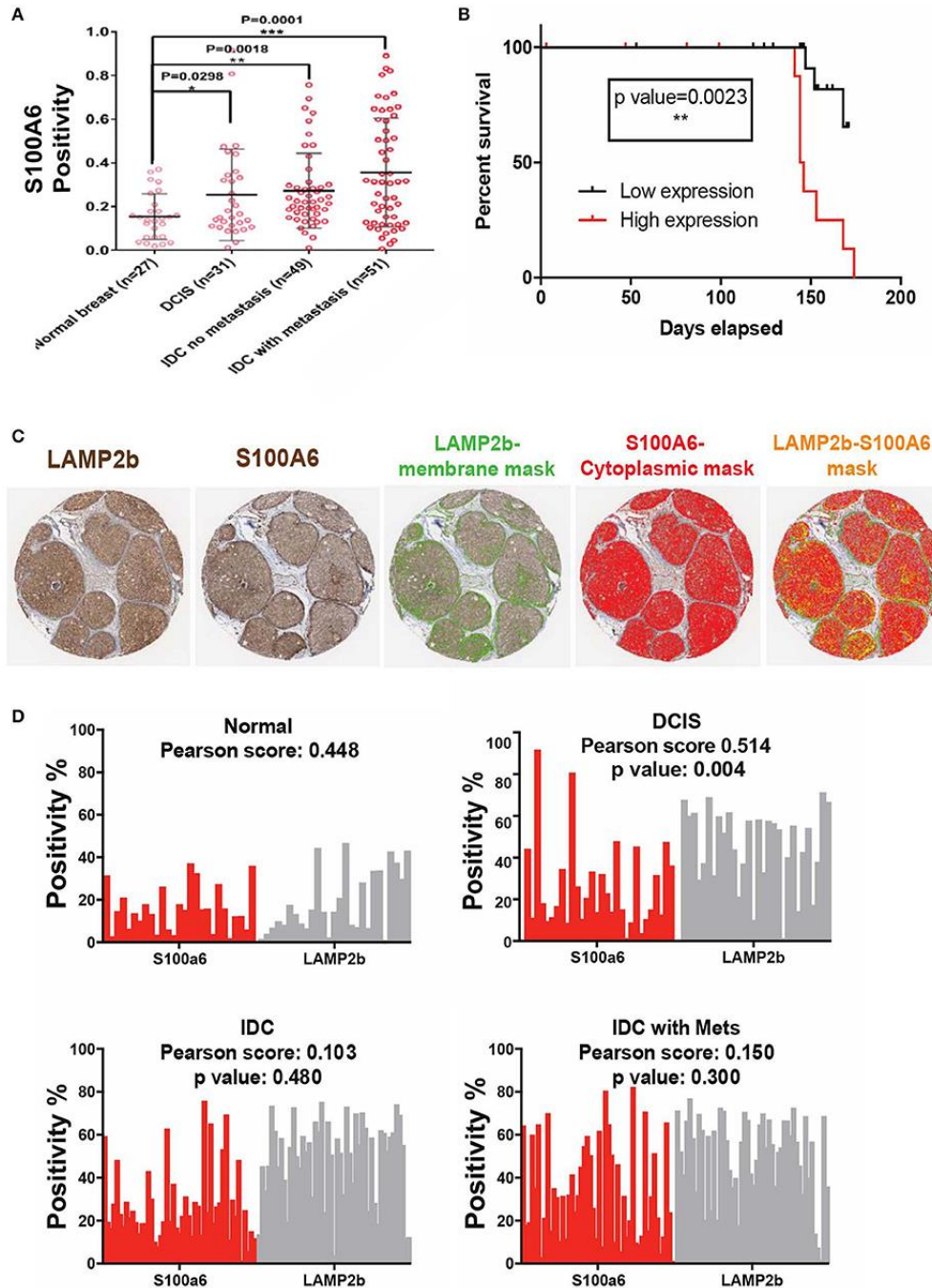


Figure 3.7. Clinical validation of S100A6 expression correlation to acid phenotype in breast cancer. (A) TMA analysis of 160 biopsy cores stained with S100A6 antibody showed increased expression of this protein from normal to DCIS, IDC, and IDC with Mets. Data are shown as mean with standard deviation as error bar. T-test was used to determine p-value. (B) Kaplan-Meier graph comparing DCIS patient's survival with low expression of S100A6 (Below the average) to patients with high S100A6 expression. Patients with high expression survived less than patients with low expression. (C) Representative images of core biopsies stained for both LAMP2b and S100A6 on sequential cuts. (D) Correlation analysis of LAMP2b and S100A6 in different stages of breast cancer.

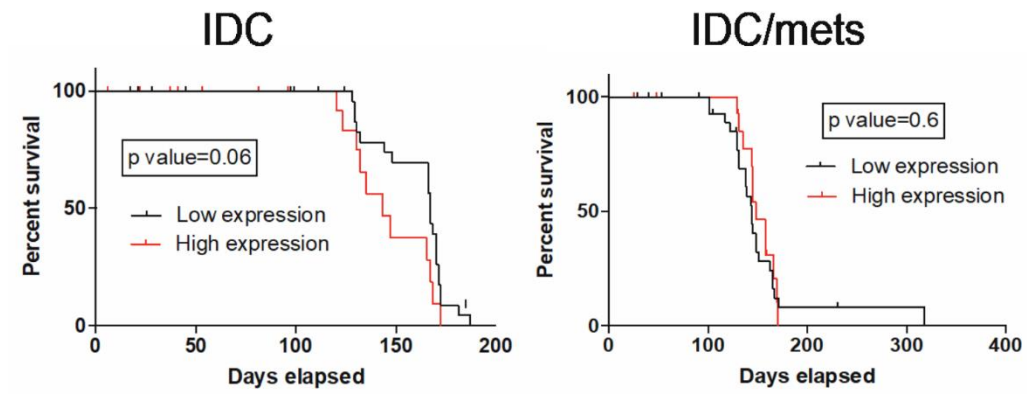


Figure 3.8. Survival analysis of patients with high and low expression of S100A6 in different stages from IDC, and IDC with local metastasis respectively.

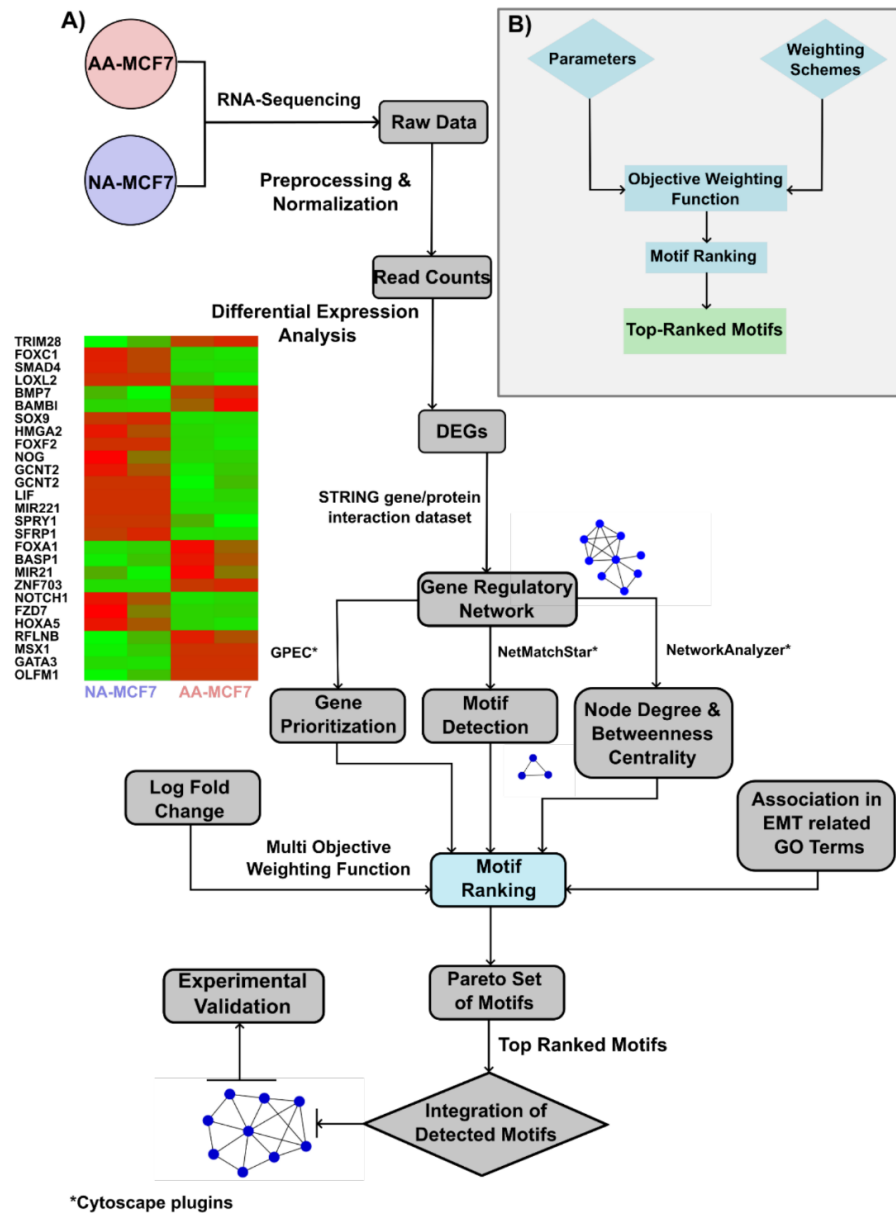


Figure 3.9. RNA sequencing data analysis workflow and the methodology of network analysis. A) Paired end reads from both Acid-Adapted (AA) and Non-AcidAdapted (NA) MCF7 cell-lines were processed and transformed to high quality trimmed reads then aligned to a reference genome to achieve count reads which have been used for differential expression analysis to explore Differentially Expressed Genes (DEGs). Based on the STRING database an experimentally validated Gene Regulatory Network (confidence = 0.7) was constructed from DEGs. Network analysis was based on a scheme to explore and rank the network motifs with respect to EMT phenotype. B) Motif ranking has been performed using a multi objective weighting function and different network topological and biological parameters for nodes. Using weighting function leads to Pareto set of motifs which has been used to explore top 10 network motifs. These motifs were considered for further experimental validation.

Chapter 4: Inhibition of glycolysis allows for breast cancer control

The vast majority of the *in vitro* work and writing of this manuscript was completed by myself. Animal studies were completed by Samantha Byrne and Dominique Abrahams, and supervised by myself and Dr. Mehdi Damaghi. This work was adapted from the publication in *Cancers (Basel)* [167].

INTRODUCTION

The initiation and development of cancers is associated with major metabolic alterations in response to dynamically changing microenvironmental conditions such as hypoxia and acidosis [38]. These forces will select for the fittest phenotype in the context of the current microenvironment. Cancer cells that are more plastic and adaptable can acclimate to an increasing array of emergent microenvironmental selective forces. Combined, these factors define tumors as highly dynamic ecosystems in which many different cancer cell subpopulations compete for space and resources [168]. The microenvironment around the cells can alter the local fitness of cancer cell subpopulations in a tumor; leading to possible dramatically different evolutionary trajectories selecting for cells with different phenotypic and genotypic properties [131]. We have previously reported how acid-producing and acid-resistant phenotypes can engineer the tumor ecosystem in order to increase their own fitness, allowing them to take over the population [19, 131]. We have also showed the different strategies that cancer cells acquire to adapt to their microenvironment [131]. Here, I investigate the impact of switching off certain phenotypes that give cancer cells a competitive advantage. By switching these off, one can influence the distribution of sub-populations with the end game of turning the majority of the

population into a less aggressive phenotype with decreased invasion and metastasis. The idea is to take away any evolutionarily acquired or selection driven advantages of the more aggressive clones in population to allow for non-aggressive cells to be able to compete [169].

Glycolysis is the prominent phenotype of cancer cells under hypoxia or normoxia (Warburg effect). Glycolysis produces acid, which must be removed from cells, resulting in an important aspect of cancer metabolism: i.e., reduced extracellular pH ($pH_e \sim 6.5\text{--}6.7$) and increased intracellular pH ($pH_i \geq 7.2$). For cells to compete they must adapt to these conditions and thus these adaptations can be used against them as a vulnerability [53]. Adaptive mechanisms include: increased expression and activity of acid extruders, such as monocarboxylate transporters (MCT) including: MCT1 and MCT4, Na^+-H^+ exchanger 1 (NHE1) and V-ATPases, as well as membrane bound exofacial carbonic anhydrases such as CA9 or CA12 to maintain an optimal pH_i [53]. An optimal pH_i gives cancer cells some proliferative advantages [53]. Herewith, we use two drugs that we are repurposing to target pH_e and pH_i metabolic adaptations so that the more aggressive cancer cell sub-populations lose their selective advantage over the less aggressive phenotypes. The first drug is diclofenac, a clinically used non-steroidal anti-inflammatory drug (NSAID), that has been shown to have an inhibitory effect on MCTs [170, 171]. Targeting MCTs is a promising approach that many groups are following to find treatment against the glycolytic phenotype of cancer cells such as MCT1/2 inhibitors [172]. However, these drugs have not yet been successful in treating cancer, as cells have shown the ability to switch isoforms from e.g., MCT1 to MCT4 [53, 172]. Diclofenac is putatively a pan-MCT inhibitor [170].

The second drug is koniginic acid (KA), a natural product produced by fungi, which inhibits the function of GAPDH [173, 174].

In previous work of systems analysis of cancer cells' metabolic vulnerabilities [53], we observed that GAPDH is highly pH_i sensitive and has a key role in promoting a WE phenotype.

This pH sensitivity of GAPDH means that the effects of its inhibition on cell proliferation are enhanced at an acidic intracellular pH. This acidic pH vulnerability is the reasoning for coupling with diclofenac, which I demonstrated to be a potent inhibitor of MCT activity, causing decreased intracellular pH. Other groups also reported GAPDH as a selective WE phenotype target [173] that can be partially and irreversibly inhibited by KA.

Evolutionary-based therapies use Darwinian principles to delay the proliferation of aggressive populations regardless of their genotype states [131, 169, 175]. These therapies can be guided by the use of mathematical models of cell population dynamics based on competing mechanisms of cancer cell sub-population within the tumor [176, 177]. Conventional maximum dose therapy (MDT) permits an unopposed proliferation of resistant and/or more plastic cells by removing sensitive and/or less plastic cancer cell populations, a phenomenon known as “competitive release” in ecology [169]. With “competitive release”, clonal and sub-clonal population balance is not maintained amongst all different clones. Alternatively, evolution-based therapies use Darwinian principles to delay the proliferation of resistant populations [131, 169], maintaining clonal and sub-clonal population balance. A form of evolutionary therapy is adaptive therapy (AT), where the competitive release of resistant clones is delayed by the application of intermittent or dose-varying therapeutic regimens, to maintain a balance between sensitive and resistant clones to successfully control tumor growth [169, 178, 179]. In this approach, I exploit metabolic adaptations to acidosis as a vulnerability for the more aggressive tumor cells in order to attenuate cancer growth. The representative cell lines, less aggressive (MCF7) and more aggressive (MDA-MB-231), were selected based on the previously described phenotypes [180-184].

RESULTS

Diclofenac and koningic acid reduce the glycolytic activity of cancer cells

H⁺-monocarboxylate transporters (MCTs) play a major role in transporting organic anions such as lactate across cell membranes. Since the transport cycle is coupled to H⁺ ions, the activity of MCTs also affects intracellular pH (pHi) within cells [185]. It has been shown that MCT inhibition decreases cancer cells' aggressive phenotypes [172, 186, 187] by reducing the lactate efflux, leading to acidification of pHi and buildup of intracellular [lactate] [53]. It has been shown that diclofenac can inhibit MCTs [170] and that koningic acid (KA) can inhibit GAPDH [173, 188, 189], which is very sensitive to pHi [53] (Figure 4.1A). As proof of principle, I measured the effect of diclofenac and KA on glucose consumption and lactate production of MCF7 and MDA-MB-231 breast cancer cell lines. In both cell lines, diclofenac and KA reduced the lactate production (Figure 4.1B) and glucose consumption (Figure 4.1C) significantly within 72 h of treatment. Notably the effect was larger in the more highly glycolytic MDA-mb-231 cells. I then measured the activity of both drugs in the 3D culture of MCF7 and MDA-MB-231 spheroids over time. I observed that both drugs showed effects as early as 24 h (Figure 4.2A,B). These results indicated that both drugs are effective in inhibiting glycolysis as proposed and can work both in 2D and 3D experiments. I also measured the glutamine and glutamate concentration in the media following treatments of both cell lines with both drugs under normoxia and hypoxia and found no differences among the groups (Figure 4.2C).

Diclofenac inhibits MCT activity

To test whether the effect of diclofenac treatment on glycolysis was due to inhibition of lactate export, I measured MCT activity before and after treatment with diclofenac using pHi as a reporter of transmembrane flux. To rule out if the effect on pHi change is because of NSAID activity of diclofenac, I also measured the MCT activity on the same cells treated with aspirin.

Using a superfusion microscopy system and cells loaded with the pH reporter dye SNARF-1, I measured the time course of pHi during superfusate maneuvers that trigger net transmembrane flux of lactate (Figure 4.1D). When presented with extracellular lactate, cells acidified, and when extracellular lactate was withdrawn, cells alkalinized. The rate of these pHi changes are measures of MCT activity. In the presence of diclofenac, however, efflux of lactate was completely inhibited in both cell lines. Controls included another NSAID, aspirin, which was without effect. As these are acute effects, cell death was not expected to play a role (vide infra), and we further ruled it out, due to the inability of dead cells to retain the SNARF-1 dye. To confirm that diclofenac was acting on a specific transport process, i.e., MCT, rather than causing a generalized tightening of membrane permeability, experiments were repeated with acetate in place of lactate. Compared to lactate, acetate can permeate the cell membrane in an MCT-independent manner by partitioning across the lipid matrix as acetic acid, and its efflux was unaffected by diclofenac (Figure 4.1E). This suggests that the action of diclofenac is targeted to MCT, the main route for lactate traffic in and out of cells. The results of this assay are not indicative of what is expected to be seen under physiological conditions. The large changes in pH observed in these experiments are not sustained for long periods of time, and are induced by superphysiological lactate levels. The purpose of these experiments was solely to determine the effects of Diclofenac on a cells ability to export lactate; not to demonstrate specific pHi values under drug treatment.

Diclofenac and koningic acid decrease the viability of cancer cells

To test if the effects on glycolysis translate into the effective killing of cancer cells, we assessed the survival of cells using CCK8 viability assays and CelltiterGlo (see Methods) in both hypoxia and normoxia. We experimented with both normoxic and hypoxic conditions as they both commonly occur in the microenvironment of solid tumors such as breast cancer, and cell viability will be expected to be much more sensitivity to glycolysis inhibition under hypoxic

conditions. In solid tumors, cells that are further than 160 micrometers from the vasculature they experience a hypoxic condition that makes the cells glycolysis dependent [20, 31]. Many cancer cells overexpress or over-activate MCTs to deplete the lactate produced under the hypoxic conditions, although this response is not universal as shown in supplemental Figure 4.3. Under normoxia (Figure 4.4A) and hypoxia (Figure 4.4B) cell survival was measured after treatment with diclofenac, KA, or both in MCF7 and MDA-MB-231 cells. As shown in Figure 4.4A, diclofenac alone reduced the viability of MDA-mb-231, and MCF10/DCIS cells, which are highly glycolytic and tumorigenic, as well as MCF-7 cells which are tumorigenic and only moderately glycolytic. Notably there was no effect on viability of MCF10AT cells, which are neither tumorigenic nor glycolytic. More pronounced effects with a similar distribution were observed with KA and the combination of DIC + KA. Surprisingly, the effect of DIC on viability under hypoxia (Figure 4.4B) was less significant cf. normoxia (Figure 4.4A), whereas the effects of KA and the DIC + KA combination were no different. To test the activity of the drug on viability and H⁺ export flux in the same experiment we performed a viability assay while monitoring the acidification of conditioned media. Inhibition of MCTs or GAPDH should reduce rate of media acidification. After treatment and before viability assays we measured the pHe of the media using the Five EasyTM/FiveGoTM pH meter (Mettler Toledo, Columbus, OH, USA see Methods). The acidification was reduced by both drugs and the pH of media was neutral, validating the effect of both diclofenac and KA on lowering glycolytic activity of cells (Figure 4.5).

To determine the effect of diclofenac and KA on the pHi of cancer cells, I measured the pHi of a panel of breast cancer cell lines (MDA-MB-231, MCF-DCIS, MCF7, 4T1, H605, and T47D), loaded with SNARF-1-AME (Figure 4.4C). For 16 h, cells were treated with diclofenac (100 μ M), KA (1 μ M), or aspirin (300 μ M), and then imaged in buffered RPMI media. All cell lines exhibited a significantly lower pHi with the treatment of diclofenac, and 4 of the 6 diclofenac treated cell lines had significantly lower pH than the aspirin group.

Considering the different microenvironment in solid tumors such as hypoxia and acidosis and their combination we wanted to test if inhibiting MCTs and GAPDH have an effect on the viability of cancer cells. These conditions are also very important to be targeted because they are specific for tumors and not experienced by normal cells. Therefore, we performed the survival assays on both MCF7 and MDA-MB-231 cells under four possible combinations of change in oxygen level and pH as following: (i) Normal pH-Normoxia, (ii) Low pH-Normoxia, (iii) Normal pH-Hypoxia, and (iv) Low pH-Hypoxia. Targeting MCTs and GAPDH under different microenvironments reduces the cancer cell's viability (Figure 4.6). The effect was greatest with the combination of both drugs and under the most unique condition of solid tumors -hypoxia, and acidic pH (Figure 4.6).

Diclofenac and koningic acid reduce the Warburg phenotype of cancer cells

The Warburg effect (WE) phenotype is defined by a high glycolytic rate even in the presence of oxygen (aerobic glycolysis) and is associated with the progression and aggressiveness of cancers [190-193]. We recently showed that inhibiting proton pumps such as MCTs and pH-sensitive glycolytic enzymes such as GAPDH or GPI, reduces the WE phenotype of cancer cells [53]. Here we used the same strategy to reduce the WE phenotype by repurposing diclofenac from a NSAID to an MCT inhibitor and a natural product produced by fungi, koningic acid to target GAPDH. Above, I already showed that these compounds can reduce the glycolytic phenotype of cancer cells, and here I am using Seahorse measurements to confirm the inhibitor effect of these products on aerobic glycolysis. Seahorse can measure the glycolytic condition through simultaneous of proton efflux (ECAR) and mitochondrial respiration (OCR), which can be used to assess WE phenotype [53, 194]. In the first experiment I interrogated at the real-time effect of diclofenac of KA on ECAR and OCR of MCF7 cancer cells (Figure 4.7A,B). KA and diclofenac monotonically increased the OCR compared to control and the combination of the two had the greatest effect (Figure 3A). KA and diclofenac both

caused an initial drop of ECAR that lasted for 150 min that slowly returned to control levels. The recovery of ECAR to KA was more rapid compared to either conditions that contained diclofenac, which may be due to differences between GAPDH and MCT regulation (Figure 4.7B). This could imply that even if the cells over-activate or overexpress the GAPDH, because the pHi is too low the phenotype can't be survived. I also measured the WE phenotype (ECAR/OCR) of these cells in three different time points: (i) right before drug injection, (ii) 5 h after injections, and (iii) 12 h after injections (black arrows in Figure 4.7A). These results showed that a combination of KA and diclofenac has the highest effect on decreasing the Warburg phenotype of cancer cells in mentioned time points (Figure 4.7C). To confirm this finding, I also performed a Seahorse experiment based on glycolytic rate assay that measured the maximum glycolytic capacity of cells by, first, shutting down mitochondrial respiration and then glycolysis (Methods). This assay also showed the highest inhibition of WE phenotype by the combination of KA and diclofenac in both MCF7 and MDA-MB-231 breast cancer cells (Figure 4.7D).

Reducing Warburg phenotype can change population dynamics

Cancer evolution is a result of genetic diversification and clonal selection within the adaptive landscapes of tissue ecosystems. Therapeutic approaches can destroy some cancer clones, but it may also create a new space and different selective pressure resulting in expansion of resistant and most probably more aggressive clones aka “competitive release” in ecology and evolution. Evolutionary based therapeutic design can be used to control cancers when a cure is not possible. For that reason, understanding Darwinian intratumoral dynamics and their interactions with microenvironmental selection forces is critical to steer a tumor into a less invasive phenotype.

In 3D spheroid experiments I investigated the competitive release strategy to develop a new treatment design. Two distinct cell types were used to provide insight into the dynamic interactions among tumor cell subpopulations, a crucial element of intratumor heterogeneity.

Mixed-culture competition experiments in spheroids can successfully track competitive outcomes amongst different cell types [195]. In 3D spheroid experiments differences in growth rates, carrying capacities and competition coefficients can be determined accurately [195]. For this experiment, I mono- and co-cultured MCF7-GFP and MDA-MB-231-RFP cells (1:1 ratio) and treated them with DMSO (control), diclofenac, KA, or combination of KA and diclofenac (Figure 4.8A–C). As a control experiment I grew spheroids in different microenvironmental conditions and with different ratios of MCF7 to MDA-MB-231 cells. In any microenvironmental condition and with any ratio of the two cancer cells, MDA-MB-231 cells always eventually dominated the MCF7 cells and took over the whole population (Figure 4.9). After treating the spheroids with diclofenac, KA, or the combination, I showed that these metabolically designed drugs can steer the population dynamics towards the less aggressive phenotype cells (MCF7-GFP). Figure 4.8A,B are controls showing effect of the agents on monocultures. Figure 4.8C shows that, in co-culture conditions, the green signal that belongs to MCF7-GFP was increased in response to both drug and the combination, compared to the control group. These results show that it may be possible to control population dynamics in tumors based on their metabolic vulnerability.

Evolutionary designed therapy controls tumor growth and metastasis in vivo

To translate my in vitro 2D and 3D results to *in vivo* we then performed animal experiments in female NSG mice. The experimental design was similar to the 3D spheroid experiment co-culture -MCF7 and MDA-MB-231 cells were mixed in 1:1 ratio and inoculated into the mice mammary fat pad. Mice were randomized into four groups of six mice per group and treated with diclofenac, KA, both, or none (DMSO). Primary tumor growth was unaffected by either monotherapy cf. controls, but there was a significant decrease caused by the combination of diclofenac and KA (Figure 4.10A).

At the end of the experiment we extracted the tumors and all the vital organs from each mouse and scored for metastasis. Notably, the diclofenac + KA combination group was metastasis-free, while all other groups had measurable metastases across multiple sites (Figure 4.10B). These results indicate that evolutionary therapeutic approaches based on metabolic targeting can be used to control tumor growth and even change aggressive phenotypes such as metastasis.

DISCUSSION

Tumor evolution follows the Darwinian principles; meaning nature selects for phenotype not genotype [169]. When cancer initiates and develops, many clones and sub-clones emerge that are genetically heterogeneous with many of them presenting the same phenotype such as the Warburg effect (WE) phenotype [45]. The emergence of one phenotype from many clones with different genetic backgrounds implies the fitness of the selected phenotype to the selection forces. The WE phenotype is associated with progression and invasion of many cancers and is defined by a high glycolytic rate in the absence or presence of oxygen (aerobic glycolysis). Most cancer cells reprogram their metabolism in favor of aerobic glycolysis despite the presence of plentiful oxygen in their microenvironment, implying higher fitness of WE phenotype.

During the evolution of tumor cells and through adaptation to constantly variable microenvironment, tumor cells adapt and acquire phenotypes helping them survive and grow. These acquired characteristics can be used as a new vulnerability against them. As mentioned previously, we recently showed that certain targets for inhibition of glycolysis have increased effects of inhibition at a lower intracellular pH [53]. To test this principle, I coupled Diclofenac, a compound I demonstrated to be a potent inhibitor of MCT's, with koningic Acid, a known inhibitor of GAPDH. The MCT inhibition by Diclofenac provided a decrease in phi in vitro which I believe enhances the effectiveness of KA, based on the previous work. In this paper I showed that targeting the WE phenotype in mixed populations of cells can stabilize the population

dynamics, preventing more glycolytic populations from taking over as they typically would. We used a simple model of co-culture of two cell lines with extremely opposing characteristics: MDA-MB-231 cells that are triple-negative fast proliferating, tumorigenic and metastatic in mouse xenograft models that are also highly glycolytic with WE phenotype and MCF7 cells that are ER/PR positive, slow-growing and tumorigenic in mouse xenografts with the help of estrogen pellets but not metastatic and very low glycolytic and not WE phenotype. The co-culture of these two cell lines was used as a simple population model of tumor heterogeneity to monitor the population dynamics of the tumor. In the future, these findings will be confirmed and expanded in a more complex, transgenic tumor model, to observe the effect of real intratumor heterogeneity in cell subpopulation. Using this metabolic targeted strategy, I showed that it may be possible to control tumor population dynamics and heterogeneity. This metabolically targeted treatment strategy was able to successfully control tumor growth and metastasis in the mouse xenograft model. Therefore, we propose a novel strategy of cancer control for the tumor where a cure is not an option. We propose evolutionary principles of tumor growth that can be used to control tumor cells' clonal or sub-clonal population in favor of slower growth and less damage to patients.

METHODS

Cell culture

MCF-7 and MDA-MB-231 cells were acquired from American Type Culture Collection (ATCC, Manassas, VA, USA, 2007–2010) and were maintained in DMEM-F12 (Life Technologies, Carlsbad, CA, USA) supplemented with 10% fetal bovine serum (HyClone Laboratories, Logan, UT, USA). Cells were tested for mycoplasma contamination and authenticated using short tandem repeat DNA typing according to ATCC's guidelines. Cells were treated with diclofenac (1 μ M) and/or koningic acid (1 μ M) dissolved in the media of the cells.

Hypoxia cell culture

For hypoxia conditions we used a Biospherix X-Vivo Hypoxia Chamber. The conditions in each hypoxia chamber kept at 37 °C, 5% CO₂, with 0.1% O₂ and 94.9% N₂ or 1.0% O₂ and 95% N₂. The chamber was quality controlled and calibrated according to the manufacturer's specifications (Biospherix, Parish, NY, USA).

Transfection (GFP/RFP plasmids)

To establish stable cell lines, the MCF-7 and MDA-MB-231 cells were infected with Plasmids expressing RFP or GFP using Fugene 6 (Promega, Madison, WI, USA) at early passage and were selected using 2 µg/mL puromycin (Sigma, St. Louis, MO, USA).

Mettler Toledo Five EasyTM/FiveGoTM pH Meter

The pH meter was first calibrated by using standard pre-made calibration buffer solutions for pH 4, 7, and 10. Then using the pH probe the pH of the control media used to grow the spheroids was measured. This pH was used as a baseline to compare the pH of the pHe media of the spheroids.

Viability assays

CCK8 Cell viability was measured after treatment with drugs (diclofenac and koningic acid or both) and DMSO as control using Cell Counting Kit-8 (CCK-8) under different microenvironmental conditions such as normoxia, hypoxia, normal pH, or low pH. CCK8 is a sensitive colorimetric-based viability assay based on Dojindo's highly water-soluble tetrazolium salt, with WST-8 as its active agent. CCK8 was used to measure viability as it is not pH sensitive and can be added to the cells directly in their niche, without fixation or change of media. For measuring viability, cells were seeded in a 96-well plate (with triplicate of the same

samples), and viability was measured at the indicated intervals. The experiments were repeated at least two times.

CellTiter-Glo® This 3D Cell Viability Assay is designed to determine the number of viable cells in 3D cell culture based on quantitation of the ATP through based on Luminescent Cell Viability Assay chemistry. The lytic capability of the reagents is much higher than the 2D assay and the assay is compatible with 96 well-plate formats of our spheroid experiments that make it ideal for high-throughput screening. In our assay 72 h after treatment of spheroid with inhibitors, the lysis buffer directly added to each well containing one sphere of MDA-MB-231 or MCF7 cells. The plates were incubated in RT for 10 min on a rocking shaker. Then the assay mixture containing luciferin and luciferase was added and the luminescent was measured after 5 min incubation in RT.

Glycolytic rate measurements (Seahorse)

Glycolytic rate of MCF7 and MDA-MB-231 cancer cells was measured using Seahorse XF96 extracellular flux analyzer and a glycolysis rate kit (Seahorse Biosciences, Billerica, MA, USA). All the seahorse experiment has been performed in the absence of $\text{CO}_2/\text{HCO}_3^-$. Oxygen consumption rate (OCR) and extracellular acidification rate (ECAR) of cancer cells were determined by seeding them on XF96 microplates in their growth medium until they reached over 90% confluence. In these studies, seeding started with 20,000 cells (80% of the well area). Measurements were determined 24 h later when the cells reached 90% confluence. One hour before the seahorse measurements culture media were removed and cells were washed 3 times with PBS followed by the addition of base medium (non-buffered DMEM supplemented with 25 mM glucose). Finally, data were normalized for total protein content of each well using the Bradford protein assay (ThermoFisher, Waltham, MA, USA). Seahorse measurements were performed with 4–6 technical replicates and these experiments were repeated at least 2 times.

The WE phenotype (“Warburgness”) can be expressed as the ratio of glycolysis (ECAR) to oxidative phosphorylation (expressed as the oxygen consumption rate, OCR) from the GST.

Metabolic profiling

Cells were seeded in a regular 96-well plate for 2D culture and in U bottom 96 well plates for 3D spheroid culture in their growth medium containing 10% FBS under standard culture condition. Once cells reach 90% confluence for 2D or carrying capacity for 3D (usually when the growth of spheres is steady and they don’t get bigger), the growth media were removed and placed in a new 96 well plate with the same order as the original plate for metabolic profiling using YSI machine (YSI 2900 multi-analyte system (YSI, Yellow Springs, OH, USA)). We used at least 150 μ L of media in each well to make sure there was enough media for each assay in the machine. Sensors in YSI were changed weekly and calibrated before each experiment. Final data of the lactate, glucose, glutamine, and glutamate in conditioned media were normalized to the protein amount per well or the confluency of each well imaged right before metabolite measurements.

MCT activity

Cells were plated on four chamber Lab-Tek chambered cover glass slides 1 day prior to experimenting, and cultured in RPMI media containing 10% FBS and 1% P/S. On day of experimentation, media was replaced with RPMI containing 10% FBS, 1% P/S, 25 mM HEPES, and 25 mM PIPES, to stabilize pH while outside of the 5% CO₂ incubator. Once the assay was ready to begin for a given group, 5-(and-6)-Carboxy SNARFTM-1, Acetoxymethyl Ester, Acetate was added 8 min prior to experimentation at a concentration of 10 μ g/mL. Prior to experimentation, the pH calibration curve of the 5-(and-6)-Carboxy SNARFTM-1, Acetoxymethyl Ester, Acetate dye was conducted using the nigericin method as described previously [196]. Once the 8 min incubation period was up, imaging began and superfusion with the 30 mM

lactate solution (solutions listed in extended data file) and the SNARF-1 ratio was allowed to stabilize. The superfusion setup used in the experiments consists of a peristaltic to flow the media, a custom manufactured fluidic switch system which allows for the rapid changing of solutions, and a vacuum pump to aspirate media from the opposite side of the chamber. Once stabilized, cells were instantaneously switched to the 0 mM lactate solution and maintained in such until the velocity of the SNARF-1 ratio began to level off. Cells were then switched back to the 30 mM lactate condition and allowed to stabilize again. Once stabilized, the cells were switched to the same 30 mM lactate solution, this time either containing (X concentration of Diclofenac or Aspirin). Cells were maintained in the drug treatment solutions for 20 min in order for the drugs to take effect, and then switched to the 0 mM lactate solution containing the same concentration of drug they were treated with.

pHi measurement

Cells were plated on four chamber Lab-Tek chambered cover glass slides 1 day prior to experimentation and cultured in RPMI media containing 10% FBS and 1% P/S. On day of experimentation, media was replaced with RPMI containing 10% FBS, 1% P/S, 25 mM HEPES, and 25 mM PIPES, to stabilize pH while outside of the 5% CO₂ incubator. Once the assay was ready to begin for a given group, 5-(and-6)-Carboxy SNARFTM-1, Acetoxymethyl Ester, Acetate was added 10 min prior to experimentation at a concentration of 10 µg/mL. After the 10 min, cells were washed 2 times with drug containing media and fresh drug containing media was resupplied to the cells. Change in pHi caused by each drug was measured by converting the SNARF-1 ratio to pHi and comparing pre- and post- treatment pHi's.

Spheroid mono- and co-culture

Perfecta3®96-Well Hanging Drop Plates or non-adhesive U shape bottom 96 well plates were used to grow the primary spheres containing 10,000 total cells. 10% Matrigel was used for

the primary spheroid construction as follows. After cells were counted they were diluted as 200 cells per μL of media. Then the cells mixture was cooled down in ice for 10 min and 10% Matrigel (melted in ice in the 4-degree Celsius walk-in fridge overnight) was added and directly seeded in the U plates. The plates were centrifuged for 1 min 500 RPM. For each experimental condition, the ratio between MCF-7-GFP and MDA-MB-231-RFP was 0, 50, or 100 percent as follows: 0/100, 50/50, 100/0. Each ratio had 4–8 replicates for each experiment. An Incucyte microscope kept at 37 °C and 5% CO₂ was used to image the spheroid growth every 6 h over approximately 30 days. Images and fluorescent intensity were analyzed in Incucyte built-in software and image J. Relative fluorescent units (RFUs) were normalized by averaging red/green fluorescence when the corresponding cell type was absent then subtracting this value from other fluorescent values of that cell type. Drug treatments were directly added to the growth media of the spheroids and renewed every 3 days.

Animal experiments

MCF7 and MDA-MB-231 breast cancer cell lines were grown in T-225 flask and harvested at 70–80% confluency. Both cells were authenticated by short tandem repeat analysis and tested for mycoplasma. 10 million cells in 200 μL cold PBS and 10% Matrigel was inoculated into cleared mammary fat pads of SCID mice (eight- to ten-week old females). Tumor measurements were done by calipers every other day and ultrasound once a week. Mice had free access to water and food for the whole duration of the experiment. For mixed cultures, a 1:1 mixture of 5 million MDA-MB-231 and 5 million MCF7 cells were injected. One week before cell injection, an estrogen pellet (0.72 mg slow-release, Innovative Research of America) was implanted to allow for the growth of ER-positive MCF7 tumors. The concentration of diclofenac given to each mouse was 40 mg/kg. As for the KA the concentration was 1 mg/kg. These concentrations remained the same when the mice were treated with both drugs. The control mice were injected with DMSO in PBS. The mice were treated by intraperitoneal injections once

on Monday, Wednesday, and Friday weekly. At the end of the experiment tumors were extracted, then the size and weight of them were measured. Vital organs were also extracted and looked for metastasis.

Animal studies were performed by the guidelines of the IACUC of the H. Lee Moffitt Cancer Center (that was approved by the University of South Florida IACUC committee: IACUC 5331R).

FIGURES

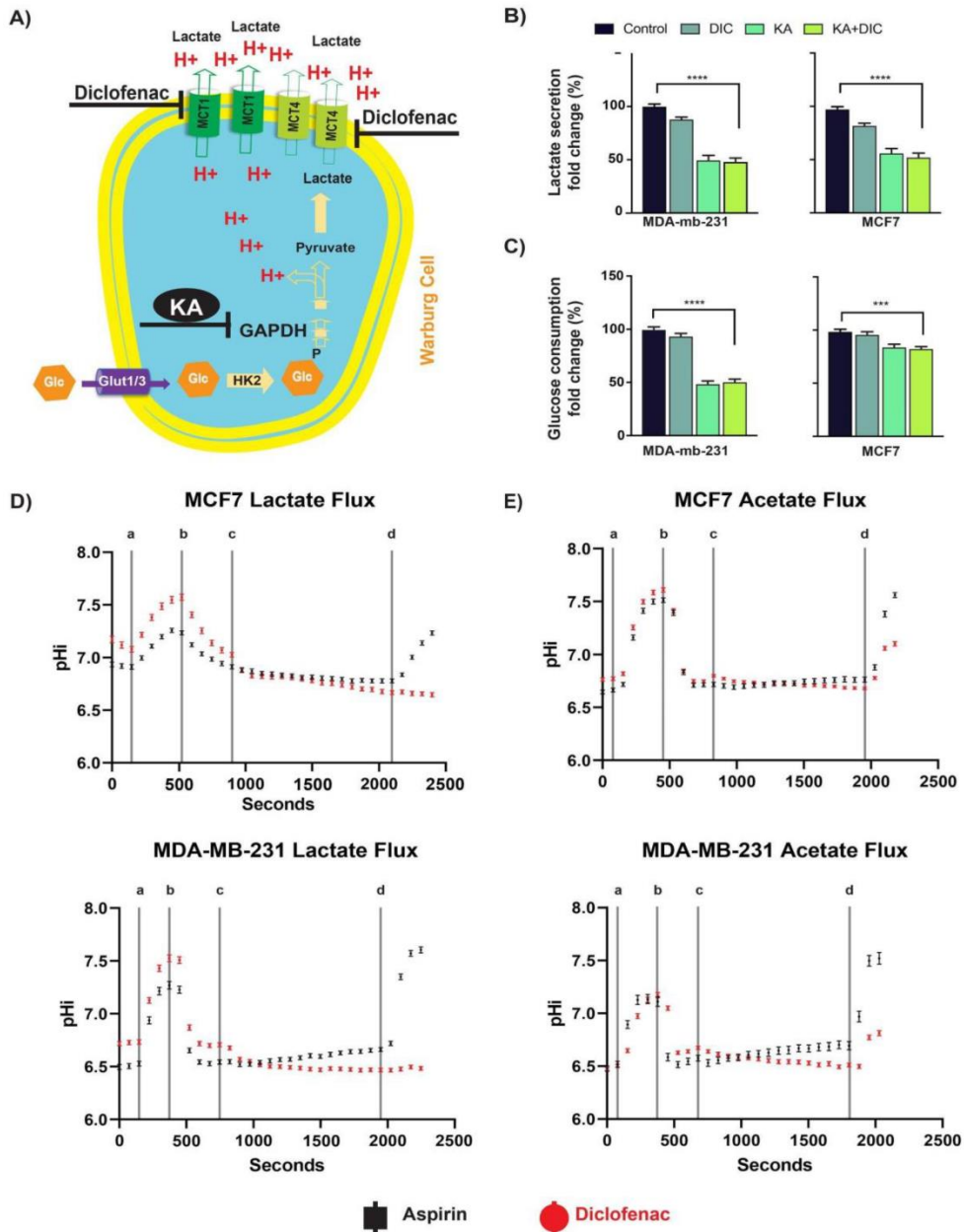


Figure 4.1. Diclofenac and koningic acid reduce the glycolytic activity of cancer cells. (A) Schematic showing effect of Diclofenac (1 μ M) to reduces the activity of MCT transporters leading to acidification of the intracellular pH_i. Koningic acid (KA) reduces glycolytic activity by inhibiting GAPDH that has an alkaline pH optimum. (B) Lactate production was reduced in both MCF7 and MDA-MB-231 cells after treatment with diclofenac, KA, or both. (C) Glucose consumption was reduced in both MCF7 and MDA-MB-231 cells after treatment with diclofenac, KA, or both. (D) MCF7 and MDA-MB-231 cells were treated with diclofenac or Aspirin to measure the effect of drug on their lactate transport abilities. Line (a) represents the switch from a 30 mM lactate environment to a 0 mM Lactate environment. Line (b) represents the switch from a 0 mM lactate environment to a 30 mM lactate environment. Line (c) represents the switch

from a 30 mM lactate environment – drug treatment to a 30 mM lactate environment + drug treatment. Line (d) represents the switch from a 30 mM lactate environment + drug treatment to a 0 mM lactate environment + drug treatment. (E) MCF7 and MDA-MB-231 cells were treated with diclofenac or Aspirin to measure the effect of drug on their pH_i altering effects. Line (a) represents the switch from a 30 mM acetate environment to a 0 mM acetate environment. Line (b) represents the switch from a 0 mM acetate environment to a 30 mM acetate environment. Line (c) represents the switch from a 30 mM acetate environment – drug treatment to a 30 mM acetate environment + drug treatment. Line (d) represents the switch from a 30 mM acetate environment + drug treatment to a 0 mM acetate environment + drug treatment. p-values are represented as follows: *** $p < 0.001$, **** $p < 0.0001$.

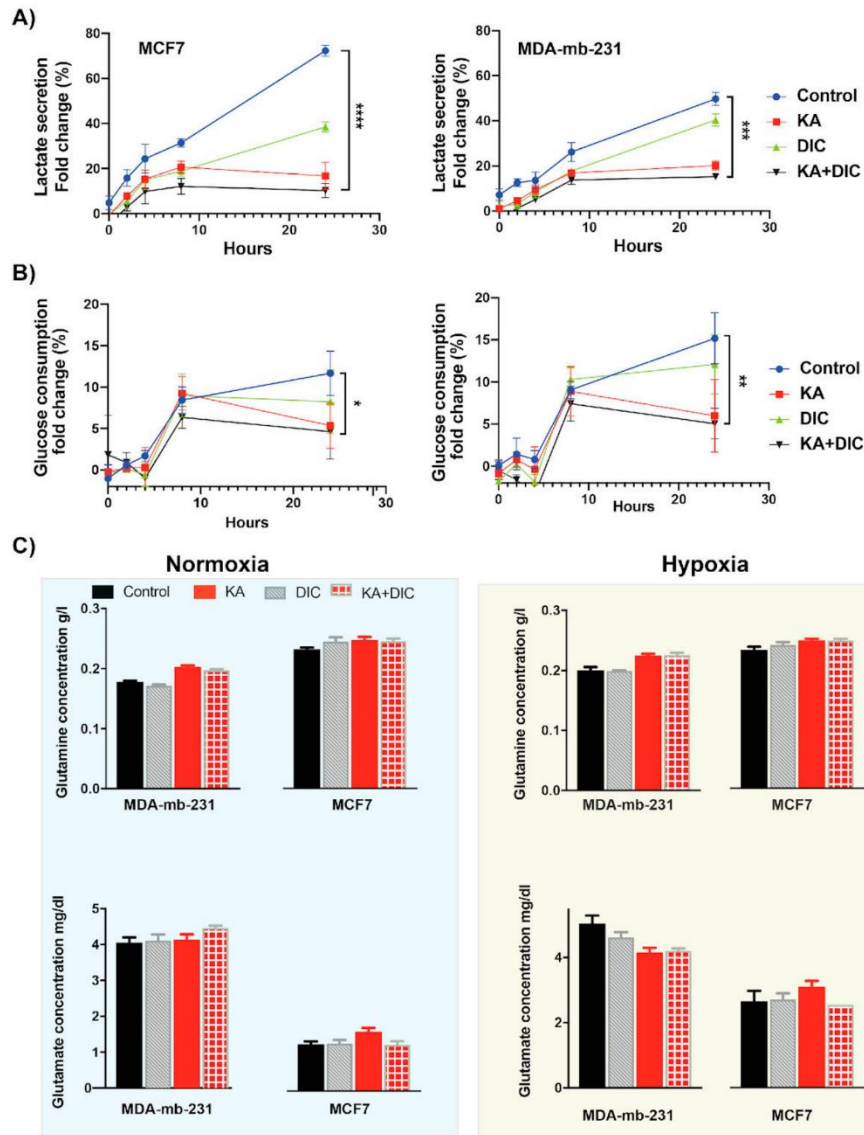


Figure 4.2. Glucose consumption was reduced in both MCF7 and MDA-MB-231 cells after 72 hours treatment with diclofenac, KA, or both. (A) Time point measurement of lactate production in both MCF7 and MDA-MB-231. (B) Time point measurement of glucose consumption in breast cancer cell lines. Data are represented as mean with SD as error bars. (C) Glutamine and

glutamate concentrations in conditioned media of MCF7 and MDA-mb-231 cells treated with Diclofenac, Koningic acid, and both compared to the non-treated control in hypoxia (0.1% oxygen) and normoxia. p-values are represented as follows: * $p < 0.05$, ** $p < 0.01$, *** $p < 0.001$, **** $p < 0.0001$.

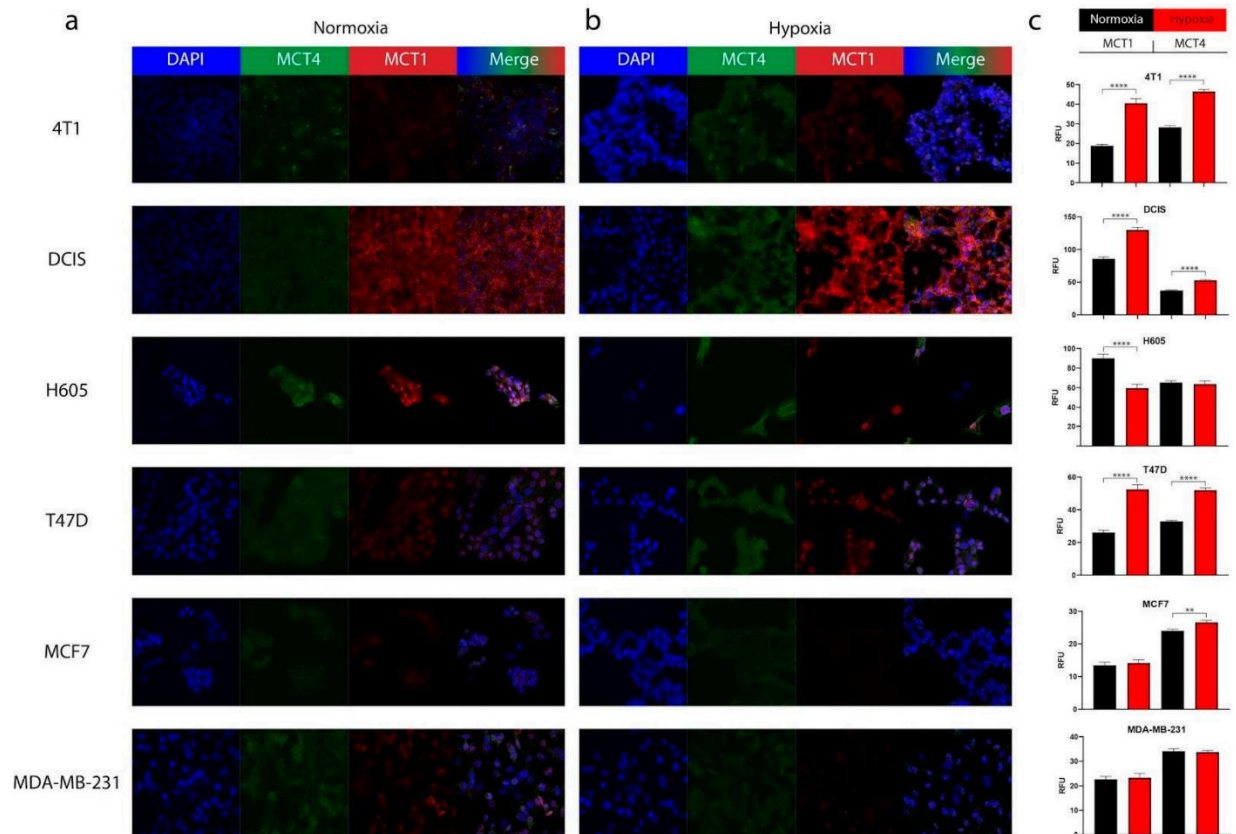


Figure 4.3. ICC Analysis of MCT Expression in Breast Cancer Cell Lines. ICC staining and analysis of 4T1, DCIS, H605, T47D, MCF7, and MDA-MB-231 cell lines. (a) DAPI, MCT4, and MCT1 staining of aforementioned breast cancer cell lines under normoxic oxygen conditions. (b) DAPI, MCT4, and MCT1 staining of aforementioned breast cancer cell lines under hypoxic oxygen conditions. (c) Quantitative analysis of ICC staining. T-test p-values are represented as follows: * $p < 0.05$, ** $p < 0.01$, *** $p < 0.001$, **** $p < 0.0001$.

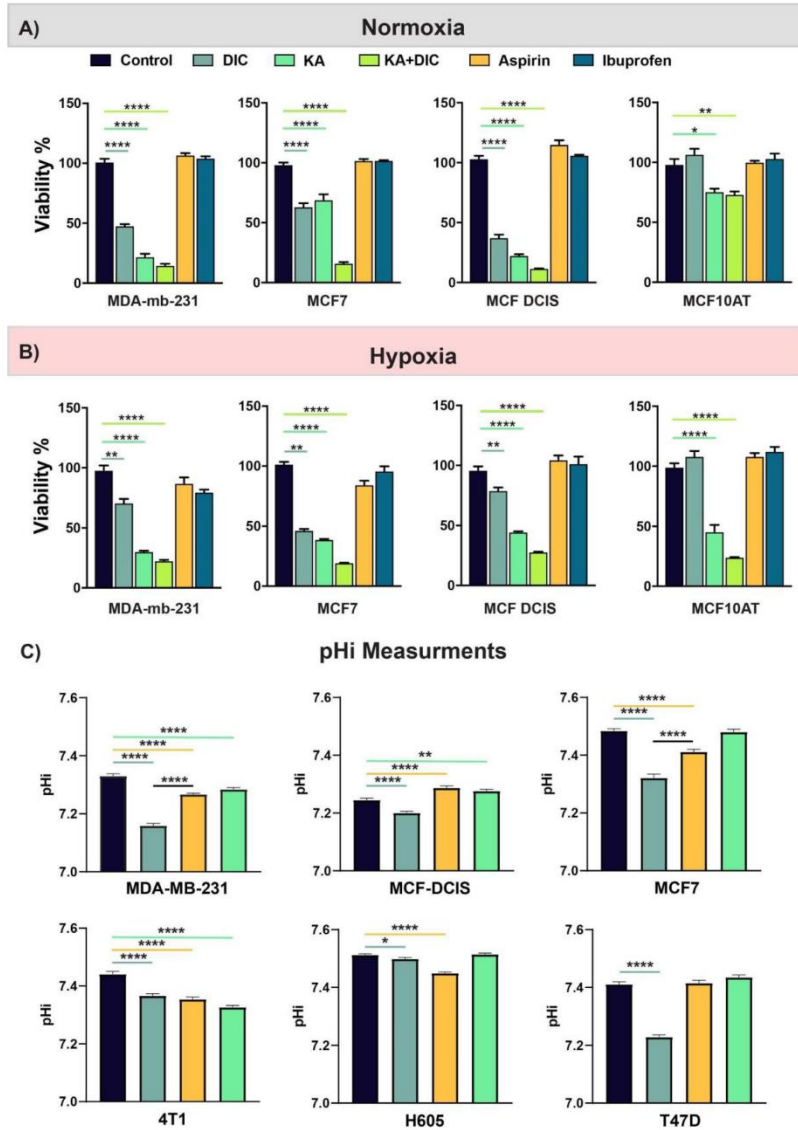


Figure 4.4. Diclofenac and koningic acid decrease the viability of cancer cells. (A,B) Viability of different breast cancer cell lines (MDA-MB-231, MCF7, MCF DCIS, MCF10AT) were measured in 2D using CCK8 kit under normoxia (A) and hypoxia (B) and different treatments. Diclofenac combination with GAPDH inhibition had the highest effect on cell viability. Interestingly other NSAID drugs such Aspirin or Ibuprofen didn't have any effect on cell viabilities. Error bars plotted as SD. (C) Intracellular pH measurement of MDA-MB-231, MCF-DCIS, MCF7, 4T1, H605, and T47D cancer cells using SNARF1, after 16 h treatment. Diclofenac decreased the pHi significantly in all cell lines. Error bars plotted as SEM. T-test p-values are represented as follows: * $p < 0.05$, ** $p < 0.01$, **** $p < 0.0001$.

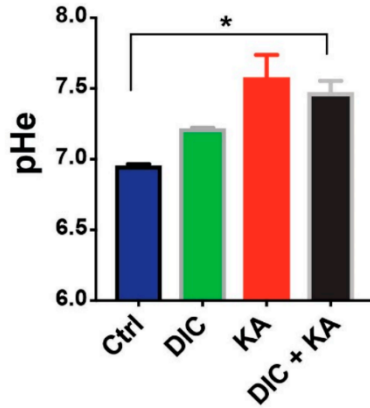


Figure 4.5. Media pH of cells treated with diclofenac, KA, or combination of both. T-test p-values are represented as follows: * $p < 0.05$, ** $p < 0.01$, *** $p < 0.001$, **** $p < 0.0001$.

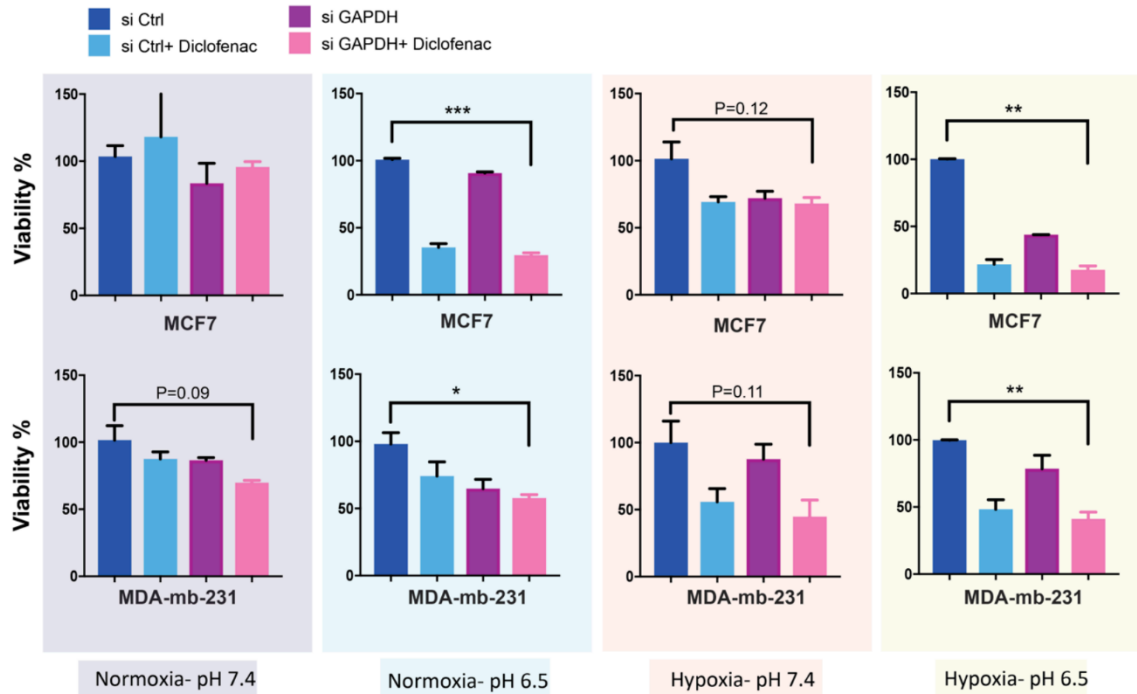


Figure 4.6. Survival assay of breast cancer cell lines in different microenvironmental conditions. Targeting MCTs and GAPDH under different microenvironments reduces the cancer cells' viability. The effect is the most with the combination of both drugs and under the most unique condition of solid tumors, hypoxia, and acidic pH. The data is normalized to non-treated for each cell line in each condition and presented as mean with error bars as SD. T-test p-values are represented as follows: * $p < 0.05$, ** $p < 0.01$, *** $p < 0.001$, **** $p < 0.0001$.

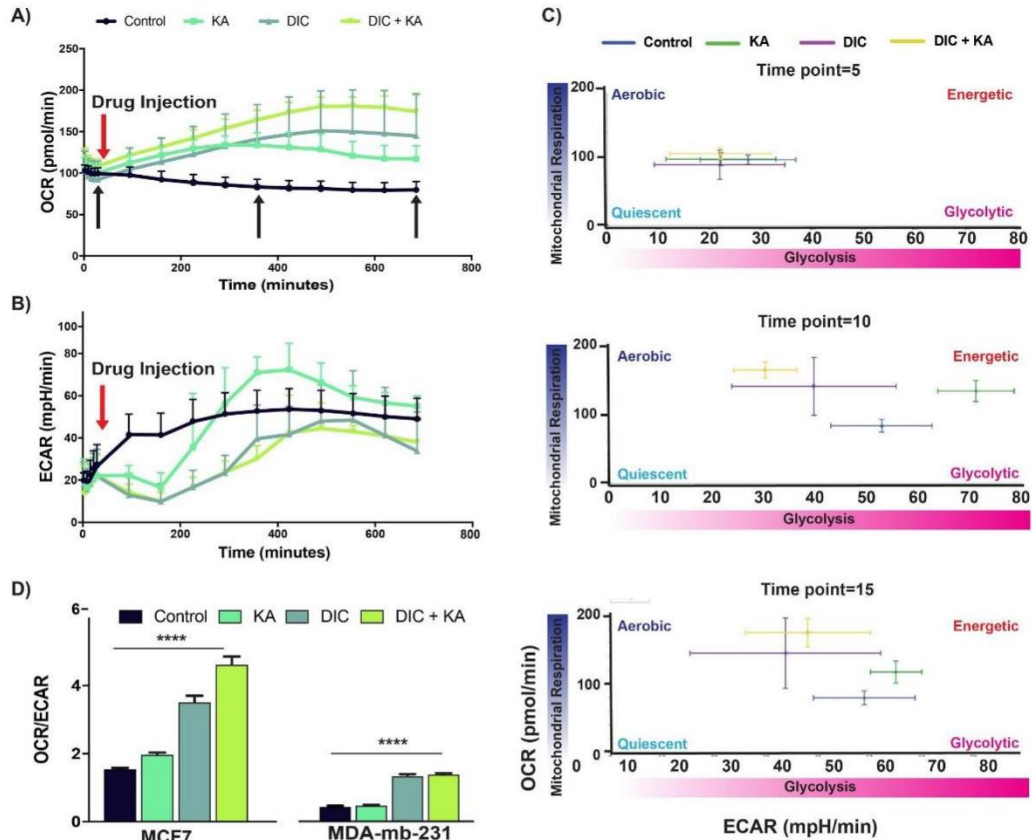


Figure 4.7. Diclofenac and koningic acid reduce the Warburg phenotype of cancer cells. (A) Oxygen Consumption Rate (OCR) and (B) Extracellular acidification rate (ECAR) of MCF7 cancer cells treated with, KA, diclofenac, and combination of both in real-time. (C) Energy map extracted from A and B under different treatments. A combination of KA and diclofenac had the highest effect on the reduction of WE phenotype in MCF7 breast cancer cells. (D) Glycolytic rate assay of both MCF7 and MDA-MB-231 cells confirmed the maximum reduction of WE phenotype with the combination of KA and diclofenac for 72 h. All the seahorse experiments were done in 6 replicates per condition and the data is normalized to the protein concentration of the cells per each well. The data is represented as the mean with the error bars as SD. T-test p-values are represented as follows: **** p < 0.0001.

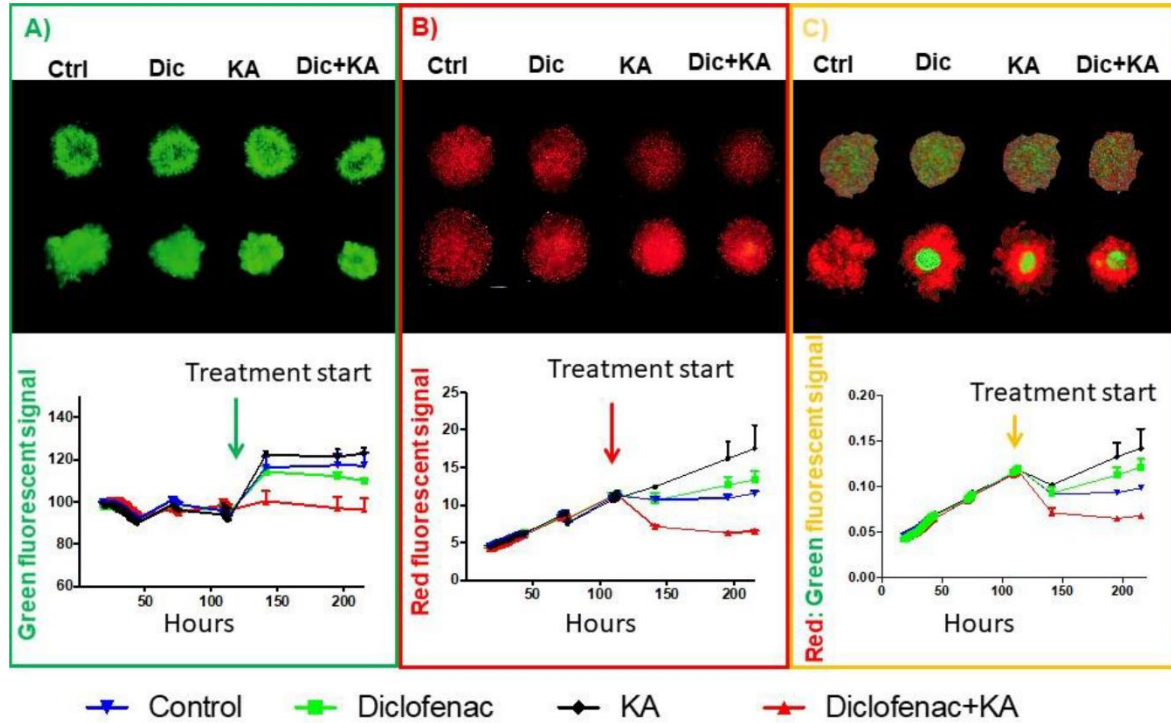


Figure 4.8. Spheroid 3D co-culture shows the role of evolutionary designed treatment in tumor cells population dynamics. (A) Images of the spheroids of MCF7 cells that were fluorescently tagged with GFP in monoculture. (B) Images of spheroids of MDA-MB-231 cells fluorescently tagged with RFP in monoculture. (C) Co-culture of MCF7-GFP and MDA-MB-231-RFP. The ratio in co-culture is 1:1 for experiment initiation. The top row are the pretreatment images and the bottom row for each condition is the last time point images. Underneath the images is a fluorescent signal analysis of the spheroid experiment under all four treatment conditions. Each experiment has 8 replicates. The data are represented as mean with the error bars as SD.

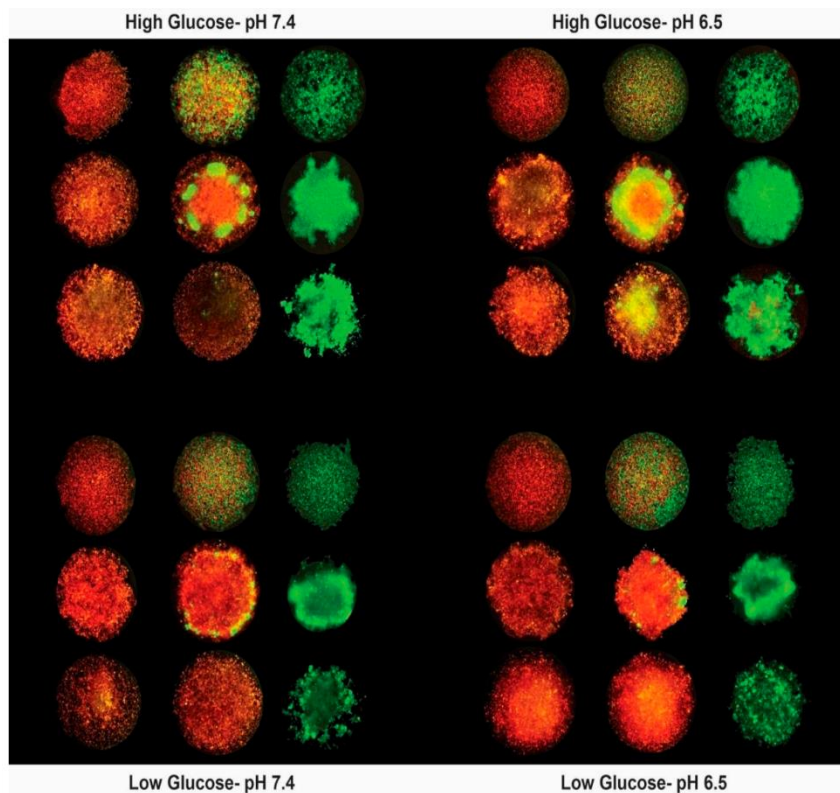


Figure 4.9. Mono- and co-culture of fluorescently tagged breast cancer cell lines. In different microenvironmental conditions and with any initial ratio of MCF7-GFP: MDA-MB-231-RFP, the more aggressive cells, MDA-MB-231 always win. The spheroids are grown in normoxia but will have hypoxia at the center; considering the size of spheres that reach 1–2 mm, we know that the oxygen concentration can vary from normoxia at the surface of spheres to hypoxia in the center.

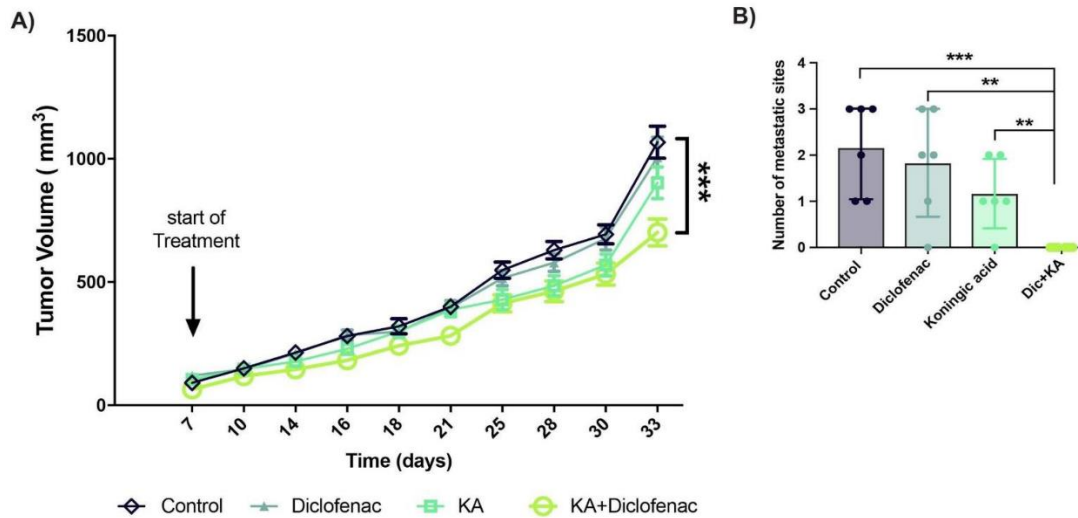


Figure 4.10. Animal experiments confirm the efficiency of evolutionary designed therapy. (A) Female NSG mice injected with a mixture of 5 million MCF7 and 5 million MDA-MB-231 breast cancer cells and randomized into four groups of 6 and treated with, DMSO, diclofenac, KA, and combination. Tumor size is measured every two or three days by calipers and also once a week with ultrasound. Data is presented is measurements by calipers and are mean with SD as their error bars. (B) The number of metastasis sites in vital organs such as liver, lungs, kidney, and spleen at the endpoint. The data is represented as mean with the error bars as the SD. T-test p-values are represented as follows: ** p < 0.01, *** p < 0.001.

Chapter 5: Implications of Findings and Future Directions

At this point it should be well conveyed that the goal of this study was to further characterize the causes and consequences of acidosis in breast cancer. Herein, the implications of the findings of each study and possible future directions to better describe phenomena observed will be discussed.

IMPLICATIONS OF FINDINGS, LIMITATIONS, AND FUTURE DIRECTIONS

Chapter 3: Breast Cancer Adaptation to Acidic Microenvironment Induces a Partial Epithelial to Mesenchymal Transition State

As mentioned, deregulated energetics is a hallmark of cancer progression. In breast cancer, the result of this metabolic rewiring is an increase in a fermentative glycolytic phenotype. Consequentially, the products of fermentation must be released by the cell in this cycle of glucose metabolism. While vasculature clears the acidic products of fermentation, the rate of glucose supply and lactate removal is nearly equal, with the steady-state pH at which a given area of the tumor reaches, depending on the rate of glucose fermentation. This environment is harsh for cells, resulting in large amounts of cells death. In order for populations to survive, cells must adapt at the population level, or acclimate at the individual level in order to be sustained. Due to the imperative of cells adapting to these conditions, understanding how this adaptation occurs and identifying key players may provide a targetable window in combating tumor evolution.

In this study, I set out to further describe how breast cancer cells are able to adapt to the harsh conditions of an acidic environment, and what phenotypic changes occur during this

adaptation. Adaptation of cancer cells to an acidic environment had been studied previously, with investigations showing the increased plasma membrane expression of the lysosomal marker LAMP2b, enhanced aggression, and an increased invasiveness and metastatic capacity [20, 137, 197]. It has also been shown that acute acidosis can induce expression of EMT markers [125, 198]. During this work, we wanted to observe the effects of chronic acidosis on this acid induced EMT phenotype.

This study used MCF7 and MCF-DCIS that were adapted for growth under acidic conditions. Over many rounds of selection, MCF7 and MCF-DCIS cancer cells were able to be adapted to grow under acidic conditions, at a rate equal to those grown under normal pH conditions. This process was done in a previous publication and the cells used were from said work [20]. The significance of the demonstration that breast cancer cells could adapt to grow in an acidic environment was notable, because this meant that there was a significant possibility that populations of cells within a tumor could also adapt to grow under these conditions. In said publication, it was also demonstrated that the markers of this acid-adaptation were present in acidic environments of the tumor, further implicating this process in tumors.

Phenotypic plasticity is a new hallmark of cancer [199]. Unlocking this plasticity is an important aspect of cancer progression because it allows cells to access different phenotypes to better adapt to whatever given current environment they are exposed to. An early indicator of this plastic phenotype was work done describing the stem-like properties of an epithelial to mesenchymal transition (EMT) observed in cancer [200]. While observed in cancer, EMT is a fundamental process in the normal development of embryos. EMT has gone on to be well described as an important factor in cancer progression, invasion and metastasis [201]. More recently, dynamic expression of markers from both epithelial and mesenchymal phenotypes has been described in circulating tumor cells of breast cancer patients [202], leading to the conclusion that a partial transition state is possible. It is now accepted that a partial EMT state is

a common cellular phenotype in breast cancer, and this partial EMT phenotype is heavily implicated in metastasis [203]. Prior to this work, it was shown that acidosis was able to modulate the expression of EMT markers in cancer cells [198, 204]. I began by confirming this phenotype in the acid-adapted breast cancer cell lines and found that the cells had characteristics of both epithelial and mesenchymal cells, placing them in the partial EMT category. This was a substantial finding, as we now know and as was just mentioned, a partial EMT phenotype is heavily associated with a metastatic phenotype in cancer [203]. Having access to both the characteristics of epithelial and mesenchymal phenotypes may allow a cell to better adapt to the dynamic environmental conditions within a tumor, if they are able to modulate their state based on the given environment. It is possible that the acid-adaptation process selects for cells already exhibiting this hybrid EMT phenotype, with an ability to tune their phenotype to the acidic environment for survival.

To further investigate this partial EMT phenotype in the acid-adapted cell populations, our collaborators conducted an integrative analysis of proteomic and transcriptomic data from the acid-adapted cell lines. This led to the discovery of the S100 family proteins, S100B and S100A6 as upregulated in the acid-adapted cell lines, associated with the EMT process. S100 proteins are Ca^{2+} binding proteins. S100B is expressed in a large number of cell types and has been shown to modulate STAT3 and NF- κ B pathways [205-207]; while also being associated with poor prognostic outcomes in breast cancer [208]. S100A6 has been shown to modulate apoptotic pathways [209, 210] and was previously associated with tumorigenesis in a variety of cancer types [211]. I further went on to validate the expression of S100B and S100A6 *in vitro* and S100A6 in samples from breast cancer patients. It was found that the expression of S100A6 was significantly higher in breast cancer patients of any stage, compared to normal breast. The significance of this finding is broad and deep, with these proteins being heavily implicated in driving the EMT process in other cancer types [212, 213], and cells expressing

high levels of S100 family of proteins being shown to be selected for in pancreatic cancer while driving a partial EMT phenotype and metastasis [214].

In total, I showed that cells adapted to an acidic microenvironment display a partial EMT phenotype. We then conducted integrative transcriptomic and proteomic analysis to identify S100A6 and S100B as upregulated hits in multiple acid-adapted breast cancer cell lines. These hits proved to be significant, as they were validated by *in vitro* ICC staining and in breast cancer patients by IHC staining of patient samples. Evidence from this work, taken with other studies conducted on the role S100 proteins play in the EMT and metastases processes, suggests that adaptation of cancer cells to an acidic environment in breast cancer may be interrelated with the EMT process and ultimately, metastasis and mortality in patients.

As mentioned previously, the goal of this study was to investigate the role adaptation to an acidic microenvironment plays in the EMT process and which protein players may be contributing to this transition. As with any study, there exist limitation to the methods of investigation.

We began the study by demonstrating a heterogeneous change in expression of EMT associated markers in the acid-adapted MCF7 cell line. I did this with both immunocytochemistry (ICC) and quantitative PCR (qPCR). The purpose of using these methods of expression detection was both to validate any changes in expression, and also to check for discrepancies between the two methods, as expression changes in protein and RNA levels are not always in agreement. While reproducible, these results are limited as there was only one method of protein detection and one method of RNA detection used. For further validation, protein expression techniques such as western blotting or flow cytometry could have been used, as functionally, protein levels matter most for the state of a cell. Additionally, these expression experiments could have been conducted in another acid-adapted cell line in order to confirm the

phenotype observed. Although, we felt this unnecessary as the association between long-term acidosis and EMT had already been demonstrated by other groups.

After we had identified the hits from the integrative proteomics and transcriptomics analysis, I then set out to validate these hits. I did so using ICC as a measure for expression of the two identified hits, S100A6 and S100B. I also stained for LAMP2B as a control, which is an established marker of an acid-adapted breast cancer phenotype. A similar critique to the validation of EMT marker expression, more *in vitro* methods could have been done here to confirm the expression of the S100A6 and S100B proteins. At the time, it was not felt to be necessary as the hits came from the previously well carried out proteomic and transcriptomic analysis from the same cell lines. It was also planned to carry out analysis of expression of S100A6 in a tumor microarray (TMA) of patient samples, which has more clinical significance than any *in vitro* analysis of cell lines.

The *in vivo* analysis of the expression of S100A6 was carried out in a TMA of breast cancer patient samples. The TMA contained samples from normal breast, DCIS, IDC and IDC with metastasis. I stratified the patients by these subtypes and compared expression of S100A6. While I found an increase in S100A6 with progressing subtypes, it may have also yielded significant results if I classified patients in another manner, such as their molecular subtype. While I validated S100B *in vitro*, resources only allowed us to validate S100A6 in the patient samples, so a clear additional step would have been to conduct these same analyses with expression of S100B in patients.

For additional experiments that could have been outside of further validating what I had shown, more could have been in implicating S100A6 and S100B in the mechanism of the EMT process. While no claims were made that the EMT process was a direct result of S100A6 or S100B expression, determining if a knockout of either of these proteins hindered the acid-adaptation process or attenuated the acid-adapted EMT phenotype would have been an

obvious additional step. Additionally, it could have been tested if over-expression of either of these proteins in the parental cell line could produce an acid-resistant phenotype similar to the acid-adapted cell lines.

In total, the work done in this study demonstrated that MCF7 cells adapted to survive under acidic conditions display a partial EMT phenotype. The answer to whether the adaptation process induced the EMT phenotype or if the EMT phenotype is preexisting and selected for, is still up for question. Our integrative analysis approach identified hits in the S100A6 and S100B proteins, which were shown to be upregulated in the acid adapted MCF7 cells at the protein level via ICC. Lastly, we demonstrated that S100A6 expression increases with staging in breast cancer patients, and a decrease in survival of patients with DCIS breast cancer is associated with higher expression of S100A6. After further investigation, S100A6 may provide a reasonable target in the selective targeting of acid-adapted cell populations in patients presenting with early stage breast cancer.

Chapter 4: Inhibition of glycolysis allows for breast cancer control

Breast tumors are reliant on glucose metabolism and ultimately carry out abnormal levels of glucose fermentation. This fermentation is the main contributor to the overarching theme of this work, tumor acidosis. By targeting glycolysis, it is possible that one would be able to not only inhibit breast cancers main metabolic pathway, but also attenuate the acidic microenvironment that is a driver of tumor evolution and progression.

In this study I set out to build upon previous work demonstrating *in silico* that inhibition of GAPDH under conditions of enhanced acidity within the cell may provide a unique therapeutic vulnerability in breast cancer [53]. Inhibition of glycolysis in the treatment of cancer is not a novel strategy, as there have been previous groups to show the effect inhibition of glycolysis has on tumor growth and cancer cell death [215, 216], but the approach used was novel.

Recently, it has been shown that discriminating tumor subpopulations by their adaptive strategies, or phenotype, rather than their genotypic or transcriptomic identity may provide better insight into tumor populations and their evolution [131]. Therefore, our strategy was to target the glycolytic phenotype as a whole, rather than a specific molecularly identifiable subpopulation.

I began this study by validating the efficacy of the drugs in slowing the glycolytic rate of breast cancer cells, via the metrics of glucose uptake and lactate secretion. The drugs chosen were diclofenac sodium and koningic acid as the pH decreasing agent and GAPDH inhibitor, respectively. I then went on to validate that the drug chosen to lower the intracellular pH of the cells, diclofenac Sodium, carried out its intended function of inhibiting monocarboxylate transporters (MCTs), the main transporters of lactate and protons in cancer. By slowing the release of protons, the intracellular pH would decrease. Previous studies suggested that diclofenac Sodium was an inhibitor of MCT transport in T-cells [170], and I confirmed this finding using an instantaneous measure of lactate transport in the breast cancer cell lines. This is significant as diclofenac Sodium is a common therapeutic agent in the formulation of creams designed to relieve arthritic and muscle pain. The accepted mechanism of action for diclofenac Sodium is as a cyclooxygenase-1 and -2 (COX-1 and -2) inhibitor, but there are many other reported mechanisms of action in the literature [171]. Demonstrating that diclofenac Sodium is a potent inhibitor of lactate transport may explain its high efficacy in relieving muscle pain and inflammation, as muscle and immune metabolism are highly dependent on lactate export [217, 218]. The use of koningic acid as a GAPDH inhibitor was not novel, as its inhibition has been heavily characterized in previous studies [189, 219], including its use in targeting the Warburg effect [173].

We then went on to demonstrate that diclofenac and koningic Acid were effective at decreasing breast cancer cell viability, both individually and in combination. Notably, decreases

in viability were not observed with treatment from aspirin or ibuprofen, both known to be inhibitors of cyclooxygenases, further strengthening the evidence for diclofenac's other mechanisms. To determine if I had achieved the desired effect of lowering the intracellular pH, I measured the intracellular pH of the breast cancer cell lines after treatment with diclofenac and observed significant decreases in most groups. Notably, the decreases in intracellular pH were not as severe as would be expected with the observation of total lactate flux inhibition from diclofenac. It has since been described that inhibition of MCT inhibitors alone does not reduce the overall flux of lactate production due to a proportional increase in the transmembrane driving force of lactate upon inhibition of extracellular lactate flux [220]. To determine how treatment with diclofenac and koningic acid effects the metabolism of breast cancer cell lines, Seahorse measurements of oxygen consumption rate (OCR) and extracellular acidification rate (ECAR). With these experiments, I showed that combination treatment with diclofenac and koningic acid results in breast cancer cells exhibiting a more oxidative state.

Cellular populations within a tumor are highly heterogeneous and independent, and as such they must compete with each other for survival. This is a result of Darwinian selection by survival of fittest, and understanding what allows one population to outcompete another may help in our understanding of tumor progression. Competition experiments among cancer cell lines have been done to model how two distinct populations within a tumor may interact and compete with one another [195]. In this work, I conducted spheroid competition experiments with MCF7 and MDA-MB-231 breast cancer cell lines. It was observed that when cultured in mixture, the MDA-MB-231 cell line quickly and consistently took over the population. Given the phenotypic nature of these two cell lines, I equate this to a highly glycolytic and aggressive cell line being able to outcompete the more benign. Interestingly, when treated with diclofenac, koningic acid, or the combination of the two, the population dynamics of the two cell lines were more stable, and the two co-existed in the spheroid. To validate if this was caused by the effect

of these drugs on metabolism, I repeated the co-culture of MDA-MB-231 and MCF7 in spheroids with media containing different concentrations of glucose and different pH levels. I found that growing these co-culture spheroids at low pH allowed for the extended maintenance of the MCF7 population. Low pH is known to be a potent inhibitor of glycolysis and lactate transport, as is the combination of diclofenac and koningic acid. Notably, it has been shown previously that competition between cancer cell populations results in tumor suppressing effects [221].

To finish this study, I wanted to measure the effect the drug combination of diclofenac and koningic acid would have on tumor growth and metastasis *in vivo*. We conducted a tumor growth experiment with injections containing a 50:50 ratio of MDA-MB-231 cells to MCF7 cells. We observed a slight but significant decrease in tumor volume at the end point in the group of mice treated with the combination of diclofenac and koningic acid. The most striking result from this experiment was the difference in presence of metastases. In the group of mice receiving treatment with the combination of diclofenac and koningic acid, there were 0 metastases present in any of the 6 mice. This result was significantly less metastases compared to not only the control group, but also the two monotherapy groups receiving only diclofenac or only koningic acid. It is estimated that 90% of cancer deaths are attributed to metastasis [222]. Creating a treatment strategy that is effective at preventing metastasis could have significant clinical impact. Most patients presenting with only a primary tumor will receive resection or some cytotoxic treatment with the goal of decreasing the tumor burden. Our treatment strategy did not reverse tumor growth, and as such would be difficult to implement as a first line therapy. Where this strategy may hold bearing is as a maintenance therapy after the tumor burden has been reduced, in order to prevent the growth of spontaneous or dormant metastasis that frequently occur in breast cancer patients who received prior treatment.

While this work holds a place in the larger sum of literature, there were limitations to the methods of investigation used. In this study I set out to test the efficacy of a proof-of-concept treatment strategy proposed in publication by our group and others, previously. This involved a dual-drug therapy targeting the glycolytic pathway, in which a GAPDH inhibitor was used, and its effect acted synergistically with a decrease in intracellular pH. Studies involving demonstration of efficacy of these drugs in achieving their intended effects on cell metabolism were comprehensive, demonstrating how these drugs worked in tandem to alter tumor population dynamics and growth could have been improved by additional experiments.

During my spheroid experiments, I conducted mixed cultures of MCF7 and MDA-MB-231 cell lines. While MCF7 and MDA-MB-231 represent two opposite ends of the breast cancer spectrum, being hormone receptor positive and lowly metastatic vs hormone receptor negative and highly metastatic, the study would have been enhanced by including competition experiments conducted with a range of cell lines. The changes in population dynamics observed with drug treatment or changes in microenvironmental conditions may not hold true if two cell lines of the same receptor status or of similar metastatic nature were pitted against one another. Another notable and contradictory finding in the spheroid experiments was that of viability. When treating spheroids with the diclofenac and koningic acid individually or in combination, decreases in growth were observed, but cell death did not appear to be occurring. In our CCK8 viability assays, it appeared that the drugs were inducing cell death. The CCK8 assay relies on dehydrogenases for its efficacy. It is possible that our drug combination was altering dehydrogenase activity, without having the large affect on viability that we observed. In the future, conducting viability assays with alternative measures would be suggested.

Once I determined that treatment with the dual-drug therapy was sufficient to maintain heterogeneity among the mixed culture of MCF7's and MDA-MB-231's, I wanted to determine what this would mean for tumor growth and metastasis. During this we showed that the drug

combination was successful in decreasing tumor volume and metastasis. While we would not have been able to ensure the same distinct heterogeneity our model had (mixture of two cell lines) it may have been beneficial to observe the effects of this treatment on a different model of breast cancer metastasis. This would have given a more broad significance to the findings, and may have aided in pushing these findings in the clinical direction. For the investigation of metastasis, it may have also been beneficial to image resected tissues to check for the presence of fluorescently labelled cells, in order to ensure that while there were no visible presence of metastasis, there were also no micro-metastases present.

An interesting relationship that was observed in this study was between cancer cell competition, metabolism, and environment. Modulating the glycolytic pathway, altering glucose concentrations, and altering media pH, were all sufficient in altering the competition between MCF7 and MDA-MB-231 cell lines. With cancer development being an evolutionary process, and competition as a main driver of natural selection, understanding how cancer cells compete with one another for resources could provide deep insight into cancer progression. I hypothesize that this competition for resources is a main driver in the initiation and progression of tumors. Further investigation into this observation with the modulation of additional resources, or the competition of additional cell lines may yield significant findings about the nature of competition for resources in a tumor.

The final conclusion of the paper was that treatment of tumor bearing mice with the diclofenac and koningic acid dual-therapy was able to completely ablate metastasis. Metastasis is the number one cause of cancer patient death, and metastasis can occur after resection of the primary. A final direction for this work would be to see how this combination therapy works in preventing metastasis in a model of breast cancer recurrence, in which the primary has been removed. If effective, this treatment strategy may be effective as a post-operative therapy for patients who do not present with metastases, but are at high risk for recurrence or metastasis.

In summary of this work, it was demonstrated that diclofenac sodium is a potent inhibitor MCT function. We also demonstrated that treatment of cells with diclofenac was able to decrease the intracellular pH of breast cancer cells, providing an opportunity to test our therapeutic strategy. The diclofenac and koningic acid combination therapy was effective in reducing the Warburg phenotype of the cells and altering the cells fermentative metabolism. Treatment of MCF7 / MDA-MB-231 co-culture spheroids with our diclofenac and koningic acid combination therapy was sufficient to maintain population heterogeneity, allowing the MCF7 population to be maintained when it otherwise would not. Lastly, treatment of *in vivo* mouse models implanted with MCF7 / MDA-MB-231 cell mixtures with our diclofenac and koningic acid combination therapy was able to significantly decrease tumor growth and completely ablate visible metastasis. With further investigation, this treatment strategy may have an opportunity to provide therapeutic benefit to post-operative breast cancer patients in the future.

CONCLUDING REMARKS

In total, the aim of this work was to further the fields' understanding of how acidosis alters the phenotype of breast cancer cells, and to present an alternative strategy for how one may go about targeting the acidotic phenotype in breast cancer. There is no doubt that acidosis contributes greatly towards altering the phenotype of breast tumors. Understanding the culmination of the effects it has, and how the causes or consequences of acidosis can be attenuated to improve patients' outcomes should be an imminent mission of the cancer research community.

References

1. *Global Cancer Observatory 2020*, International Agency for Research on Cancer.
2. Azamjah, N., Y. Soltan-Zadeh, and F. Zayeri, *Global Trend of Breast Cancer Mortality Rate: A 25-Year Study*. Asian Pac J Cancer Prev, 2019. **20**(7): p. 2015-2020.
3. Hendrick, R.E., M.A. Helvie, and D.L. Monticciolo, *Breast Cancer Mortality Rates Have Stopped Declining in U.S. Women Younger than 40 Years*. Radiology, 2021. **299**(1): p. 143-149.
4. Sung, H., et al., *Global Cancer Statistics 2020: GLOBOCAN Estimates of Incidence and Mortality Worldwide for 36 Cancers in 185 Countries*. CA Cancer J Clin, 2021. **71**(3): p. 209-249.
5. Hendrick, R.E., et al., *Age distributions of breast cancer diagnosis and mortality by race and ethnicity in US women*. Cancer, 2021. **127**(23): p. 4384-4392.
6. *TNM staging*. 2020 July 21, 2020; Available from: <https://www.cancerresearchuk.org/about-cancer/breast-cancer/stages-types-grades/tnm-staging>.
7. Knight, W.A., et al., *Estrogen receptor as an independent prognostic factor for early recurrence in breast cancer*. Cancer Res, 1977. **37**(12): p. 4669-71.
8. Meyer, J.S., et al., *Low incidence of estrogen receptor in breast carcinomas with rapid rates of cellular replication*. Cancer, 1977. **40**(5): p. 2290-8.
9. Samal, B.A., et al., *Estrogen receptors and responsiveness of advanced breast cancer to chemotherapy*. Cancer, 1980. **46**(12 Suppl): p. 2925-7.
10. Horwitz, K.B. and W.L. McGuire, *Specific progesterone receptors in human breast cancer*. Steroids, 1975. **25**(4): p. 497-505.

11. Pauletti, G., et al., *Detection and quantitation of HER-2/neu gene amplification in human breast cancer archival material using fluorescence in situ hybridization*. *Oncogene*, 1996. **13**(1): p. 63-72.
12. Siadati, S., et al., *Correlation of ER, PR and HER-2/Neu with other Prognostic Factors in Infiltrating Ductal Carcinoma of Breast*. *Iran J Pathol*, 2015. **10**(3): p. 221-6.
13. Perou, C.M., et al., *Molecular portraits of human breast tumours*. *Nature*, 2000. **406**(6797): p. 747-52.
14. Cheang, M.C., et al., *Ki67 index, HER2 status, and prognosis of patients with luminal B breast cancer*. *J Natl Cancer Inst*, 2009. **101**(10): p. 736-50.
15. Cappelletti, V., et al., *Metabolic Footprints and Molecular Subtypes in Breast Cancer*. *Dis Markers*, 2017. **2017**: p. 7687851.
16. Avril, N., et al., *Metabolic characterization of breast tumors with positron emission tomography using F-18 fluorodeoxyglucose*. *J Clin Oncol*, 1996. **14**(6): p. 1848-57.
17. Anemone, A., et al., *Tumour acidosis evaluated in vivo by MRI-CEST pH imaging reveals breast cancer metastatic potential*. *Br J Cancer*, 2021. **124**(1): p. 207-216.
18. Ghergurovich, J.M., et al., *Local production of lactate, ribose phosphate, and amino acids within human triple-negative breast cancer*. *Med (N Y)*, 2021. **2**(6): p. 736-754.
19. Estrella, V., et al., *Acidity generated by the tumor microenvironment drives local invasion*. *Cancer Res*, 2013. **73**(5): p. 1524-35.
20. Damaghi, M., et al., *Chronic acidosis in the tumour microenvironment selects for overexpression of LAMP2 in the plasma membrane*. *Nat Commun*, 2015. **6**: p. 8752.
21. Sadeghi, M., et al., *Integrative Analysis of Breast Cancer Cells Reveals an Epithelial-Mesenchymal Transition Role in Adaptation to Acidic Microenvironment*. *Front Oncol*, 2020. **10**: p. 304.
22. Rattigan, Y.I., et al., *Lactate is a mediator of metabolic cooperation between stromal carcinoma associated fibroblasts and glycolytic tumor cells in the tumor microenvironment*. *Exp Cell Res*, 2012. **318**(4): p. 326-35.

23. Fischbeck, A.J., et al., *Tumor Lactic Acidosis: Protecting Tumor by Inhibiting Cytotoxic Activity Through Motility Arrest and Bioenergetic Silencing*. Front Oncol, 2020. **10**: p. 589434.
24. Varanasi, U.R., B. Carr, and D.P. Simpson, *Lactic acidosis associated with metastatic breast carcinoma*. Cancer Treat Rep, 1980. **64**(12): p. 1283-5.
25. Warner, E., *Type B lactic acidosis and metastatic breast cancer*. Breast Cancer Res Treat, 1992. **24**(1): p. 75-9.
26. Evans, T.R., et al., *Lactic acidosis. A presentation of metastatic breast cancer arising in pregnancy*. Cancer, 1992. **69**(2): p. 453-6.
27. Schornack, P.A. and R.J. Gillies, *Contributions of cell metabolism and H⁺ diffusion to the acidic pH of tumors*. Neoplasia, 2003. **5**(2): p. 135-45.
28. Stubbs, M., et al., *Causes and consequences of tumour acidity and implications for treatment*. Mol Med Today, 2000. **6**(1): p. 15-9.
29. Gillies, R.J., Z. Liu, and Z. Bhujwalla, *³¹P-MRS measurements of extracellular pH of tumors using 3-aminopropylphosphonate*. Am J Physiol, 1994. **267**(1 Pt 1): p. C195-203.
30. van Sluis, R., et al., *In vivo imaging of extracellular pH using ¹H MRSI*. Magn Reson Med, 1999. **41**(4): p. 743-50.
31. Damaghi, M. and R. Gillies, *Phenotypic changes of acid-adapted cancer cells push them toward aggressiveness in their evolution in the tumor microenvironment*. Cell Cycle, 2017. **16**(19): p. 1739-1743.
32. Bellone, M., et al., *The acidity of the tumor microenvironment is a mechanism of immune escape that can be overcome by proton pump inhibitors*. Oncoimmunology, 2013. **2**(1): p. e22058.
33. Ibrahim Hashim, A., et al., *Reduction of metastasis using a non-volatile buffer*. Clin Exp Metastasis, 2011. **28**(8): p. 841-9.
34. Ibrahim-Hashim, A., et al., *Systemic buffers inhibit carcinogenesis in TRAMP mice*. J Urol, 2012. **188**(2): p. 624-31.

35. Bailey, K.M., et al., *Mechanisms of buffer therapy resistance*. Neoplasia, 2014. **16**(4): p. 354-64 e1-3.
36. Zucca-Matthes, G., C. Urban, and A. Vallejo, *Anatomy of the nipple and breast ducts*. Gland Surg, 2016. **5**(1): p. 32-6.
37. Tobon, H. and H. Salazar, *Ultrastructure of the human mammary gland. II. Postpartum lactogenesis*. J Clin Endocrinol Metab, 1975. **40**(5): p. 834-44.
38. Gatenby, R.A. and R.J. Gillies, *Why do cancers have high aerobic glycolysis?* Nat Rev Cancer, 2004. **4**(11): p. 891-9.
39. Ordway, B., et al., *Causes and Consequences of Variable Tumor Cell Metabolism on Heritable Modifications and Tumor Evolution*. Front Oncol, 2020. **10**: p. 373.
40. Lorusso, G. and C. Ruegg, *The tumor microenvironment and its contribution to tumor evolution toward metastasis*. Histochem Cell Biol, 2008. **130**(6): p. 1091-103.
41. Yuan, Y., *Spatial Heterogeneity in the Tumor Microenvironment*. Cold Spring Harb Perspect Med, 2016. **6**(8).
42. Gillies, R.J. and R.A. Gatenby, *Hypoxia and adaptive landscapes in the evolution of carcinogenesis*. Cancer Metastasis Rev, 2007. **26**(2): p. 311-7.
43. Gillies, R.J. and R.A. Gatenby, *Adaptive landscapes and emergent phenotypes: why do cancers have high glycolysis?* J Bioenerg Biomembr, 2007. **39**(3): p. 251-7.
44. Gatenby, R.A., R.J. Gillies, and J.S. Brown, *Evolutionary dynamics of cancer prevention*. Nat Rev Cancer, 2010. **10**(8): p. 526-7.
45. Gatenby, R.A. and R.J. Gillies, *A microenvironmental model of carcinogenesis*. Nat Rev Cancer, 2008. **8**(1): p. 56-61.
46. Pouyssegur, J., F. Dayan, and N.M. Mazure, *Hypoxia signalling in cancer and approaches to enforce tumour regression*. Nature, 2006. **441**(7092): p. 437-43.
47. Semenza, G.L., *Life with oxygen*. Science, 2007. **318**(5847): p. 62-4.

48. Bracken, C.P., et al., *Cell-specific regulation of hypoxia-inducible factor (HIF)-1alpha and HIF-2alpha stabilization and transactivation in a graded oxygen environment*. J Biol Chem, 2006. **281**(32): p. 22575-85.
49. Majmundar, A.J., W.J. Wong, and M.C. Simon, *Hypoxia-inducible factors and the response to hypoxic stress*. Mol Cell, 2010. **40**(2): p. 294-309.
50. Hardie, D.G., *Molecular Pathways: Is AMPK a Friend or a Foe in Cancer?* Clin Cancer Res, 2015. **21**(17): p. 3836-40.
51. Harachi, M., et al., *mTOR Complexes as a Nutrient Sensor for Driving Cancer Progression*. Int J Mol Sci, 2018. **19**(10).
52. Epstein, T., et al., *Separation of metabolic supply and demand: aerobic glycolysis as a normal physiological response to fluctuating energetic demands in the membrane*. Cancer Metab, 2014. **2**: p. 7.
53. Persi, E., et al., *Systems analysis of intracellular pH vulnerabilities for cancer therapy*. Nat Commun, 2018. **9**(1): p. 2997.
54. Damaghi, M., J.W. Wojtkowiak, and R.J. Gillies, *pH sensing and regulation in cancer*. Front Physiol, 2013. **4**: p. 370.
55. Offermanns, S., *Hydroxy-Carboxylic Acid Receptor Actions in Metabolism*. Trends Endocrinol Metab, 2017. **28**(3): p. 227-236.
56. Wu, Y., et al., *Acid-sensing ion channels contribute to the effect of extracellular acidosis on proliferation and migration of A549 cells*. Tumour Biol, 2017. **39**(6): p. 1010428317705750.
57. Zhou, Z.H., et al., *The acid-sensing ion channel, ASIC2, promotes invasion and metastasis of colorectal cancer under acidosis by activating the calcineurin/NFAT1 axis*. J Exp Clin Cancer Res, 2017. **36**(1): p. 130.
58. Sadeghi, M., Ordway, B., Rafiei, I., Borad, P., Fang, B., Koomen, J.L., Zhang, C., Yoder, S., Johnson, J., Damaghi, M., *Integrative Analysis of Breast Cancer Cells Reveals an Epithelial-Mesenchymal Transition Role in Adaptation to Acidic Microenvironment*. Frontiers in Oncology, 2020. **10**.
59. Handy, D.E., R. Castro, and J. Loscalzo, *Epigenetic modifications: basic mechanisms and role in cardiovascular disease*. Circulation, 2011. **123**(19): p. 2145-56.

60. Feinberg, A.P. and B. Vogelstein, *Hypomethylation distinguishes genes of some human cancers from their normal counterparts*. Nature, 1983. **301**(5895): p. 89-92.
61. Feinberg, A.P. and B. Vogelstein, *Hypomethylation of ras oncogenes in primary human cancers*. Biochem Biophys Res Commun, 1983. **111**(1): p. 47-54.
62. Goelz, S.E., et al., *Hypomethylation of DNA from benign and malignant human colon neoplasms*. Science, 1985. **228**(4696): p. 187-90.
63. Cheah, M.S., C.D. Wallace, and R.M. Hoffman, *Hypomethylation of DNA in human cancer cells: a site-specific change in the c-myc oncogene*. J Natl Cancer Inst, 1984. **73**(5): p. 1057-65.
64. Cox, R. and M.T. Tuck, *Alteration of methylation patterns in rat liver histones following administration of ethionine, a liver carcinogen*. Cancer Res, 1981. **41**(4): p. 1253-6.
65. Miranda-Goncalves, V., et al., *Corrigendum: Metabolism and Epigenetic Interplay in Cancer: Regulation and Putative Therapeutic Targets*. Front Genet, 2019. **10**: p. 784.
66. Helmlinger, G., et al., *Interstitial pH and pO₂ gradients in solid tumors in vivo: high-resolution measurements reveal a lack of correlation*. Nat Med, 1997. **3**(2): p. 177-82.
67. Tafreshi, N.K., R.J. Gillies, and D.L. Morse, *Molecular imaging of breast cancer lymph node metastasis*. Eur J Radiol, 2012. **81 Suppl 1**: p. S160-1.
68. Latham, T., et al., *Lactate, a product of glycolytic metabolism, inhibits histone deacetylase activity and promotes changes in gene expression*. Nucleic Acids Res, 2012. **40**(11): p. 4794-803.
69. Wagner, W., W.M. Ciszewski, and K.D. Kania, *L- and D-lactate enhance DNA repair and modulate the resistance of cervical carcinoma cells to anticancer drugs via histone deacetylase inhibition and hydroxycarboxylic acid receptor 1 activation*. Cell Commun Signal, 2015. **13**: p. 36.
70. Corbet, C., et al., *The SIRT1/HIF2 α axis drives reductive glutamine metabolism under chronic acidosis and alters tumor response to therapy*. Cancer Res, 2014. **74**(19): p. 5507-19.
71. Corbet, C., et al., *Acidosis Drives the Reprogramming of Fatty Acid Metabolism in Cancer Cells through Changes in Mitochondrial and Histone Acetylation*. Cell Metab, 2016. **24**(2): p. 311-23.

72. Fodor, B.D., et al., *Jmjd2b antagonizes H3K9 trimethylation at pericentric heterochromatin in mammalian cells*. Genes Dev, 2006. **20**(12): p. 1557-62.
73. Whetstine, J.R., et al., *Reversal of histone lysine trimethylation by the JMJD2 family of histone demethylases*. Cell, 2006. **125**(3): p. 467-81.
74. Wu, H. and Y. Zhang, *Mechanisms and functions of Tet protein-mediated 5-methylcytosine oxidation*. Genes Dev, 2011. **25**(23): p. 2436-52.
75. Cimmino, F., et al., *HIF-1 transcription activity: HIF1A driven response in normoxia and in hypoxia*. BMC Med Genet, 2019. **20**(1): p. 37.
76. Thienpont, B., et al., *Tumour hypoxia causes DNA hypermethylation by reducing TET activity*. Nature, 2016. **537**(7618): p. 63-68.
77. Bungard, D., et al., *Signaling kinase AMPK activates stress-promoted transcription via histone H2B phosphorylation*. Science, 2010. **329**(5996): p. 1201-5.
78. Yi, S.A., et al., *S6K1 Phosphorylation of H2B Mediates EZH2 Trimethylation of H3: A Determinant of Early Adipogenesis*. Mol Cell, 2016. **62**(3): p. 443-452.
79. Csibi, A., et al., *The mTORC1 pathway stimulates glutamine metabolism and cell proliferation by repressing SIRT4*. Cell, 2013. **153**(4): p. 840-54.
80. Anderson, K.A., et al., *SIRT4 Is a Lysine Deacylase that Controls Leucine Metabolism and Insulin Secretion*. Cell Metab, 2017. **25**(4): p. 838-855 e15.
81. Toska, E., et al., *PI3K Inhibition Activates SGK1 via a Feedback Loop to Promote Chromatin-Based Regulation of ER-Dependent Gene Expression*. Cell Rep, 2019. **27**(1): p. 294-306 e5.
82. Koren, S. and M. Bentires-Alj, *Tackling Resistance to PI3K Inhibition by Targeting the Epigenome*. Cancer Cell, 2017. **31**(5): p. 616-618.
83. Sidoli, S., et al., *Integrated Analysis of Acetyl-CoA and Histone Modification via Mass Spectrometry to Investigate Metabolically Driven Acetylation*. Methods Mol Biol, 2019. **1928**: p. 125-147.
84. Lee, J.V., et al., *Akt-dependent metabolic reprogramming regulates tumor cell histone acetylation*. Cell Metab, 2014. **20**(2): p. 306-319.

85. Zhang, D., et al., *Metabolic regulation of gene expression by histone lactylation*. Nature, 2019. **574**(7779): p. 575-580.
86. Kawazu, M., et al., *Histone demethylase JMJD2B functions as a co-factor of estrogen receptor in breast cancer proliferation and mammary gland development*. PLoS One, 2011. **6**(3): p. e17830.
87. Toyokawa, G., et al., *The histone demethylase JMJD2B plays an essential role in human carcinogenesis through positive regulation of cyclin-dependent kinase 6*. Cancer Prev Res (Phila), 2011. **4**(12): p. 2051-61.
88. Fu, L., et al., *HIF-1alpha-induced histone demethylase JMJD2B contributes to the malignant phenotype of colorectal cancer cells via an epigenetic mechanism*. Carcinogenesis, 2012. **33**(9): p. 1664-73.
89. Kim, J.G., et al., *Histone demethylase JMJD2B-mediated cell proliferation regulated by hypoxia and radiation in gastric cancer cell*. Biochim Biophys Acta, 2012. **1819**(11-12): p. 1200-7.
90. Mariani, C.J., et al., *TET1-mediated hydroxymethylation facilitates hypoxic gene induction in neuroblastoma*. Cell Rep, 2014. **7**(5): p. 1343-1352.
91. Good, C.R., et al., *TET1-Mediated Hypomethylation Activates Oncogenic Signaling in Triple-Negative Breast Cancer*. Cancer Res, 2018. **78**(15): p. 4126-4137.
92. Goel, A., S.P. Mathupala, and P.L. Pedersen, *Glucose metabolism in cancer. Evidence that demethylation events play a role in activating type II hexokinase gene expression*. J Biol Chem, 2003. **278**(17): p. 15333-40.
93. Wolf, A., et al., *Developmental profile and regulation of the glycolytic enzyme hexokinase 2 in normal brain and glioblastoma multiforme*. Neurobiol Dis, 2011. **44**(1): p. 84-91.
94. Ma, Z., et al., *Epigenetic drift of H3K27me3 in aging links glycolysis to healthy longevity in Drosophila*. Elife, 2018. **7**.
95. Miyo, M., et al., *Tumour-suppressive function of SIRT4 in human colorectal cancer*. Br J Cancer, 2015. **113**(3): p. 492-9.
96. Sun, H., et al., *SIRT4 acts as a tumor suppressor in gastric cancer by inhibiting cell proliferation, migration, and invasion*. Onco Targets Ther, 2018. **11**: p. 3959-3968.

97. Toska, E., et al., *PI3K pathway regulates ER-dependent transcription in breast cancer through the epigenetic regulator KMT2D*. Science, 2017. **355**(6331): p. 1324-1330.
98. Camarda, R., J. Williams, and A. Goga, *In vivo Reprogramming of Cancer Metabolism by MYC*. Front Cell Dev Biol, 2017. **5**: p. 35.
99. Fisel, P., et al., *DNA methylation of the SLC16A3 promoter regulates expression of the human lactate transporter MCT4 in renal cancer with consequences for clinical outcome*. Clin Cancer Res, 2013. **19**(18): p. 5170-81.
100. Gatenby, R.A. and R.J. Gillies, *Glycolysis in cancer: a potential target for therapy*. Int J Biochem Cell Biol, 2007. **39**(7-8): p. 1358-66.
101. Choi, Y.K. and K.G. Park, *Targeting Glutamine Metabolism for Cancer Treatment*. Biomol Ther (Seoul), 2018. **26**(1): p. 19-28.
102. Cluntun, A.A., et al., *Glutamine Metabolism in Cancer: Understanding the Heterogeneity*. Trends Cancer, 2017. **3**(3): p. 169-180.
103. Jiang, J., S. Srivastava, and J. Zhang, *Starve Cancer Cells of Glutamine: Break the Spell or Make a Hungry Monster?* Cancers (Basel), 2019. **11**(6).
104. Medina, M.A. and I. Nunez de Castro, *Glutaminolysis and glycolysis interactions in proliferant cells*. Int J Biochem, 1990. **22**(7): p. 681-3.
105. DeBerardinis, R.J. and T. Cheng, *Q's next: the diverse functions of glutamine in metabolism, cell biology and cancer*. Oncogene, 2010. **29**(3): p. 313-24.
106. Kim, S., et al., *Metabolic phenotypes in triple-negative breast cancer*. Tumour Biol, 2013. **34**(3): p. 1699-712.
107. Wang, L., et al., *Autophagy mediates glucose starvation-induced glioblastoma cell quiescence and chemoresistance through coordinating cell metabolism, cell cycle, and survival*. Cell Death Dis, 2018. **9**(2): p. 213.
108. Li, Y., D.A. Petrov, and G. Sherlock, *Single nucleotide mapping of trait space reveals Pareto fronts that constrain adaptation*. Nat Ecol Evol, 2019. **3**(11): p. 1539-1551.
109. Gouirand, V., F. Guillaumond, and S. Vasseur, *Influence of the Tumor Microenvironment on Cancer Cells Metabolic Reprogramming*. Front Oncol, 2018. **8**: p. 117.

110. Gravenmier, C.A., M. Siddique, and R.A. Gatenby, *Adaptation to Stochastic Temporal Variations in Intratumoral Blood Flow: The Warburg Effect as a Bet Hedging Strategy*. Bull Math Biol, 2018. **80**(5): p. 954-970.
111. Epstein, T., R.A. Gatenby, and J.S. Brown, *The Warburg effect as an adaptation of cancer cells to rapid fluctuations in energy demand*. PLoS One, 2017. **12**(9): p. e0185085.
112. Brooks, A.N., et al., *Adaptation of cells to new environments*. Wiley Interdiscip Rev Syst Biol Med, 2011. **3**(5): p. 544-61.
113. Marjanovic, N.D., R.A. Weinberg, and C.L. Chaffer, *Cell plasticity and heterogeneity in cancer*. Clin Chem, 2013. **59**(1): p. 168-79.
114. Cabrera, M.C., R.E. Hollingsworth, and E.M. Hurt, *Cancer stem cell plasticity and tumor hierarchy*. World J Stem Cells, 2015. **7**(1): p. 27-36.
115. Karacosta, L.G., et al., *Mapping lung cancer epithelial-mesenchymal transition states and trajectories with single-cell resolution*. Nat Commun, 2019. **10**(1): p. 5587.
116. Lovisa, S., M. Zeisberg, and R. Kalluri, *Partial Epithelial-to-Mesenchymal Transition and Other New Mechanisms of Kidney Fibrosis*. Trends Endocrinol Metab, 2016. **27**(10): p. 681-695.
117. Aiello, N.M., et al., *EMT Subtype Influences Epithelial Plasticity and Mode of Cell Migration*. Dev Cell, 2018. **45**(6): p. 681-695 e4.
118. Jolly, M.K., et al., *Hybrid epithelial/mesenchymal phenotypes promote metastasis and therapy resistance across carcinomas*. Pharmacol Ther, 2019. **194**: p. 161-184.
119. Dirkse, A., et al., *Stem cell-associated heterogeneity in Glioblastoma results from intrinsic tumor plasticity shaped by the microenvironment*. Nat Commun, 2019. **10**(1): p. 1787.
120. Gupta, P.B., et al., *Phenotypic Plasticity: Driver of Cancer Initiation, Progression, and Therapy Resistance*. Cell Stem Cell, 2019. **24**(1): p. 65-78.
121. Enderling, H., *Cancer stem cells: small subpopulation or evolving fraction?* Integr Biol (Camb), 2015. **7**(1): p. 14-23.

122. Tan, E.J., A.K. Olsson, and A. Moustakas, *Reprogramming during epithelial to mesenchymal transition under the control of TGFbeta*. Cell Adh Migr, 2015. **9**(3): p. 233-46.
123. Valcourt, U., et al., *Analysis of Epithelial-Mesenchymal Transition Induced by Transforming Growth Factor beta*. Methods Mol Biol, 2016. **1344**: p. 147-81.
124. Tang, C., et al., *Transcriptional regulation of FoxM1 by HIF1alpha mediates hypoxia-induced EMT in prostate cancer*. Oncol Rep, 2019.
125. Suzuki, A., et al., *Acidic extracellular pH promotes epithelial mesenchymal transition in Lewis lung carcinoma model*. Cancer Cell Int, 2014. **14**(1): p. 129.
126. Wykoff, C.C., et al., *Hypoxia-inducible expression of tumor-associated carbonic anhydrases*. Cancer Res, 2000. **60**(24): p. 7075-83.
127. Gerlinger, M., et al., *Intratumor heterogeneity and branched evolution revealed by multiregion sequencing*. N Engl J Med, 2012. **366**(10): p. 883-92.
128. Sottoriva, A., et al., *Intratumor heterogeneity in human glioblastoma reflects cancer evolutionary dynamics*. Proc Natl Acad Sci U S A, 2013. **110**(10): p. 4009-14.
129. Baird, R.D. and C. Caldas, *Genetic heterogeneity in breast cancer: the road to personalized medicine?* BMC Med, 2013. **11**: p. 151.
130. Yachida, S. and C.A. Iacobuzio-Donahue, *Evolution and dynamics of pancreatic cancer progression*. Oncogene, 2013. **32**(45): p. 5253-60.
131. Ibrahim-Hashim, A., et al., *Defining Cancer Subpopulations by Adaptive Strategies Rather Than Molecular Properties Provides Novel Insights into Intratumoral Evolution*. Cancer Res, 2017. **77**(9): p. 2242-2254.
132. Ercan, D., et al., *Amplification of EGFR T790M causes resistance to an irreversible EGFR inhibitor*. Oncogene, 2010. **29**(16): p. 2346-56.
133. Gillies, R.J., I. Robey, and R.A. Gatenby, *Causes and consequences of increased glucose metabolism of cancers*. J Nucl Med, 2008. **49 Suppl 2**: p. 24S-42S.

134. Xu, L., D. Fukumura, and R.K. Jain, *Acidic extracellular pH induces vascular endothelial growth factor (VEGF) in human glioblastoma cells via ERK1/2 MAPK signaling pathway: mechanism of low pH-induced VEGF*. J Biol Chem, 2002. **277**(13): p. 11368-74.
135. Lardner, A., *The effects of extracellular pH on immune function*. J Leukoc Biol, 2001. **69**(4): p. 522-30.
136. Pilon-Thomas, S., et al., *Neutralization of tumor acidity improves antitumor responses to immunotherapeutic interventions*. Cancer Res, 2015.
137. Damaghi, M. and R. Gillies, *Phenotypic changes of acid adapted cancer cells push them toward aggressiveness in their evolution in the tumor microenvironment*. Cell Cycle, 2016: p. 0.
138. Kelley, D.Z., et al., *Integrated Analysis of Whole-Genome ChIP-Seq and RNA-Seq Data of Primary Head and Neck Tumor Samples Associates HPV Integration Sites with Open Chromatin Marks*. Cancer Res, 2017. **77**(23): p. 6538-6550.
139. Wang, J., et al., *Pathway and network approaches for identification of cancer signature markers from omics data*. (1837-9664 (Print)).
140. Wolchok, J.D., et al., *Nivolumab plus ipilimumab in advanced melanoma*. N Engl J Med, 2013. **369**(2): p. 122-33.
141. Wang, Z., M. Gerstein, and M. Snyder, *RNA-Seq: a revolutionary tool for transcriptomics*. Nature reviews. Genetics, 2009. **10**(1): p. 57-63.
142. Kreeger, P.K. and D.A. Lauffenburger, *Cancer systems biology: a network modeling perspective*. Carcinogenesis, 2009. **31**(1): p. 2-8.
143. Patt, A., et al., *Integration of Metabolomics and Transcriptomics to Identify Gene-Metabolite Relationships Specific to Phenotype*. Methods Mol Biol, 2019. **1928**: p. 441-468.
144. Schmitz, L., et al., *Transcripts and tumors: regulatory and metabolic programming during biotrophic phytopathogenesis*. F1000Res, 2018. **7**.
145. Sadeghi, M., et al., *MicroRNA and Transcription Factor Gene Regulatory Network Analysis Reveals Key Regulatory Elements Associated with Prostate Cancer Progression*. PLoS One, 2016. **11**(12): p. e0168760.

146. Guo, N.L. and Y.W. Wan, *Network-based identification of biomarkers coexpressed with multiple pathways*. (1176-9351 (Print)).
147. Le, D.H. and Y.K. Kwon, *GPEC: a Cytoscape plug-in for random walk-based gene prioritization and biomedical evidence collection*. *Comput Biol Chem*, 2012. **37**: p. 17-23.
148. Geiger, T., et al., *Use of stable isotope labeling by amino acids in cell culture as a spike-in standard in quantitative proteomics*. *Nat Protoc*, 2011. **6**(2): p. 147-57.
149. Cox, J., et al., *A practical guide to the MaxQuant computational platform for SILAC-based quantitative proteomics*. *Nat Protoc*, 2009. **4**(5): p. 698-705.
150. Wojtkowiak, J.W., et al., *Chronic autophagy is a cellular adaptation to tumor acidic pH microenvironments*. *Cancer Res*, 2012. **72**(16): p. 3938-47.
151. Avnet, S., et al., *Cancer-associated mesenchymal stroma fosters the stemness of osteosarcoma cells in response to intratumoral acidosis via NF-kappaB activation*. *Int J Cancer*, 2017. **140**(6): p. 1331-1345.
152. Armour, C.D., et al., *Digital transcriptome profiling using selective hexamer priming for cDNA synthesis*. *Nat Methods*, 2009. **6**(9): p. 647-9.
153. Bolger, A.M., M. Lohse, and B. Usadel, *Trimmomatic: a flexible trimmer for Illumina sequence data*. (1367-4811 (Electronic)).
154. Kim, D., B. Langmead, and S.L. Salzberg, *HISAT: a fast spliced aligner with low memory requirements*. 2015. **12**: p. 357.
155. Anders, S., P.T. Pyl, and W. Huber, *HTSeq--a Python framework to work with high-throughput sequencing data*. (1367-4811 (Electronic)).
156. Team, R.C., *A Language and Environment for Statistical Computing*.
157. Love, M.I., W. Huber, and S. Anders, *Moderated estimation of fold change and dispersion for RNA-seq data with DESeq2*. *Genome Biology*, 2014. **15**(12): p. 550.
158. von Mering, C., et al., *STRING: a database of predicted functional associations between proteins*. (1362-4962 (Electronic)).

159. Alon, U., *Network motifs: theory and experimental approaches*. Nature Reviews Genetics, 2007. **8**: p. 450.
160. Shannon, P., et al., *Cytoscape: a software environment for integrated models of biomolecular interaction networks*. (1088-9051 (Print)).
161. Rinnone, F., et al., *NetMatchStar: an enhanced Cytoscape network querying app*. F1000Research, 2015. **4**: p. 479-479.
162. Le, D.-H. and V.-H. Pham, *HGPEC: a Cytoscape app for prediction of novel disease-gene and disease-disease associations and evidence collection based on a random walk on heterogeneous network*. BMC systems biology, 2017. **11**(1): p. 61-61.
163. Assenov, Y., et al., *Computing topological parameters of biological networks*. (1367-4811 (Electronic)).
164. Khan, F.M., et al., *Unraveling a tumor type-specific regulatory core underlying E2F1-mediated epithelial-mesenchymal transition to predict receptor protein signatures*. (2041-1723 (Electronic)).
165. Razavi, P., et al., *The Genomic Landscape of Endocrine-Resistant Advanced Breast Cancers*. Cancer Cell, 2018. **34**(3): p. 427-438 e6.
166. Curtis, C., et al., *The genomic and transcriptomic architecture of 2,000 breast tumours reveals novel subgroups*. Nature, 2012. **486**(7403): p. 346-52.
167. Ordway, B., et al., *Targeting of Evolutionarily Acquired Cancer Cell Phenotype by Exploiting pHi-Metabolic Vulnerabilities*. Cancers (Basel), 2020. **13**(1).
168. Gatenby, R.A. and J. Brown, *Mutations, evolution and the central role of a self-defined fitness function in the initiation and progression of cancer*. Biochim Biophys Acta Rev Cancer, 2017. **1867**(2): p. 162-166.
169. Enriquez-Navas, P.M., et al., *Exploiting evolutionary principles to prolong tumor control in preclinical models of breast cancer*. Sci Transl Med, 2016. **8**(327): p. 327ra24.
170. Renner, K., et al., *Restricting Glycolysis Preserves T Cell Effector Functions and Augments Checkpoint Therapy*. Cell Rep, 2019. **29**(1): p. 135-150 e9.

171. Gan, T.J., *Diclofenac: an update on its mechanism of action and safety profile*. Curr Med Res Opin, 2010. **26**(7): p. 1715-31.
172. Doherty, J.R., et al., *Blocking lactate export by inhibiting the Myc target MCT1 Disables glycolysis and glutathione synthesis*. Cancer Res, 2014. **74**(3): p. 908-20.
173. Liberti, M.V., et al., *A Predictive Model for Selective Targeting of the Warburg Effect through GAPDH Inhibition with a Natural Product*. Cell Metab, 2017. **26**(4): p. 648-659 e8.
174. Liberti, M.V., et al., *Evolved resistance to partial GAPDH inhibition results in loss of the Warburg effect and in a different state of glycolysis*. J Biol Chem, 2020. **295**(1): p. 111-124.
175. Commander, R., et al., *Subpopulation targeting of pyruvate dehydrogenase and GLUT1 decouples metabolic heterogeneity during collective cancer cell invasion*. Nat Commun, 2020. **11**(1): p. 1533.
176. Picco, N., et al., *Integrating Models to Quantify Environment-Mediated Drug Resistance*. Cancer Res, 2017. **77**(19): p. 5409-5418.
177. Nichol, D., et al., *Steering Evolution with Sequential Therapy to Prevent the Emergence of Bacterial Antibiotic Resistance*. PLoS Comput Biol, 2015. **11**(9): p. e1004493.
178. West, J., et al., *Towards Multidrug Adaptive Therapy*. Cancer Res, 2020. **80**(7): p. 1578-1589.
179. Zhang, J., et al., *Integrating evolutionary dynamics into treatment of metastatic castrate-resistant prostate cancer*. Nat Commun, 2017. **8**(1): p. 1816.
180. Holliday, D.L. and V. Speirs, *Choosing the right cell line for breast cancer research*. Breast Cancer Res, 2011. **13**(4): p. 215.
181. Neve, R.M., et al., *A collection of breast cancer cell lines for the study of functionally distinct cancer subtypes*. Cancer Cell, 2006. **10**(6): p. 515-27.
182. Kao, J., et al., *Molecular profiling of breast cancer cell lines defines relevant tumor models and provides a resource for cancer gene discovery*. PLoS One, 2009. **4**(7): p. e6146.

183. Horwitz, K.B., M.E. Costlow, and W.L. McGuire, *MCF-7; a human breast cancer cell line with estrogen, androgen, progesterone, and glucocorticoid receptors*. Steroids, 1975. **26**(6): p. 785-95.
184. Levenson, A.S. and V.C. Jordan, *MCF-7: the first hormone-responsive breast cancer cell line*. Cancer Res, 1997. **57**(15): p. 3071-8.
185. Andersen, A.P., et al., *Roles of acid-extruding ion transporters in regulation of breast cancer cell growth in a 3-dimensional microenvironment*. Mol Cancer, 2016. **15**(1): p. 45.
186. Caruso, J.P., et al., *pH, Lactate, and Hypoxia: Reciprocity in Regulating High-Affinity Monocarboxylate Transporter Expression in Glioblastoma*. Neoplasia, 2017. **19**(2): p. 121-134.
187. Counillon, L., et al., *Na(+)/H(+) antiporter (NHE1) and lactate/H(+) symporters (MCTs) in pH homeostasis and cancer metabolism*. Biochim Biophys Acta, 2016. **1863**(10): p. 2465-80.
188. Liberti, M.V. and J.W. Locasale, *The Warburg Effect: How Does it Benefit Cancer Cells?* Trends Biochem Sci, 2016. **41**(3): p. 211-218.
189. Endo, A., et al., *Specific inhibition of glyceraldehyde-3-phosphate dehydrogenase by koniginic acid (heptelidic acid)*. J Antibiot (Tokyo), 1985. **38**(7): p. 920-5.
190. Warburg, O., *The Chemical Constitution of Respiration Ferment*. Science, 1928. **68**(1767): p. 437-43.
191. Warburg, O., *On respiratory impairment in cancer cells*. Science, 1956. **124**(3215): p. 269-70.
192. Warburg, O., *On the origin of cancer cells*. Science, 1956. **123**(3191): p. 309-14.
193. Warburg, O., F. Wind, and E. Negelein, *The Metabolism of Tumors in the Body*. J Gen Physiol, 1927. **8**(6): p. 519-30.
194. De Luca, A., et al., *Mitochondrial biogenesis is required for the anchorage-independent survival and propagation of stem-like cancer cells*. Oncotarget, 2015. **6**(17): p. 14777-95.
195. Freischel, A.R., et al., *Frequency-dependent interactions determine outcome of competition between two breast cancer cell lines*. Sci Rep, 2021. **11**(1): p. 4908.

196. Hulikova, A., et al., *Intracellular carbonic anhydrase activity sensitizes cancer cell pH signaling to dynamic changes in CO₂ partial pressure*. J Biol Chem, 2014. **289**(37): p. 25418-30.
197. Sutoo, S., et al., *Adaptation to chronic acidic extracellular pH elicits a sustained increase in lung cancer cell invasion and metastasis*. Clin Exp Metastasis, 2020. **37**(1): p. 133-144.
198. Riemann, A., et al., *Extracellular Acidosis Modulates the Expression of Epithelial-Mesenchymal Transition (EMT) Markers and Adhesion of Epithelial and Tumor Cells*. Neoplasia, 2019. **21**(5): p. 450-458.
199. Hanahan, D., *Hallmarks of Cancer: New Dimensions*. Cancer Discov, 2022. **12**(1): p. 31-46.
200. Mani, S.A., et al., *The epithelial-mesenchymal transition generates cells with properties of stem cells*. Cell, 2008. **133**(4): p. 704-15.
201. Thiery, J.P., et al., *Epithelial-mesenchymal transitions in development and disease*. Cell, 2009. **139**(5): p. 871-90.
202. Yu, M., et al., *Circulating breast tumor cells exhibit dynamic changes in epithelial and mesenchymal composition*. Science, 2013. **339**(6119): p. 580-4.
203. Luond, F., et al., *Distinct contributions of partial and full EMT to breast cancer malignancy*. Dev Cell, 2021. **56**(23): p. 3203-3221 e11.
204. Corbet, C., et al., *TGFbeta2-induced formation of lipid droplets supports acidosis-driven EMT and the metastatic spreading of cancer cells*. Nat Commun, 2020. **11**(1): p. 454.
205. Zhang, L., et al., *S100B attenuates microglia activation in gliomas: possible role of STAT3 pathway*. Glia, 2011. **59**(3): p. 486-98.
206. Bianchi, R., et al., *S100B protein stimulates microglia migration via RAGE-dependent up-regulation of chemokine expression and release*. J Biol Chem, 2011. **286**(9): p. 7214-26.
207. Donato, R., et al., *Functions of S100 proteins*. Curr Mol Med, 2013. **13**(1): p. 24-57.

208. McIlroy, M., et al., *Interaction of developmental transcription factor HOXC11 with steroid receptor coactivator SRC-1 mediates resistance to endocrine therapy in breast cancer [corrected]*. Cancer Res, 2010. **70**(4): p. 1585-94.
209. Slomnicki, L.P., B. Nawrot, and W. Lesniak, *S100A6 binds p53 and affects its activity*. Int J Biochem Cell Biol, 2009. **41**(4): p. 784-90.
210. Tsoporis, J.N., S. Izhar, and T.G. Parker, *Expression of S100A6 in cardiac myocytes limits apoptosis induced by tumor necrosis factor-alpha*. J Biol Chem, 2008. **283**(44): p. 30174-83.
211. Lesniak, W., L.P. Slomnicki, and A. Filipek, *S100A6 - new facts and features*. Biochem Biophys Res Commun, 2009. **390**(4): p. 1087-92.
212. Chen, X., et al., *S100 calcium-binding protein A6 promotes epithelial-mesenchymal transition through beta-catenin in pancreatic cancer cell line*. PLoS One, 2015. **10**(3): p. e0121319.
213. Li, A., et al., *S100A6 promotes the proliferation and migration of cervical cancer cells via the PI3K/Akt signaling pathway*. Oncol Lett, 2018. **15**(4): p. 5685-5693.
214. Simeonov, K.P., et al., *Single-cell lineage tracing of metastatic cancer reveals selection of hybrid EMT states*. Cancer Cell, 2021. **39**(8): p. 1150-1162 e9.
215. Wood, T.E., et al., *A novel inhibitor of glucose uptake sensitizes cells to FAS-induced cell death*. Mol Cancer Ther, 2008. **7**(11): p. 3546-55.
216. Chan, D.A., et al., *Targeting GLUT1 and the Warburg effect in renal cell carcinoma by chemical synthetic lethality*. Sci Transl Med, 2011. **3**(94): p. 94ra70.
217. Hargreaves, M. and L.L. Spriet, *Skeletal muscle energy metabolism during exercise*. Nat Metab, 2020. **2**(9): p. 817-828.
218. Caslin, H.L., et al., *Lactate Is a Metabolic Mediator That Shapes Immune Cell Fate and Function*. Front Physiol, 2021. **12**: p. 688485.
219. Kato, M., K. Sakai, and A. Endo, *Koningic acid (heptelidic acid) inhibition of glyceraldehyde-3-phosphate dehydrogenases from various sources*. Biochim Biophys Acta, 1992. **1120**(1): p. 113-6.

220. Blaszczak, W., H. Williams, and P. Swietach, *Autoregulation of H(+)/lactate efflux prevents monocarboxylate transport (MCT) inhibitors from reducing glycolytic lactic acid production*. Br J Cancer, 2022.
221. Chen, C.L., et al., *Tumor suppression by cell competition through regulation of the Hippo pathway*. Proc Natl Acad Sci U S A, 2012. **109**(2): p. 484-9.
222. Chaffer, C.L. and R.A. Weinberg, *A perspective on cancer cell metastasis*. Science, 2011. **331**(6024): p. 1559-64.

Appendices


APPENDIX 1: IACUC APPROVAL LETTER



RESEARCH INTEGRITY & COMPLIANCE
INSTITUTIONAL ANIMAL CARE & USE COMMITTEE

MEMORANDUM

TO: Robert Gatenby, M.D.

FROM: 
Farah Moulvi, MSPH, IACUC Coordinator
Institutional Animal Care & Use Committee
Research Integrity & Compliance

DATE: 10/28/2020

PROJECT TITLE: Cancer as a Complex Adaptive System (Investigating phenotypic & microenvironmental mechanisms for immunotherapy response)
Evolution of Lung and Ovarian

FUNDING SOURCE: Federal government or major agency that awards grants based on peer-reviewed proposals (NIH, NSF, DOD, AHA, ACS, etc.)
Non-Profit (Private Foundations, H. Lee Moffitt Cancer Center, etc.), For Profit (Industry Sponsored) or Other
National Institute of Health DeBartolo Family Foundation

IACUC PROTOCOL #: R IS00005331

PROTOCOL STATUS: **APPROVED**

Your request for continuation of this study was received and will be reported to the Institutional Animal Care and Use Committee (IACUC). The IACUC acknowledges that this study is currently on going as previously approved. Please be advised that **continuation of this study is in effect for a one-year period beginning 11/25/2020:**

Please take note of the following:

- **IACUC approval is granted for a one-year period at the end of which, an annual renewal form must be submitted for years two (2) and three (3) of the protocol through the eIACUC system.** After three years all continuing studies must be completely re-described in a new electronic application and submitted to IACUC for review.
 - **All modifications to the IACUC-Approved Protocol must be approved by the IACUC prior to initiating the modification.** Modifications can be submitted to the IACUC for review and approval as an Amendment or Procedural Change through the eIACUC system. These changes must be within the scope of the original research hypothesis, involve the original species and justified in writing. Any change in the IACUC-approved protocol that does not meet the latter definition is considered a major protocol change and requires the submission of a new application.
-

INSTITUTIONAL ANIMAL CARE AND USE COMMITTEE
PHS No. A4100-01, AAALAC No. 000434, USDA No. 58-R-0015
University of South Florida • 12901 Bruce B. Downs Blvd., MDC35 • Tampa, FL 33612-4799
(813) 974-7106 • FAX (813) 974-7091

APPENDIX 2: COPYRIGHT STATEMENTS

Copyright statement for “Causes and Consequences of Variable Tumor Cell Metabolism on Heritable Modifications and Tumor Evolution”

© 2020 Ordway, Swietach, Gillies and Damaghi. This is an open-access article distributed under the terms of the Creative Commons Attribution License (CC BY). The use, distribution or reproduction in other forums is permitted, provided the original author(s) and the copyright owner(s) are credited and that the original publication in this journal is cited, in accordance with accepted academic practice. No use, distribution or reproduction is permitted which does not comply with these terms.

Copyright statement for “Integrative Analysis of Breast Cancer Cells Reveals an Epithelial-Mesenchymal Transition Role in Adaptation to Acidic Microenvironment”

© 2020 Sadeghi, Ordway, Rafiei, Borad, Fang, Koomen, Zhang, Yoder, Johnson and Damaghi. This is an open-access article distributed under the terms of the Creative Commons Attribution License (CC BY). The use, distribution or reproduction in other forums is permitted, provided the original author(s) and the copyright owner(s) are credited and that the original publication in this journal is cited, in accordance with accepted academic practice. No use, distribution or reproduction is permitted which does not comply with these terms.

Copyright statement for “Targeting of Evolutionarily Acquired Cancer Cell Phenotype by Exploiting pHi-Metabolic Vulnerabilities”

© 2020 by the authors. Licensee MDPI, Basel, Switzerland. This article is an open access article distributed under the terms and conditions of the Creative Commons Attribution (CC BY) license

APPENDIX 3: PUBLICATIONS

1. Sadeghi M*, Ordway B*, Rafiei I, Borad P, Fang B, Koomen JL, Zhang C, Yoder S, Johnson J, Damaghi M. Integrative Analysis of Breast Cancer Cells Reveals an Epithelial-Mesenchymal Transition Role in Adaptation to Acidic Microenvironment. (Primary). *Front. Oncol.* 2020, 10:304. doi: 10.3389/fonc.2020.00304. (* Authors contributed equally)
2. Ordway B, Swietach P, Gillies RJ, Damaghi M. Causes and Consequences of Variable Tumor Cell Metabolism on Heritable Modifications and Tumor Evolution (Review). *Front. Oncol.* 2020, 10:373. doi: 10.3389/fonc.2020.00373
3. Ordway B, Tomaszewski M, Byrne S, Abrahams D, Swietach P, Gillies RJ, Damaghi M. Targeting of Evolutionarily Acquired Cancer Cell Phenotype by Exploiting pHi-Metabolic Vulnerabilities. (Primary) *Cancers.* 2021, 13, 64.
4. Ordway B, Gillies RJ, Damaghi M. Extracellular Acidification Induces Lysosomal Dysregulation. (Review) *Cells.* 2021, 10, 1188.
5. Russell S, Xu L, Kam Y, Abrahams D, Ordway B, Lopez A, Bui M, Johnson J, Epstein T, Ruiz E, Lloyd M, Swietach P, Verduzco D, Wojtkowiak J, Gillies RJ., Proton export upregulates aerobic glycolysis. (Primary) *BMC Biology.* 2022.
6. Ibrahim-Hashim A, Gillies RJ, Ordway B, Gatenby R., Back to basic: Trials and tribulations of alkalizing agents in Cancer. (Clinical Trial). Accepted.
7. Sunassee E, Jardim-Perassi BV, Ordway B*, Ramanujam N., Metabolic Imaging in Breast Cancer: Can we combat chemoresistance?. (Review). In preparation. (*Corresponding Author)
8. Ordway B, Xu L, Gillies RJ. Metabolic feedback of the Warburg phenotype. (Primary). In preparation.